Fall 12-2021

Mechanisms of Stress Survival in Gram Positive Bacterial Pathogens

Asia Poudel
Old Dominion University, asiapoudel@gmail.com

MECHANISMS OF STRESS SURVIVAL IN GRAM POSITIVE BACTERIAL PATHOGENS

by

Asia Poudel
M.Sc. September 2010, Tribhuvan University, Nepal
M.S. May 2021, Old Dominion University

A Dissertation Submitted to the Faculty of
Old Dominion University in Partial Fulfillment of the
Requirements for the Degree of

DOCTOR OF PHILOSOPHY

CHEMISTRY

OLD DOMINION UNIVERSITY
December 2021

Approved by:

Erin B. Purcell (Director)

Steven M. Pascal (Member)

James W. Lee (Member)

Christopher Osgood (Member)

ABSTRACT

MECHANISMS OF STRESS SURVIVAL IN GRAM POSITIVE BACTERIAL PATHOGENS

Asia Poudel
Old Dominion University, 2021
Director: Dr. Erin B. Purcell

Anaerobic Gram-positive bacteria are not a well-characterized group but include many human pathogens that are resilient against stresses caused by the human immune system or by antibiotic treatment. This dissertation investigated the survival mechanisms of two clinically relevant Gram-positive organisms, *Clostridioides difficile* and *Cutibacterium acnes* under extracellular stresses. The response of the opportunistic skin pathogen *Cutibacterium acnes* to nanosecond electric pulses is characterized and found that growth in a biofilm, which usually protects bacteria from stress, renders this species more killable by this treatment. In addition, the stringent response (SR), a conserved bacterial stress survival mechanism, is studied in the intestinal pathogen *Clostridioides difficile*. The SR contributes to antibiotic tolerance and virulence in many pathogens, but there is no homogeneity in its operation and regulation among diverse bacterial species. The SR is driven by the guanosine nucleotide signaling alarmones, (pp)pGpp, that are synthesized by conserved enzymes. We identified environmental cues that induce clostridial synthetase expression and implicated (pp)pGpp signaling in antibiotic survival. Interestingly, we have discovered that both the clostridial stringent response synthetases synthesize pGpp rather than pppGpp/ppGpp as the only alarmone, which is unique among bacteria that use the SR. *C. difficile* must cope with rapidly changing and diverse gastrointestinal environments and survive

antibiotic treatment to establish *Clostridioides difficile* infection (CDI). The results from this study elucidated its survival mechanism in hostile environments and offer significant insights to develop targeted therapeutics against CDI.

This dissertation is dedicated to my family for their unrelenting love and support; especially to my deceased grandmother, Lila Devi Poudel.

ACKNOWLEDGEMENTS

I express my heartfelt appreciation and earnest compliment to all the helping hands who supported me in one or other way for completing my dissertation work. First and foremost, I would like to thank my advisor, Dr. Erin B. Purcell for her dedicated guidance and encouragement throughout my PhD study at Old Dominion University. I would like to extend my sincere thanks to the members of my dissertation committee, Drs. Steven M. Pascal, James W. Lee and Christopher J. Osgood for their helpful knowledge and support through my graduate study. In addition, I would like to acknowledge current and previous Purcell lab group members for their contribution and support in this work. I extend my sincere gratitude to Dr. David Courson for his support and guidance on my research. I would like to thank all the faculties and staffs at the Department of Chemistry and Biochemistry at ODU for their support during my graduate study. I am thankful to Dr. Alvin Holder for allowing me to use his lab's ITC instrument and Dr. Michael J. Celestine for his help in doing ITC experiments. I would like to reaffirm my admiration and special thanks to all my colleagues who supported me with their invaluable suggestions. Furthermore, I would like to acknowledge Dr. Rita Tamayo (UNC-Chapel Hill), Dr. Carl E. Bauer (Indiana University) and Dr. Fang Minxu (UC-San Francisco) for their support on my projects.

I am greatly obliged to my wife, Divya Thapa, my parents and all other family members without whose constant inspiration and unconditional support, this work would not have been completed. Lastly, I would like to thank my newly born son, Aadrik Poudel, for giving my life a powerful sense of purpose since the day of his birth.

This dissertation research is supported by NIH (NIAID K22 AI118929-01) and Pulse Biosciences.

NOMENCLATURE

Abbreviations	Full forms/definitions
CDI	*Clostridioides difficile* infection
FMT	Fecal microbiota transplantation
FDA	Food and Drug Administration
SR	Stringent response
GMP	Guanosine-5’-monophosphate
GDP	Guanosine-5’-diphosphate
GTP	Guanosine-5’-triphosphate
AMP	Adenosine-5’monophosphate
ADP	Adenosine-5’diphosphate
ATP	Adenosine-5’triphosphate
pGpp	GMP-3’-diphosphate
ppGpp	GDP-3’-diphosphate/guanosine tetraphosphate
pppGpp	GTP-3’-diphosphate/guanosine pentaphosphate
(pp)ppGpp	pppGpp, ppGpp, and pGpp
Magic spot	Product catalyzed by RSH enzymes
RSH	RelA/SpoT homolog
SAS	Small alramone synthetase
SAH	Small alarmone hydrolase
TGS	ThrRS, GTPase, and SpoT
ACT	Aspartate kinase, chorismite, and TyrA
ZFD	Zinc-finger or conserved cysteine domain
NUDIX	Nucleoside diphosphate linked moiety X
ROS	Reactive oxygen species
RNS	Reactive nitrogen species

PPi	Inorganic pyrophosphate
Pi	Inorganic phosphate
TLC	Thin layer chromatography
PEI-cellulose	Polyethyleneimine-cellulose
NMR	Nuclear Magnetic Resonance
ITC	Isothermal titration calorimetry
kDa	Kilo Dalton
OD	Optical density
PCR	Polymerase chain reaction
°C	Degree Celsius
BHIS	Brain heart infusion supplemented
TY	Tryptone yeast
LB	Luria-Bertani
×g	Times gravity
ANOVA	Analysis of variance
DNA	Deoxyribinucleotide
SDS-PAGE	Sodium dodecyl sulfate-polyacrylamide gel
DTT	Dithiothreitol
PMSF	Phenylmethylsulphonyl fluoride
IPTG	Isopropyl β-D-thiogalactoside
CdRelQ	*C. difficile* RelQ
CdRSH	*C. difficile* RSH
BSRelQ	*B. subtilis* RelQ
P_{rsh}	Promoter region upstream of *C. dfficile rsh*
P_{relQ}	Promoter region upstream of *C. dfficile relQ*
P_{tet}	Promoter region of tetracycline inducible vector
PBS	Phosphate buffered saline
Ni-NTA	Nickel-nitrilotriacetic acid
DIC	Differential interface
PI	Propidium iodide

CFU	Colony forming unit Nickel-nitrilotriacetic acid
nsPEF	nanosecond pulsed electric field
ITO	Indium titanium oxide
ATCC	American type culture collection
PEF	Pulsed electric field
LY	Lysozyme
ECM	Extracellular matrix

TABLE OF CONTENTS

Page

LIST OF TABLES

Table Page

LIST OF FIGURES

Figure Page

CHAPTER I

INTRODUCTION

GRAM POSITIVE BACTERIA

Gram stain differentiates bacteria between Gram-positive and Gram-negative species based on their cell wall composition.(1) Gram-positive bacteria possess a thick cell wall (20-80nm) whereas Gram-negative bacteria have a relatively thin (<10nm) cell wall.(2) Its thickness, composition and the extent of cross linking determines the bacterial cell shape and morphology.(3) Besides its function in maintaining cell morphology, the bacterial cell wall is the first line of defense against harmful environmental stresses and plays a significant role in signal transduction.(4) The differences in cell wall composition between Gram-positive bacteria and Gram-negative bacteria confer different cellular properties particularly while responding to external stresses including antibiotics, physical stresses, and host immune responses.(2,4) The thick cell wall of Gram-positive bacteria is a major factor that allows them to withstand a wide range of challenging conditions including antibiotic and physical stress.

Gram-positive bacteria include several human pathogens that cause severe infections. Increasing antimicrobial resistance is a major public health problem that compromises the care of thousands of patients worldwide. In the US, Gram-positive bacterial infections are the most common multidrug resistant infections including infections due to methicillin resistant *Staphylococcus aureus*, vancomycin resistant Enterococci and *Clostridioides difficile*.(5) Gram-positive bacteria are less well characterized than Gram-negative species and very few data exist to inform best management practices against these infections. The molecular mechanisms of antimicrobial resistance are diverse and frequently differ within bacterial genera and/or species

and are influenced by the presence of other environmental stressors.(6) In fact, bacterial survival largely depends on their capacity to sense and react to the changes in environmental conditions. Several response mechanisms are activated during stress conditions which differ between the species.(7) Therefore, studies concentrating on Gram-positive bacterial stress survival strategies are important to mitigate the growing problem of drug resistance. Understanding their stress survival mechanisms would provide valuable information in designing targeted therapies against these organisms. This dissertation focuses on studying the survival mechanisms against several environmental stresses of two clinically relevant Gram-positive anerobic organisms: *Clostridioides difficile* and *Cutibacterium acnes*.

Clostridioides difficile

Clostridioides difficile is a Gram-positive, spore forming anaerobic gastrointestinal pathogen that causes *Clostridioides difficile* infection (CDI).(8) CDI is one of the most common causes of healthcare-associated diarrhea in the developed world with increasing recurrence rates in the 21st century.(9) The incidence of CDI is rising around the globe due in part to the emergence of the so-called hypervirulent epidemic strains including ribotype 027, which is prevalent in Europe and North America.(9-11) Antibiotic usage and diet also play a role in increasing CDI.(12-14) In the United States, over 450,000 patients are infected with *C. difficle* per year resulting in 29,000 deaths with an associated annual health care cost of $4.8 billion.(15) *C. difficile* is transmitted to susceptible hosts via faeco-oral transmission.(16) Once spores are ingested, they survive the acidic pH of the stomach and travel through the intestine where they interact with primary bile salts and amino acids(17,18) that facilitate their germination into vegetative cells.(16) These vegetative cells colonize the intestinal epithelium and secrete toxins, TcdA and TcdB, resulting in a host inflammatory response including rapid infiltration of neutrophils into the

intestinal mucosa that causes increased intestinal epithelial permeability and formation of pseudomembranes.(19-21) The clinical manifestations of CDI range from mild diarrhea to life threatening pseudomembranous colitis, fulminant colitis and toxic megacolon.(16) The most significant risk factor for CDI development is the exposure of the normal gut microflora to broad spectrum antibiotics.(13) Many broad-spectrum antibiotics including ampicillin, cephalosporins, clindamycin, amoxicillin and fluoroquinolones are associated with the spread of CDI (Table 1).(11,13,22,23) The gut microflora maintains a healthy gut ecosystem and prevents *C. difficile* colonization. However, when these microflorae are disrupted by antibiotics, many of which are ineffective against *C. difficile*, it facilitates the multiplication and colonization of *C. difficile* to cause disease.(19)

Table 1: Antibiotics and their association with CDI. Adapted and modified from Leffler DA and Lamont JT 2015.(13)

Antibiotics	Association with CDI
Ampicillin	Very common
Clindamycin	Very common
Amoxcillin	Very common
Cephalosporins	Very common
Fluoroquinolones	Very common
Sulfonamides	Somewhat common
Trimethoprim	Somewhat common
Maacrolides	Somewhat common
Aminoglycosides	Uncommon
Bacitracin	Uncommon
Metronidazole	Uncommon
Rifampin	Uncommon
Chloramphenicol	Uncommon
Tetracyclines	Uncommon
Carbapenems	Uncommon

Gastrointestinal pathogens experience diverse environments once they come in contact with the host during infection.(24) Therefore, *C. difficile* must navigate a rapidly changing and hostile environment to establish symptomatic infection. The proliferation of vegetative cells in the gut environment is impacted by several factors including host immune response, oxygen levels, nutrient limitation, secondary bile acids, short chain fatty acids, competing gut microflora and varying pH throughout the gastrointestinal tract.(24-32) The immune response can include fever, antimicrobial host defense peptides, sequestration of metals to limit their availability, and oxidative stress from reactive oxygen species (ROS) and reactive nitrogen species (RNS) produced by phagocytic cells.(33-35) ROS and RNS are also produced during metabolism by both host cells and commensal microbiota within the gut.(24,36,37) Commensal microorganisms also exert nutritional stress on pathogens by limiting availability of carbohydrates and amino acids.(34) In addition, they limit the production of secondary bile salts required for the sporulation as well as produce short chain fatty acids such as propionate, butyrate and acetate that are believed to limit the proliferation of *C. difficile* vegetative cells.(38,39) The pH within the gastrointestinal tract also varies from acidic to alkaline depending on the region as well as the established microbiome, host diet and health state as well as drug intake.(26) The varying pH signals the invasive bacterial population about its localization within the gut environment and regulate the synthesis of pH stress proteins.(34)

C. difficile colonization is disproportionately common in older adult population due to inadequate innate or humoral immune responses and loss of commensal bacterial diversity in this age group (Figure 1).(40-42) Patients above 65 years of age are at an increased risk by ~5 to 10-fold for CDI development than younger patients.(43) In addition, the frequency of developing CDI increases with the prolonged stay at healthcare institutions. The incidence of bacterial colonization

during the first few days of hospitalization ranges from 2.1 to 20% and gradually increases with extended stay.(43,44) Similarly, nursing home patients are at higher risk of developing CDI due to older age, poor health status, underlying diseases, frequent hospitalizations, and antibiotics exposure compared to the noninstitutionalized population.(43)

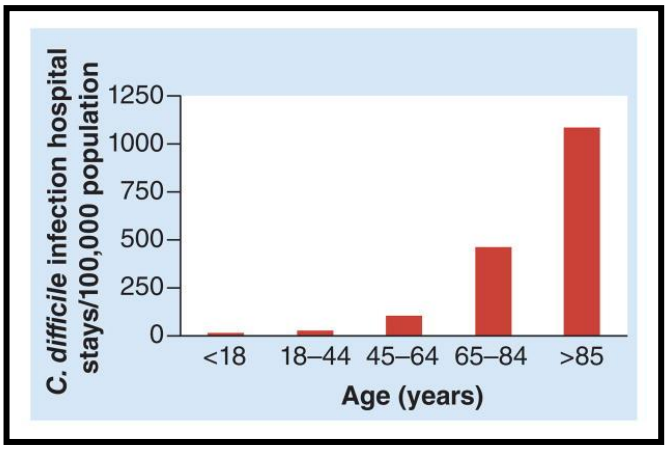

Figure 1. Hospitalization with CDI increases with age. Adapted and modified from Jump RL 2013.(42)

Since CDI transmission occurs via spores through fecal-oral route, use of personal protective equipment such as gloves and disposable gowns in health care settings are recommended.(43) In clinical settings, it is advised to wash hands with soap and water after direct contact with CDI patients.(43) As alcohol-based disinfectants are ineffective in killing *C. difficile* spores, chlorine-based solutions such as hypochlorite solutions are recommended for environmental cleaning.(45) CDI treatment depends on the nature and severity of the infection.(46) Primary therapy of initial episode of non-severe CDI includes the use of oral vancomycin or oral fidaxomicin, however,

there are reports of development of resistance against these drugs. (22,46) Metronidazole, once regarded as a first line therapy against CDI, is no longer recommended due to its reduced efficacy.(22) Fecal microbiota transplant (FMT) is emerging as a reasonable treatment option for recurrent CDI with high cure rates in patients experiencing multiple recurrent episodes.(46,47) FMT in combination with multiple classes of antibiotics including beta-lactams, cephalosporins, clindamycin, and fluoroquinolones restored healthy gut bacteria and prevented the intestinal colonization of *C. difficile* in clinical trials.(46) However, the US-FDA has not yet authorized the routine use of FMT as a CDI treatment option due to the inherent risk of transmitting undetected pathogens and chemical agents to the recipient.(48) Furthermore, antibody-based therapy in combination with antibiotics have shown promising outcomes against recurrent CDI.(47) Bezlotoxumab is an FDA approved monoclonal antibody that targets toxin B and has been shown to reduce the risk of recurrent CDI in those at a high risk of recurrence.(47) As of now, there are no known approved vaccines available against CDI but, clinical trials with some candidates are in progress. As there are no universal therapies against CDI, understanding the stress survival mechanisms of the infecting bacterium would provide valuable foundation in developing targeted therapies against this organism.

Cutibacterium acnes

Cutibacterium acnes, formerly known as *Propionibacterium acnes*, is a Gram-positive, non-spore forming, facultative anaerobic rod-shaped biofilm-forming bacterium that colonizes human skin.(49,50) It is an opportunistic pathogen associated with invasive skin infections such as acne vulgaris as well as medical device related infections.(51) The most common acne therapeutic strategies such as topical and systemic antimicrobial treatments are less effective in reducing the infection due to the emergence of bacterial resistance.(52-54) As biofilm forming

cells are more resilient to antimicrobial stress, antibiotic therapy against *C. acnes* is quite challenging eventually leading to the recurrence of the inflammation and emergence of antibiotic resistant strains.(55) Recent studies suggest that biofilm formation is one of the important factors contributing to the chronic pathophysiology of acne vulgaris.(56)

Acne vulgaris is very common skin disorder affecting most of the adolescents, however individuals of other ages also may be affected.(57) Approximately 70% of adolescents at some point of time suffer from this kind of skin disorder and the prevalence of adult acne vulgaris is increasing especially in women of 25 years and older.(57,58) In the US, the estimated direct health care burden for all kinds of skin related disease is around $75 billion out of which acne vulgaris is the most common target of spending.(59) The most common treatments include the topical application of retinoids as well as the systemic treatments, photosensitizers and natural approaches.(60,61) However, the efficacy of these treatments is minimum and results into unpleasant side effects such as hyperpigmentation, exfoliation and crusting.(60) In addition to these conventional therapeutics, new light and thermal treatment strategies have been developed, however these treatments include high energy low wavelength light that results into an increase in the temperature to 49°C which is detrimental to tissue underlying the skin.(58) Therefore, it is important to develop alternative therapeutics to control and prevent the infections.

Development of novel antimicrobial compounds usually takes decades and eventually faces similar problems as most microbes develop resistance against a new drug after its prolonged usage.(62-64) Most commonly clindamycin and erythromycin in combination with benzoyl peroxide or retinoids are used as therapeutics against all grades of acne.(65) However, these treatment strategies have failed to reduce the bacterial burden, altered the skin microbiota, and resulted into recurrence of the infection and emergence of antibiotic resistance.(66,67) As an

alternative, scientific community have started looking into non-chemical therapies which could be useful in addressing the problem of drug resistance. Among them, noninvasive nanosecond pulse stimulation (NPS) has emerged as a potential alternative for microbial inactivation.(68-71)

THE BACTERIAL STRINGENT RESPONSE

The stringent response (SR) is a stress survival mechanism that enables bacterial cells to quickly adapt to extracellular stress and constantly switch between growth, survival and death.(72,73) It is an adaptive bacterial response that regulates the transcriptional as well as translational machinery via nucleotide signaling.(73) It was first described in *E. coli* when the cells were under the stress of amino acid deprivation.(74) Following its discovery, the SR has been established as a conserved bacterial stress response, induced under various nutritional and environmental stresses, which directs the cellular machinery to temporarily halt growth and division and induce transcription of stress survival genes that include virulence factors in several pathogens.(75-78) This molecular switching of bacterial physiology is canonically driven by the accumulation of two intracellular ‘alarmone’ nucleotides, guanosine pentaphosphate (pppGpp) and guanosine tetraphosphate (ppGpp) collectively known as (p)ppGpp and sometimes referred to as ‘magic spot’.(75) These signaling molecules are metabolized by multidomain bifunctional synthetase/hydrolase enzymes in the RelA-SpoT (RSH) family and by monofunctional small alarmone synthetase (SAS, RelP/RelQ) and the recently discovered small alarmone hydrolase (SAH) domains (Figure 2).(73,79,80) Gram-negative bacteria typically employ two long RSH family enzymes, one bifunctional SpoT and one monofunctional RelA in which the hydrolase domain has weak or no activity.(81) On the other hand, Gram-positive Firmicutes typically encode a single RSH and one or two SAS.(81)

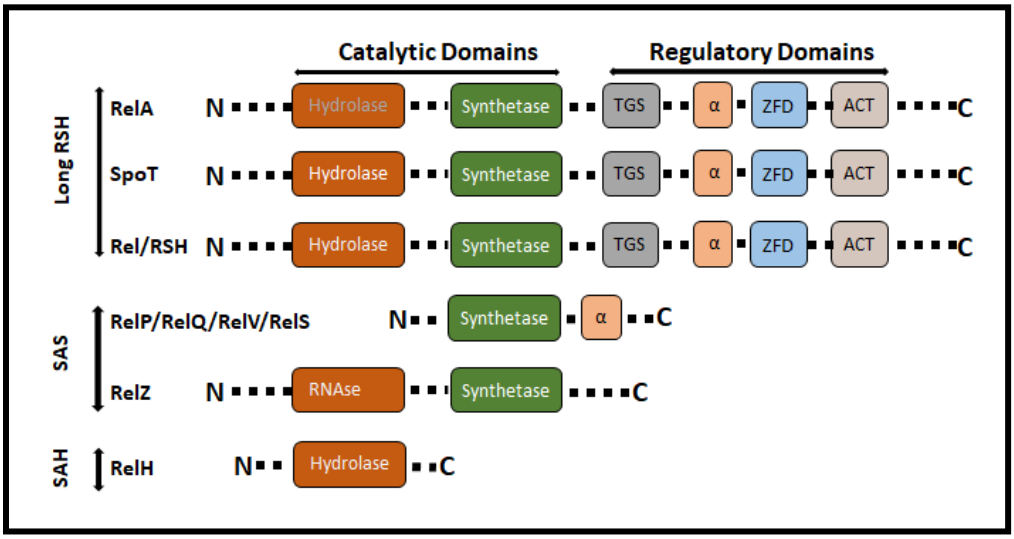

Figure 2. Domain organization of (pp)pGpp metabolizing enzymes. Each enzyme is composed of two regions: an N-terminal catalytic domain and a C-terminal regulatory domain. Both synthetase and hydrolase domains are functional in bifunctional enzymes (Rel/RSH/SpoT). Hydrolase activity is lost in monofunctional multidomain (p)ppGpp synthetase enzymes. *E. coli* RelA has only synthetase activity as its hydrolase activity has been lost due to accumulation of mutations in the catalytic residues. The regulatory region of multidomain proteins contains a TGS domain (ThrRS, GTPase, and SpoT), a conserved α helical domain, a ZFD domain (zinc-finger or conserved cysteine domain), and an ACT (aspartate kinase, chorismate, and TyrA) RNA recognition motif. The small alarmone synthetase (SAS) enzymes (RelV/RelP/RelQ/RelS) contain a synthetase domain and a small oligomeric α-domain. RelZ from *Mycobacterium smegmatis* contains additional RNAse domain. The RelH/small alarmone hydrolase (SAH) contains only the hydrolase domain. Adapted and modified from Das B and Bhadra RK 2020.(82)

The highly conserved synthetase domains of both families catalyze the transfer of a pyrophosphate moiety from ATP to 3'-OH of GDP and/or GTP to produce ppGpp or pppGpp, respectively.(83) A potential third alarmone, pGpp, has been recently discovered which may be synthesized directly from GMP or generated by hydrolysis from the longer forms of magic spot, but its biological role is largely unexplored (Figure 3). (84,85)

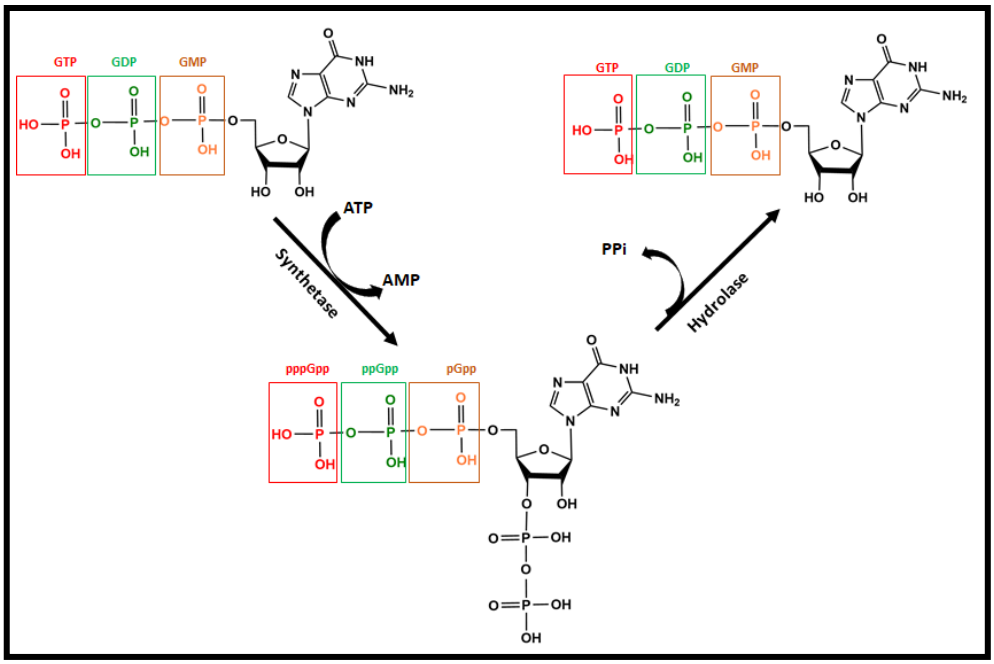

Figure 3. (pp)pGpp metabolism. The synthetase domain of RelA/SpoT homologue enzyme catalyzes the transfer of pyrophosphate group from ATP to the ribose moiety of GTP, GDP or GMP to produce pppGpp, ppGpp and pGpp respectively. The hydrolase domain regenerates GTP, GDP and GMP by removing the 3' pyrophosphate group from respective magic spots. Adapted and modified from Irving *et al.* 2021.(86)

Extracellular stresses including amino acid starvation, alkaline shock, cell wall stress from cell wall active antibiotics, heat stress, oxidative stress and acid stress can trigger the SR by modulating the transcription of either RSH or SAS genes in several pathogens.(77,87,88) (89,90) However, the mechanisms by which the SR induce cellular responses vary among bacterial species but the end result is similar: adjust cellular physiology in a way that helps restore and maintain homeostasis, even in the face of challenging environmental circumstances. Post-transcriptional regulation of RSH enzymes typically involves protein-protein interactions or binding of uncharged tRNAs, while post-transcriptional regulation of SAS enzymes seems to depend on allosteric binding of (p)pGpp. (91-94) The SAS enzymes also appear to play a stress-independent role in maintaining basal (p)ppGpp levels and regulating guanosine homeostasis in *Bacillus subtilis* and *E. faecalis*.(95-97)

Table 2. Substrate affinities of SAS of representative Gram-positive organisms. SAS have diverse substrate affinities, higher number of stars indicating higher affinities to respective guanosine nucleotides. Adapted and modified from Steinchen W *et al.* 2018(94), Gaca AO *et al.* 2015(84), Sajish M *et al.* 2009(98) and Petchiappan A *et al.* 2020(99).

SAS	GMP	GDP	GTP
E. fecalis RelQ	★★	★★★	★
B. subtilis RelQ	★	★★★	★★
S. aureus RelQ/RelP	★	★★★	★★
S. mutans RelQ/RelP	★	★★★	★★
M. smegmatis RelZ	★★★	★★	★

Guanosine nucleotide substrate utilization varies among organisms.(84) Bifunctional RSH synthetases in Gram-positive organisms generally have higher affinity for GTP than GDP.(98,100) In contrast, the SAS enzyme RelQ preferentially utilizes GDP over GTP in *Bacillus subtilis, Enterococcus faecalis, Streptococcus mutans, Staphylococcus aureus,* and *Mycobacterium smegmatis* (Table 2). (84,85,99,101) SAS enzymes do not universally prefer GDP to GTP, as RelS from *C. glutamicum* utilizes GTP with higher affinity than GDP.(102) Recently, SAS enzymes are reported to be able to utilize GMP as a pyrophosphate acceptor and synthesize pGpp in Gram-positive bacteria including *E. faecalis*, *S. mutans*, *B. subtilis*, *S. aureus*, *Corynebacterium glutamicum*, and *Mycobacterium smegmatis*. In addition, the recently discovered NUDIX hydrolases remove 5' phosphates or pyrophophates from (p)ppGpp to produce pGpp, but the physiological role of this third alarmone is still under investigation.(84,85,99,103,104)

RESEARCH AIMS

The main objectives of the work presented in this dissertation are to:

1. Express and purify the small alarmone synthetase RelQ from *C. difficile* for functional characterization using recombinant gene expression and protein purification techniques; perform *in vitro* biochemical characterization of *C. difficile* RelQ using autoradiography, thin layer chromatography, and phosphorous NMR (Chapter II). This chapter is based on the publication Poudel *et al.* 2021.(105)
2. Identify potential environmental signals triggering the expression of *C. difficile* stringent response genes, *rsh* and *relQ*, using lab-constructed oxygen-independent fluorescent transcriptional reporters. Various environmental stresses mimicking the bacterial host environment were examined for the regulation of the stringent response in *C. difficile*

(Chapter III). This chapter is based on the publications Poudel *et al.* 2021(105) and Pokhrel et al. 2020.(106)

3. Determine the effect of nanosecond pulsed electric fields (nsPEF) in the growth of *C. acnes* using a noninvasive nanosecond pulse stimulation technique. The survival of both the planktonic and biofilm cells against nsPEF treatment were studied (Chapter IV). This chapter is based on the publication Poudel *et al.* 2021.(107)

CHAPTER II

FUNCTIONAL CHARACTERIZATION OF *CLOSTRIDIOIDES DIFFICILE'S* SMALL ALARMONE SYNTHETASE, RELQ

PREFACE

The content of this chapter was published in bioRxiv in August 2021. Reprinted with permission from Poudel, A., Pokhrel, A., Oludiran, A., Coronado, E. J., Alleyne, K., Gilfus, M. M., Gurung, R. K., Adhikari, S. B., and Purcell, E. B. (2021) Unique features of magic spot metabolism in *Clostridioides difficile*. *bioRxiv*, 2021.2008.2002.454818

INTRODUCTION

Bacteria develop several survival strategies to cope with a wide variety of environmental stresses including nutrient limitation, antibiotics, or changes in abiotic factors during their life cycle. The stringent response is a ubiquitous bacterial signaling pathway that has been linked to many bacterial functions such as environmental adaptation, virulence, motility, cell division, biofilm formation, persister formation and development.(73,108,109) As mentioned in chapter I, the SR is governed by secondary nucleotide messengers collectively known as (pp)pGpp.(75) Three main groups of RelA/SpoT homolog (RSH) super family enzymes are responsible in controlling the intracellular levels of these nucleotide signaling molecules as a response to various external and internal stresses encountered by the organisms.(81) These proteins are categorized as long-RSH enzymes, small alramone synthetases (SAS) and small alrmone hydrolases (SAH).(81,86) N-terminal domain of long RSH typically comprise catalytic regions including a

hydrolase and a synthetase domain whereas C-terminal domain consist of regulatory regions.(81,86) Two small alarmone enzymes consist of either a single synthetase or a hydrolase domain and lack regulatory domains.(81,86) Gram negative organisms of beta and gamma subgroups of proteobacteria accommodate two long RSH enzymes, RelA and SpoT, where RelA primarily functions as (pp)pGpp synthetase and SpoT is involved in both the synthesis and hydrolysis of (pp)pGpp.(81,86) In contrast, Gram positive firmicutes carry a long bifunctional RSH enzymes and one or two small alarmone synthetases.(81,86)

Small alarmone synthetases were recently discovered and classified into 30 subfamilies that spread across multiple bacterial species.(110) The discovery of SASs has widened the scope of understanding bacterial stress response induced under several environmental circumstances. Two highly homologous SAS enzymes named as RelQ (SAS1, YjbM) and RelP (SAS2, YwaC) exist among most of the reported bacterial species (77) These SAS are predominantly found in firmicutes and share nearly 50% sequence similarity at amino acid level.(77) Two common SAS found in both *Bacillus subtilis* and *Staphylococcus aureus* are similar in structural architecture but differ significantly in their ability to produce (p)ppGpp and their substrate selectivity.(79,94,101) Beside RelP and RelQ, several additional SASs have now been characterized. *Corynebacterium glutamicum*, a Gram-positive soil bacterium, carry one common SAS protein, RelP and a new small alarmone synthetase RelS.(102) RelP do not exhibit (pp)pGpp synthesis activity whereas RelS shares sequence similarity with synthetase domain of RelQ and demonstrate maximum activity at low temperature.(102) *Mycobacterium smegmatis*, an actinobacterium, encodes a dual domain bifunctional protein named as RelZ which has a C-terminal domain like the other SAS protein however contains an additional N-terminal RNase HII domain in the same polypeptide chain.(99) *Vibrio cholerae*, a Gram-negative proteobacterium, possesses RelV protein which has

a (pp)pGpp synthetase domain and exhibits activity upon glucose or fatty acid starvation.(111) Since the bacterium is phylogenetically different from firmicutes, RelV shares poor homology with RelP and RelQ.(111)

Previously, our group has identified the genes encoding RSH and RelQ in *C.difficile*, confirmed the pyrophosphotransferase activity of RSH to GDP exclusively, and identified a role for *C.difficile* RSH in antibiotic survival.(112) Therefore, biochemical characterization of both the enzymes and regulation of expression of the genes encoding these enzymes under various environmental conditions would shed light into their potential roles in survival in diverse environments. The major objective of the project described in this chapter was to express and purify *C. difficile* small alarmone synthetase, RelQ for its functional characterization. We aimed to study its *in vitro* activity under various environmental conditions as well as determine its substrate preferences. The work presented in this study represents an important step in understanding the mechanisms of magic spot synthesis in *C. difficile*.

MATERIALS AND METHODS

Cloning of *C. difficile* RelQ *(CdRelQ)*

The *relQ* gene (CDR20291_0350) was amplified from *C. difficile* R20291 genomic DNA using primers relQ_a_F and relQ_a_R (Appendix B) that added a C-terminal hexahistidine tag. The gene was subsequently ligated into the pMMBneo expression vector at the KpnI (New England Biolabs, NEB) and PstI (NEB) restriction sites, and chemically transformed into *E. coli* BL21. The resulting plasmid, pMMBneo::relQ was confirmed via PCR using pMMBneo plasmid-specific primers, pMMB_F & pMMB_R (Appendix B). Because expression from pMMBneo did not result in a visible protein band on an SDS-PAGE gel, the relQ gene (CDR20291_0350)

was amplified from *C. difficile* R20291 genomic DNA using gene specific primers 5'relQ_NdeI & 3'relQ_XhoI (Appendix B). The relQ amplicon was ligated into pET24a expression vector at the NdeI-XhoI restriction sites and upstream of the vector derived 6xHis-tag to generate pET24a::relQ plasmid (Appendix A). The plasmid was transformed into *E. coli* BL21 (NEB) and confirmed by PCR using relQ gene specific primers (relQ_a_F & relQ_a_R). (Appendix B). Q5 high fidelity DNA polymerase from NEB was used in all the PCR reactions.(105)

In vivo overexpression of CdRelQ

Growth curve assays following the induction of *C. difficile relQ* in *E. coli* BL21 cells carrying pMMBneo:: relQ were performed in 96 well microtiter plates (Brand Plates) using a BioTek Synergy plate reader. Exponential phase cultures of *E. coli* were inoculated in luria Bertani (LB) medium with 50µg/mL kanamycin in the presence or absence of 0.5 mM isopropyl-β-D-thiogalactopyranoside (IPTG) inducer. The plate was incubated at 37°C with shaking for a total of 16 hours while monitoring cell growth every 30 minutes.(105)

Overexpression and purification of CdRelQ

Saturated starter cultures of *E. coli* BL21 cells containing pET24a-CdRelQ-His plasmid (Appendix A) were grown overnight in LB medium with 50 µg/mL kanamycin in a shaking incubator at 250 rpm and 37°C. Cultures were diluted at 1:20 into LB medium with 50 µg/mL kanamycin and grown at 37°C with shaking until the optical density at 600 nm reached 0.5-0.6. Once cells reached the desired OD_{600}, they were allowed to stand at room temperature for 10 mins and induced with 0.5 mM isopropyl β-D-1-thiogalactopyranoside (IPTG) for 3 hours at 30°C for protein expression. Cells were centrifuged at 4030 rcf using a Beckman coulter JA12 rotor for 30 mins at 4°C and pellets were frozen at -20°C. Cells were lysed using lysis buffer (50 mM Tris-

HCl, pH 8.0, 500 mM NaCl, 5 mM MgCl2, 10 mM imidazole, 3 mM BME, and 100 mM PMSF) via sonication. The cells were burst for 10 secs at 40% amplitude with 30 secs pause for 8 cycles followed by centrifugation at 13680×g for 15 mins at 4°C in a bench top Scilogex centrifuge. The soluble protein fraction was collected as supernatant and subjected for purification using HisPur Ni-NTA Resin affinity chromatography (Thermo Fisher Scientific). Briefly, the supernatant was mixed with equilibrating buffer (same as lysis buffer) in 1:1 ratio and subjected to 1.0 mL Ni-NTA resin column equilibrated with the equilibrating buffer. Initially the column was washed with five column volumes of the lysis buffer, and further washed and eluted using a gradient of imidazole- 30 mM, 50 mM and 75 mM imidazole were used for column washing while the protein was eluted using 150 mM and 300 mM imidazole in two fractions. Purified protein was subsequently dialyzed overnight at 4°C in a buffer consisting of 30 mM Tris, pH 8.0, 300 mM NaCl, 5 mM MgCl2, 5 mM BME, and 20 % glycerol using 8-10 kDa molecular weight cutoff Float-A-Lyzer®G2 dialysis device (Spectra/Por Spectrum® Laboratories Inc.). Protein concentration was determined spectroscopically measuring A_{280} using BioDrop. Molar extinction coefficient of 36455 $M^{-1}cm^{-1}$ as determined by ExPASY(113) for CdRelQ was used to estimate the concentration.(105)

Expression and purification of the control synthetase

E. coli BL21 cells carrying pET28 bearing the *Bacillus subtilis* SAS1/RelQ gene were generously provided by Mingxu Fang, University of California, San Diego and Carl E. Bauer, Indiana University, Bloomington. *Bacillus subtilis* RelQ (BsRelQ) was expressed and purified using a protocol developed by Mingxu Fang as previously published.(114) Briefly, *E. coli* BL21 cells bearing pET28a::BsRelQ were grown in LB media containing 50 µg/mL kanamycin at 37°C with shaking until the OD_{600} reached 0.4. Protein expression was induced overnight at 16°C by the addition of 200 µM IPTG. Cell pellet was collected by centrifugation at 4°C and resuspended

in StrepTactin buffer containing 50 mM Tris pH 8.9, 1 M NaCl and 20% glycerol along with 2 mM PMSF. The cells were sonicated with 10 secs burst and 30 secs pause cycle at 40% amplitude for 8 cycles followed by centrifugation to collect the clarified lysate. The protein was purified by using StrepTactin resin column (IBA Life sciences) following the manufacturer's instructions.(105)

***In vitro* measurement of synthetase activity**

(pp)pGpp synthesis was carried in a reaction volume of 10.0 µL as described previously(106,112) with a fixed concentration of CdRelQ (2.0µM) or BsRelQ (3.0µM). The reaction mixture consists of a buffer containing 10 mM Tris-HCl (pH 7.5), 5 mM ammonium acetate, 2 mM KCl, 0.2 mM DTT, 0.15 mM ATP, 5mM $MgCl_2$, 1.0 µCi of γ-^{32}P-ATP (PerkinElmer), and indicated concentrations of AMP (Acros organics)/ADP/ATP (Bio Basic)/GMP (BioPlus Chemicals)/GDP/GTP (BioBasic) phosphoacceptor. The use of γ-^{32}P-ATP radioisotope was presented as a proposal to and approved by the University's Radiation Safety Office committee prior to experiment designing and conduction (Appendix K). Where indicated, the pH of the reaction was adjusted with HCl or NaOH. Where indicated, $MgCl_2$ was substituted with 5 mM metal salts in the +2oxidation state ($MnCl_2$, $CoCl_2$, $CuCl_2$, $ZnCl_2$, $NiBr_2$, $CaCl_2$, and $FeSO_4$). The reactions were carried out at 37°C and stopped by spotting 2.0 µL of each sample onto PEI-cellulose TLC plates, allowing the spots to dry. Unless otherwise indicated, reactions were run for 60 minutes before quenching. The plates were subsequently developed in 1.5 M KH_2PO_4 (pH 3.64 ± 0.03) and autoradiographed using a Storm 860 Phosphorimager (GE Healthcare Life Sciences). pGpp signal was quantitated using ImageJ software.(115) RelQ activity was expressed as the percentage of γ-^{32}P-ATP substrate converted into product at each timepoint.(112) Michaelis-Menten assays were performed by running the reactions for 5 minutes

at the indicated concentration of GDP or GTP. The line of best fit for the Michaelis-Menten equation was calculated using non-linear regression with least squares fit and the equation $y = (V_{max}*X)/(K_M + X)$ where X represents the GXP substrate concentration and y represents the initial reaction velocity and graphed with Prism (GraphPad).(105)

Hydrolase contaminant check

BsRelQ synthesis reactions containing either GDP or GTP as substrates were conducted for 60 minutes at 37°C as described above. CdRelQ was added to each reaction at a final concentration of 2.0 μM and incubated for an additional 60 minutes. At 0, 30, and 60 minutes after CdRelQ addition, 2.0 μL of each reaction were spotted into the PEI-TLC plates for development as described above.(105)

GXP phosphatase activity

Guanosine nucleotide hydrolysis was assessed through synthetase assays performed as above using guanosine 5'-β-thio-diphosphate trilithuim salt (GDPβS) as the only nucleotide phosphoacceptor (Millipore Sigma). The reactions were caried out for 60 mins at 37°C and the spots were autoradiographed as reported above.(105)

^{31}P NMR spectroscopy

The structural properties of the newly synthesized product from pyrophosphate transfer reactions were evaluated by phosphorous NMR. Synthesis reactions were carried out with clostridial synthetases as mentioned above for 40 mins at 37°C and the reaction mixtures were subjected to acquire phosphorous NMR spectra. In addition, phosphorous NMR spectra of the standard nucleotides (ATP, GTP, GDP, GMP, AMP) solutions in the reaction buffer were also acquired for signal comparison and assignments. D_2O at 15% was added into each of the samples

to enable locking of the magnetic field in the NMR spectrometer. NMR spectra were indirectly referenced to 85% external phosphoric acid. ^{31}P NMR recordings with proton decoupling were performed using 400 MHz Bruker Avance III HD NMR spectrometer at 162 MHz (^{31}P) equipped with 5 mm PABBO BB/19F-1H/D Z-GRD Z108618/0798 probe. A total of 14000 scans for each sample at 303K were performed to acquire NMR spectra. All the measurements were carried out using pulse sequences supplied by the spectrometer manufacturer (Bruker-TopSpin 3.2).(105)

Isothermal calorimetry (ITC)

ITC200 microcalorimeter (Malvern) was employed for the analysis of the binding affinity of CdRelQ towards GXP as described previously.(106) Briefly, a total volume of 300 µL reaction buffer containing 0.006 mM of the protein was added into the cell component and 40 µL of 0.06 mM GXP was filled into the syringe from which a total of 38 injections were made for the analysis at 37°C. Both the protein and ligands were prepared in the same buffer containing 10 mM Tris-Cl, 5 mM AmAce, 5 mM $MgCl_2$, 0.2 mM DTT, 0.12 mM ATP and 2 mM KCl. The data obtained were processed in Origin software using a single-binding-site model. The heats of dilution acquired through the titration of ligand into the reference solution was subtracted from the binding curves during peak integration and the calculation of thermodynamic parameters. Two independent samples were measured.(105)

RESULTS

C. difficile encodes one conserved SAS and one divergent SAS

Earlier we have reported that *C. difficile* encodes an RSH family enzyme and the SAS RelQ and confirmed the enzymatic activity of RSH.(106) Upon further exploration, we found that *C. difficile* encodes another putative SAS enzyme, CDR20291_1607 in addition to RelQ, which we

have named RelC. It contains a putative SAS domain and a C-terminal 250 residue region that contains no conserved domain, and its only homologs are in *Firmicutes* species.(81) CdRelQ exhibits high sequence conservation in the ATP and GDP binding motifs identified in crystal structures of *B. subtilis* RelQ and *S. aureus* RelP (Figure 3).(116,117) Similarly, CdRelC has a highly conserved ATP-binding motif, but the putative GDP-binding motif lacks several conserved residues including a tyrosine (Y116 in BsRelQ, Y151 in SaRelP, Q137 in RelC) that stacks with the guanosine base in the GDP substrate and is invariant in SAS and RSH synthetase domains.(116,117) In addition, RelC contains a ten residue insert within the GDP recognition motif that has no homolog in any characterized SAS (Figure 3). Our initial attempts to express RelC in *E. coli* for purification were unsuccessful, but further experimentation will be necessary to determine whether RelC binds any form of guanosine substrate or serves as a pyrophosphotransferase. (Figure 4).(105)

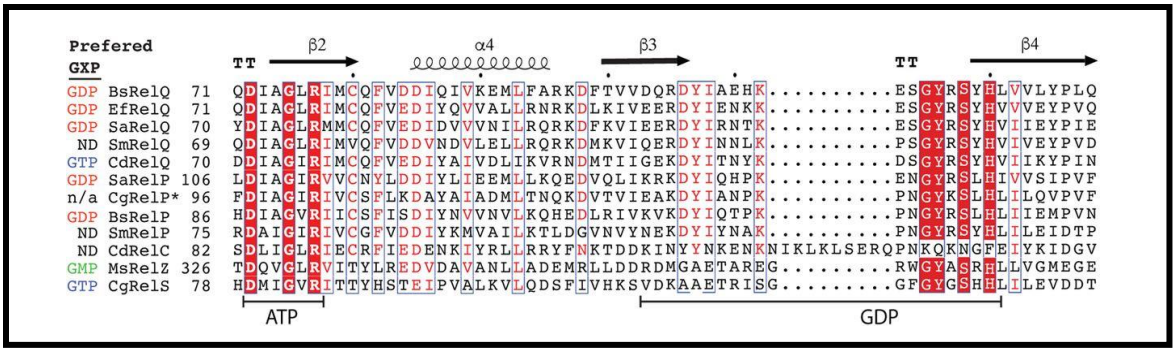

Figure 4. Substrate binding sites of SAS enzymes. The sequences of characterized SAS enzymes are aligned with the crystal structure of *Bacillus subtilis* RelQ (PDB 5DED). β-strands are shown as arrows and α-helices are shown as corkscrews. Conserved residues are shown in red and highly conserved residues are shown in white on a red background. The ATP and GDP binding motifs identified in BsRelQ and SaRelP are indicated on the bottom. The preferred guanosine nucleotide substrate of enzymes that have been kinetically characterized are shown on the left. ND indicates that the substrate preference of an enzyme has not been determined; n/a indicates that the enzyme is not active as a (pp)pGpp synthetase. Alignment generated with ESPript3 (https://espript.ibcp.fr/ESPript/ESPript/). Adapted from Poudel *et al.* 2021.(105)

CdRelQ is an active (pp)pGpp synthetase

In our earlier work, we have reported the *in vitro* synthetase activity of *C. difficile* RSH, CdRSH.(106) We performed a similar experiment with CdRelQ and confirmed that it is also capable of transferring a pyrophosphate moiety from γ-32P-ATP to a guanosine nucleotide phosphoacceptor (Figure 5 A). However, CdRelQ activity is concentration dependent and exhibits little to no pyrophosphotransfer activity at concentrations below 0.4 μM (Figure 5 A & B) Unlike,

CdRSH, CdRelQ when overexpressed in *E. coli* does not arrest cell division (Appendix C) suggesting a lack of *in vivo* (pp)pGpp synthesis activity. Several reports suggest that oligomerization plays an important role in the regulation of RSH family enzymes. Small alarmone synthetases in Gram-positive bacteria such as *B. subtilis*, *S. aureus,* and *E. faecalis* function as tetramers.(116-118) The inactivity of CdRelQ below certain concentration indicates that it may need to undergo oligomerization for its functional activity like other small alarmone synthetases. For instance, *E. faecalis's* RelQ is lost when its oligomerization state is disrupted.(118) Similarly, the allosteric binding of *B. subtilis*'s RelQ with (pp)pGpp depends on its tetramerization.(116)

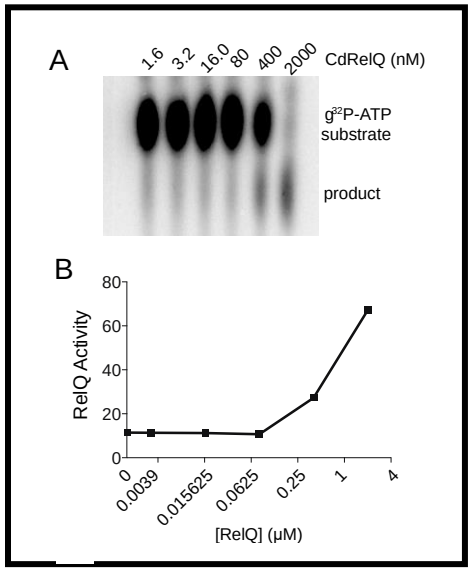

Figure 5. CdRelQ activity *in vitro* is concentration dependent. (A) A representative activity assay shows transfer of pyrophosphate from γ-^{32}P-ATP to a GDP acceptor requires a high concentration of RelQ. (B) Quantification of pyrophosphotransfer activity shown in panel A. Adapted from Poudel *et al.* 2021.(105)

CdRelQ utilizes GDP and GTP but synthesizes pGpp exclusively

We performed synthesis assays utilizing the monophosphate, diphosphate and triphosphate forms of both adenosine and guanosine nucleotides as phospphoacceptors to assess the substrate specificity of CdRelQ. TLC enzymatic assays have demonstrated that CdRelQ is incapable of catalyzing the transfer of pyrophosphate from ATP to any adenosine nucleotides or to guanosine monophosphate (Figure 6 A). However, it utilizes both GDP and GTP as phosphoacceptors and synthesizes the same size product rather than the expected ppGpp and pppGpp (Figure 6 A). In order to identify the CdRelQ synthesized product, we performed synthesis assay using the same range of adenosine and guanosine phosphoacceptors with *Bacillus subtilis* BsRelQ. As has been previously demonstrated, it utilized all three forms of guanosine nucleotides and synthesized three different sized products, pGpp, ppGpp and pppGpp. Surprisingly, the single product synthesized by CdRelQ exhibited the same apparent size and charge as pGpp synthesized by BsRelQ from ATP and GMP (Figure 6 A). We also performed synthesis assay including CdRSH, BsRelQ, and CdRelQ for further exploration of guanosine nucleotides utilization and found that CdRSH utilized only GDP and synthesized the product having same apparent size of pGpp (Figure 6 B). In this assay, CdRSH exhibited some trace synthesis of an apparent pGpp product using GTP as a substrate, although the pGpp spot was very faint and could have resulted from GDP contamination in the GTP sample (Figure 6 B).(105)

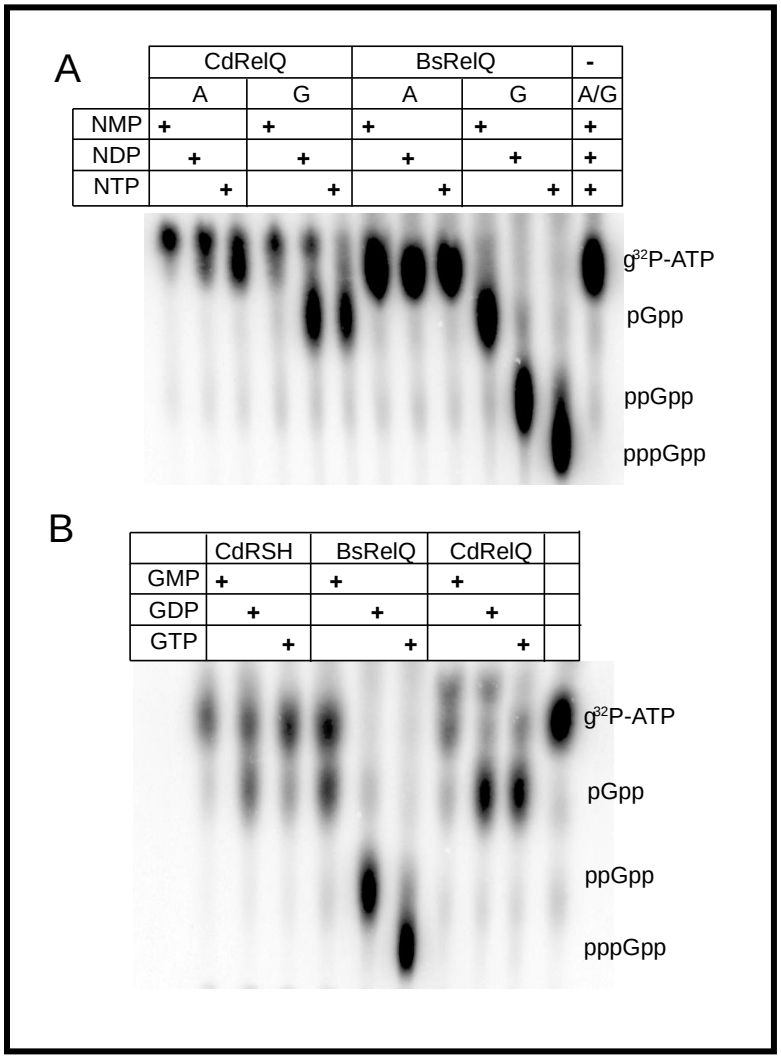

Figure 6. CdRelQ utilizes GDP and GTP but exclusively synthesizes pGpp. (A) Pyrophosphotransfer after 60 minutes from γ-^{32}P-ATP to 500 μM of the indicated purine nucleotide phosphoacceptors by 2.0 μM CdRelQ or 3.0 μM BsRelQ. (B) Pyrophosphotransfer after 60 minutes from γ-^{32}P-ATP to 500 μM of the indicated guanosine nucleotide phosphoacceptors by 3.0 μM CdRSH, 3.0 μM SAS1, or 2.0 μM CdRelQ. Adapted from Poudel *et al.* 2021.(105)

The affinity of CdRelQ towards its guanosine nucleotide substrates was estimated using isothermal titration calorimetry (ITC) where CdRelQ was titrated individually against GDP and GTP for the measurement of thermodynamic parameters (Table 3 and Appendix D).

Table 3. Substrate affinity of CdRelQ at 37°C. The binding of CdRelQ at 0.006 mM to GDP/GTP at 0.060 mM was measured by ITC. The data were fitted to a single-binding site model. Shown are the values for K, the equilibrium binding constant; ΔH, the enthalpy change associated with protein binding to the ligand; ΔS, the entropy change associated with binding and ΔG, the Gibbs free energy change associated with binding. Adapted from Poudel *et al.* 2021.(105)

Substrate	K (M^{-1})	ΔH (cal/mol)	ΔS (cal/mol/°C)	ΔG (cal/mol)
GDP	2.04E3 ± 2.25E3	-8.18E7 ± 8.21E7	-2.64E5	7.96E4
GTP	4.87E4 ± 3.64E3	-1.639E6 ± 7.412E4	-5.25E3	-1.07E4

We observed that the affinity constant of CdRelQ for GDP is roughly half to that for GTP suggesting that the enzyme has a higher affinity for GTP under experimental conditions. The calculated Gibbs free energy change associated with CdRelQ binding also demonstrates its higher affinity for GTP. The ITC data with CdRelQ are in consistence with our TLC assay (Figure 6 A) where CdRelQ appeared to completely deplete the radioactive ATP substrate when combined with GTP but could not completely utilize the ATP substrate when mixed with GDP indicating CdRelQ prefers GTP over GDP. In similar experiments we have previously observed that CDRSH prefers GDP over GTP as substrate for its invitro synthetic activity.(106) Kinetic analysis of CDRelQ

activity at multiple concentrations of guanosine substrate yielded calculated Michaelis constants of 45.4 μM for GTP and 53.6 μM for GDP, consistent with the visual observations (Figure 7). Overall, our data indicates that *C. difficile* synthetases have unique guanosine substrate preferences. In addition, the differential substrate specificity of the clostridial synthetases suggest that these two enzymes may function in discreet cellular conditions depending upon the availability of either GTP or GDP.(105)

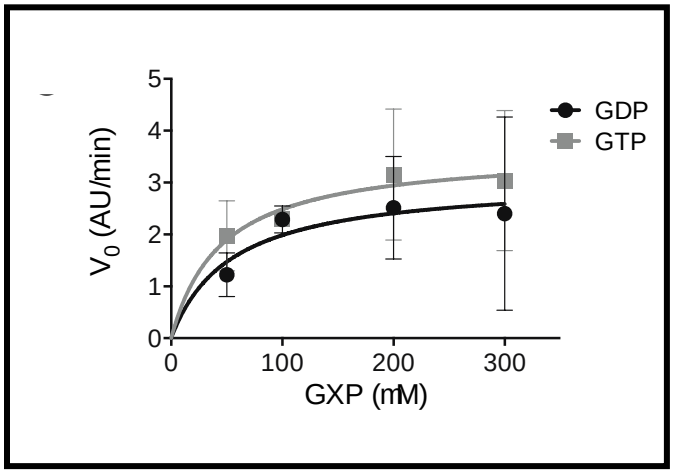

Figure 7. Kinetic analysis of CdRelQ. Michaelis-Menten plot showing the initial reaction velocity at the indicated concentrations of GDP or GTP. Adapted from Poudel *et al.* 2021.(105)

CdRelQ synthesizes pGpp directly

Once we observed the unexpected synthesis of pGpp by CdRelQ, we further checked for its intrinsic (pp)pGpp hydrolysis capability by incubating it with ppGpp and pppGpp produced by BsRelQ. After an hour of incubation, we did not observe any signs of hydrolysis of exogenously

produced magic spots and no pGpp spot had emerged indicating that CdRelQ synthesizes pGpp directly rather than converting (pp)pGpp intermediates (Figure 8).

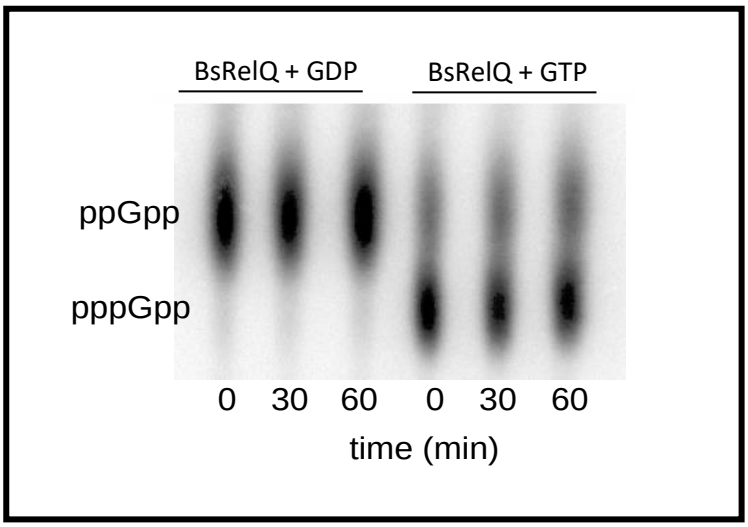

Figure 8. RelQ does not hydrolyze exogenously produced ppGpp or pppGpp. BsRelQ was incubated with GTP or GDP for 60 minutes to produce ppGpp and pppGpp. CdRelQ was added to the mixture and incubated for 60 minutes. Shown are samples taken at 0, 30, and 60 minutes after the addition of CdRelQ. Adapted from Poudel *et al.* 2021.(105)

Clostridial synthetases require phosphorolysis of the guanosine substrate

From the magic spot synthesis experiments including both the clostridial synthetases, we were convinced that the guanosine substrate must undergo hydrolysis during the synthesis. To conform it, we employed 5'-β-thio-diphosphate (GDPβS), which has a non-hydrolyzable thiol bond between the α and β phosphates, as a phosphoacceptor. Both CdRelQ and CdRSH synthesized pGpp when GDP was supplied as a substrate, but neither of clostridial enzymes

generated any form of magic spot when GDPβS was the substrate (Figure 9). However, BsRelQ did appear to utilize the radioactive ATP substrate in the presence of GDPβS. The product formed by BsRelQ using GDPβS is larger in size than ppGpp formed from GDP since the non-hydrolysable analogue contains three lithium atoms that make the product heavier than ppGpp and closer in apparent size to pppGpp formed from GTP (Figure 9). Overall, these data demonstrated that the need to hydrolyze a beta-phosphate bond is specific to the clostridial synthetases.(105)

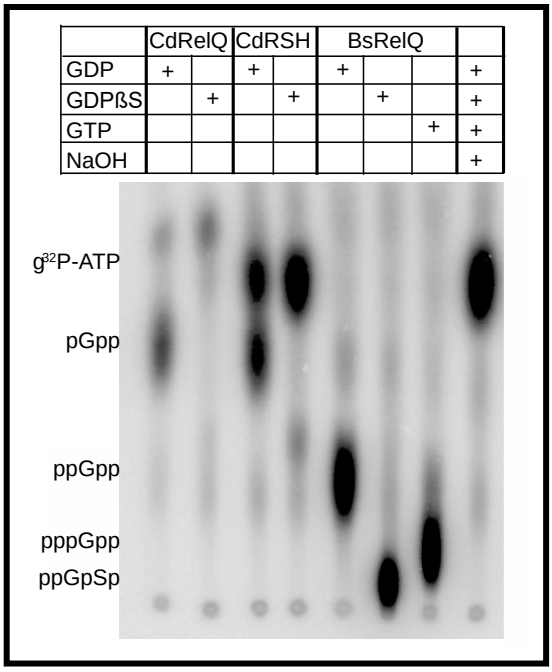

Figure 9. Clostridial synthetases hydrolyze the beta phosphate bond on GXP to synthesize pGpp. Phosphotransfer from γ-^{32}P-ATP by 2.0 μM CdRelQ, 3.0 μM CdRSH, or 3.0 μM BsRelQ to 500 μM of GDP, non-hydrolyzable GDPβS, or GTP. Adapted from Poudel *et al.* 2021.(105)

The addition of a pyrophosphate moiety to GTP/GDP concurrent with or after hydrolysis of the GXP β-phosphate bond could theoretically produce 5'GTP or pGpp. β phosphates at the 3'OH position of ribonucleotides are alkali-labile while phosphates on the 5'OH are not.(98) To confirm this, both the CdRelQ and BsRelQ synthesized reaction were treated with sodium hydroxide before spotting in TLC plate. The spots produced by RelQ and BsRelQ pyrophosphotransfer are blurred and diminished by NaOH treatment, indicating that they are pGpp rather than GTP (Appendix E).

CdRelQ and CdRSH both synthesize pGpp

We performed ^{31}P NMR spectroscopy with proton decoupling and investigated the chemical shifts of the (pp)pGpp synthesis reactions of both the clostridial synthetases. When ATP is mixed pair-wise with the guanosine phosphoaccepters GDP, and GTP, the resonant peaks of each of the phosphorous from each nucleotide are clearly visible and are consistent with the reported values, as are the resonant peaks of AMP and GMP (Figure 10 A, B, E, G).(119,120) The chemical shifts of each of the phosphorous group are listed in Table 4. When ATP and GDP are incubated with CdRelQ, the beta and gamma phosphate peaks of ATP at -19.16 ppm and -5.58 ppm are reduced and an AMP 5' phosphate peak at 3.52 ppm appears, consistent with ATP hydrolysis occurring (Figure 10 A, B, C). The peaks of ATP and GDP were assigned by comparison to their peaks when analyzed individually (Appendix F). Additionally, distinct peaks at 3.52 ppm and 4.02 ppm emerge after incubation with RelQ. These are close to the 5' phosphate peaks of AMP and GMP and may together be ascribed to the formation of AMP from ATP hydrolysis and a 5' guanosine phosphate from hydrolysis of the beta phosphate bond of GDP (Figure 10 A, C, G). We speculate that the 5' phosphate peak of pGpp is offset from the 3.28 ppm peak of GMP by its proximity to the 3' disphosphate moiety (Figure 10 C, G). The peaks of the

GDP 5’ alpha and beta phosphates, at -10.10 ppm and -6.18 ppm, are broadened, presumably by overlap with the peaks of the chemically similar pGpp 3’ alpha and beta phosphate (Figure 10 B, C). Similarly, when ATP and GDP are incubated with CdRSH, the beta and gamma phosphate peaks of ATP are almost completely abolished and the alpha and beta phosphate peaks of the GDP substrate differentiate into doublet peaks, presumably from the pGpp 3’ alpha and beta phosphates, while a pronounced peak at 4.06 ppm emerges (Figure 10 B, D). We attribute the greater loss of ATP peaks and greater differentiation of the guanosine alpha and beta phosphate peaks to greater enzymatic activity by RSH, for which GDP is the preferred substrate, and subsequently less residual ATP and GDP in the reaction mixture. When ATP and GTP are mixed, the alpha and gamma phosphates of the two triphosphate substrates present as doublet peaks, while the beta phosphates present as one broad peak (Figure 10 E). When ATP and GTP are incubated with CdRelQ, peaks at 4.03 ppm, -10.39 ppm, and -5.83 ppm, consistent with the 5’ phosphate and 3’ alpha and beta phosphates, respectively, emerge (Figure 10 E, F). (105)

Table 4. ^{31}P NMR chemical shifts (ppm) of standard nucleotides and the magic spot synthesis reactions. Adapted from Poudel *et al.* 2021.(105)

Nucleotides	5’ αP	5’ βP	5’ γP	3’ αP	3’ βP
AMP	3.49				
ATP	-10.71	-19.04	-5.58		
GMP	3.28				
GDP	-10.10	-6.18			
GTP	-10.70	-19.14	-5.72		
(GDP + ATP) CdRelQ product	4.02			-10.49	-6.13
(GDP + ATP) CdRSH product	4.06			-10.47	-5.93
(GTP + ATP) CdRelQ product	4.03			-10.39	-5.83

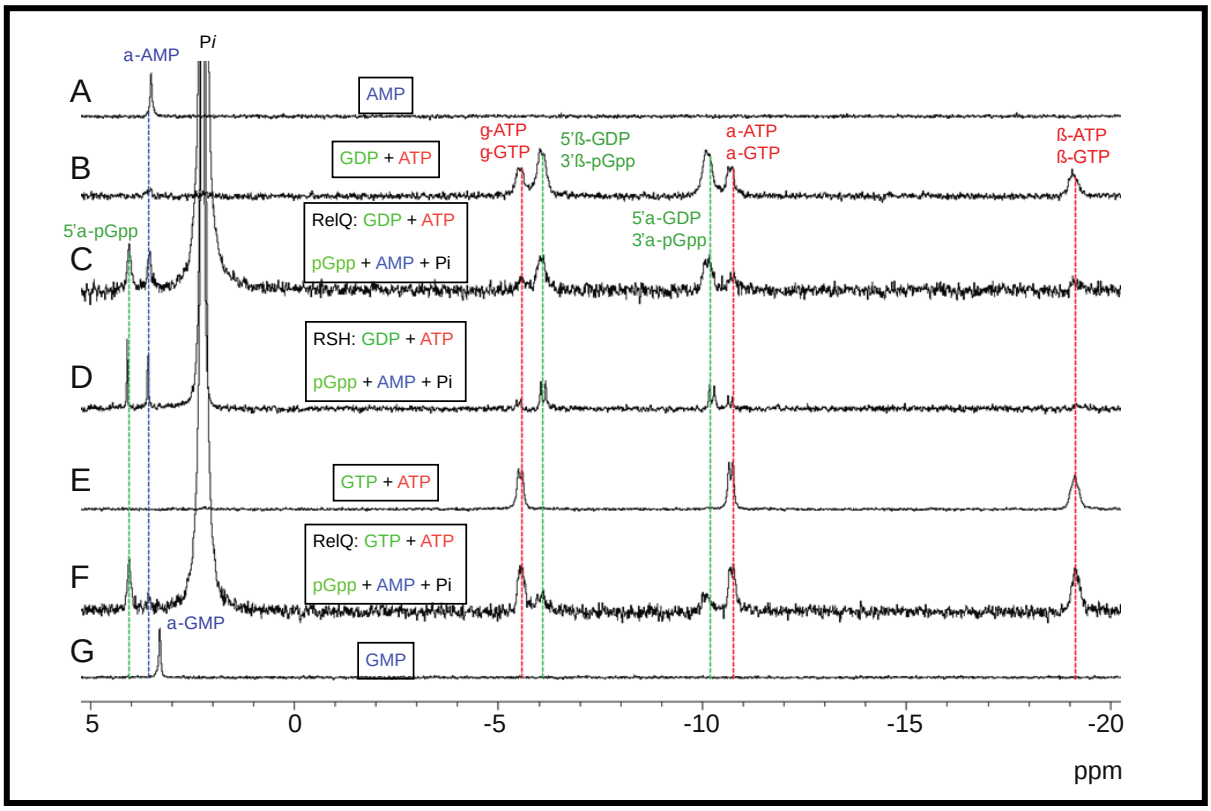

Figure 10. ^{31}P NMR evidence that clostridial magic spot is pGpp (A) AMP standard. (B) GDP and ATP standards. (C) GDP and ATP incubated with 2.0 µM CdRelQ for 40 min. (D) GDP and ATP incubated with 3.0 µM CdRSH for 60 min. (E) GTP and ATP standards. (F) GTP and ATP incubated with 2.0 µM CdRelQ for 40 minutes. (G) GMP standard. The activity of the clostridial synthetases transfers a pyrophosphate from ATP to the 3' hydroxyl of GTP or GDP, creating alpha and beta phosphate groups with chemical environments similar to those of the 5' alpha and beta phosphates of GDP. The clostridial synthetases also cleave the 5' beta phosphate bond of the guanosine substrate, leaving a single 5' alpha phosphate whose chemical environment is similar to that of the 5' alpha phosphate of GMP. Adapted from Poudel *et al.* 2021.(105)

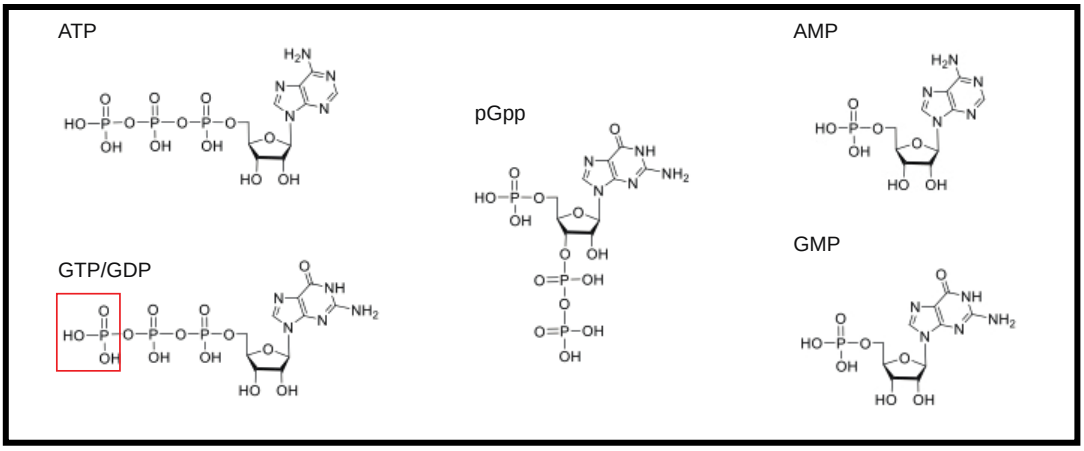

Figure 11. Structures of nucleotide substrates and products. GTP and GDP are differentiated by a third phosphate (outlined in red) on the 5' hydroxyl group.

Interestingly, an enormous peak at 2.2 ppm, identical to published values for inorganic phosphate, is present in all the reactions utilizing clostridial synthetases, consistent with hydrolysis of the 5'β phosphate bond on GXP substrates by clostridial enzymes (Figure 10 C, D, F). We speculate that the large inorganic phosphate peak present in the clostridial reactions shifts the 5'αP peak in the clostridial reactions away from the peak of GMP alone,(121,122) When the enzymes are incubated with guanosine substrates in absence of ATP, the inorganic phosphate peaks are much smaller relative to the peaks from the guanosine phosphates, suggesting that either ATP hydrolysis or formation of the 3'β phosphate bond on the alarmone product stimulate the phosphorolysis of the guanosine substrate (Figure 11). No peaks attributable to pGpp emerge, confirming that hydrolysis depends on ATP (Figure 12).(105)

It is clear that the product of the clostridial synthetases is a guanosine nucleotide containing three phosphorous atoms. This product cannot be ppGp produced by transfer of a single phosphate to the 3' hydroxyl of GDP, as the synthetases must hydrolyze the 5' beta phosphate bond of the guanosine substrate and cannot utilize GDPβS as a phosphate acceptor. Theoretically, the enzymes could transfer a single phosphate onto the 5' beta phosphate of GDP (or replace the 5' gamma phosphate of GTP) to synthesize 5'guanosine triphosphate, but we did not observe the characteristic beta phosphate peak of GTP at -19.14 ppm in our NMR spectra unless exogenous GTP was provided as a substrate (Figure 10 C, D, F), Therefore, pGpp is the only possible product of the clostridial synthetases.(105)

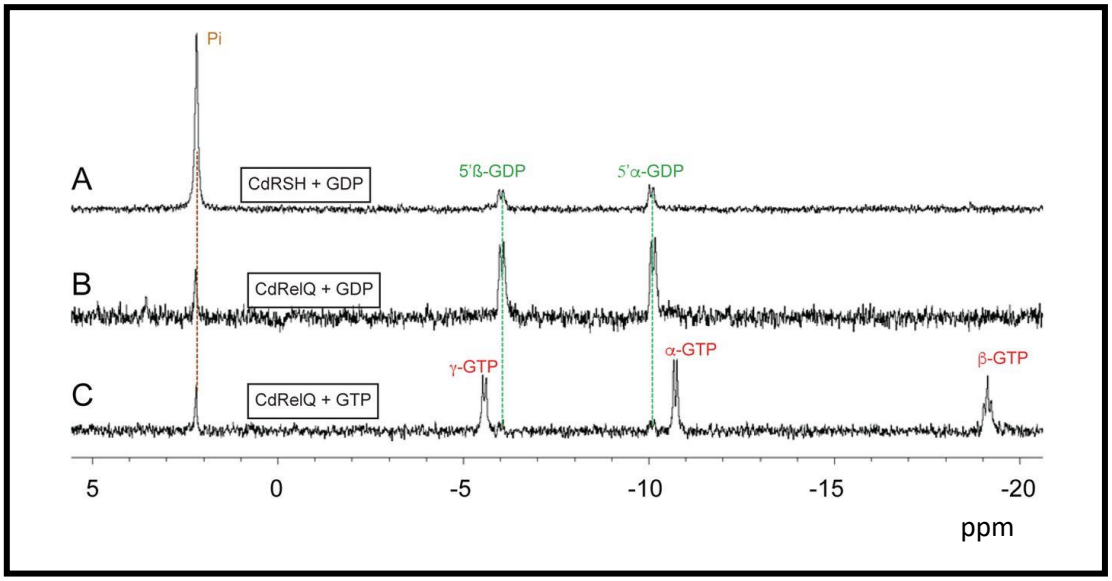

Figure 12. ^{31}P NMR of clostridial synthetase reactions without ATP. (A) GDP incubated with 3.0 µM CdRSH for 40 min. (B) GDP incubated with 2.0 µM CdRelQ for 40 min. (C) GTP incubated with 2.0 µM CdRelQ for 40 min. Adapted from Poudel *et al.* 2021.(105)

CdRelQ is insensitive to varying pH and utilizes diverse metal cofactors

We further characterized CdRelQ activity at pH ranging from 5.0 to 11.0 and in the presence of different divalent cations of varying ionic sizes in separate phosphortransfer reactions. We found that like CdRSH,(106) CdRelQ activity is not altered under varying pH (Figure 13).

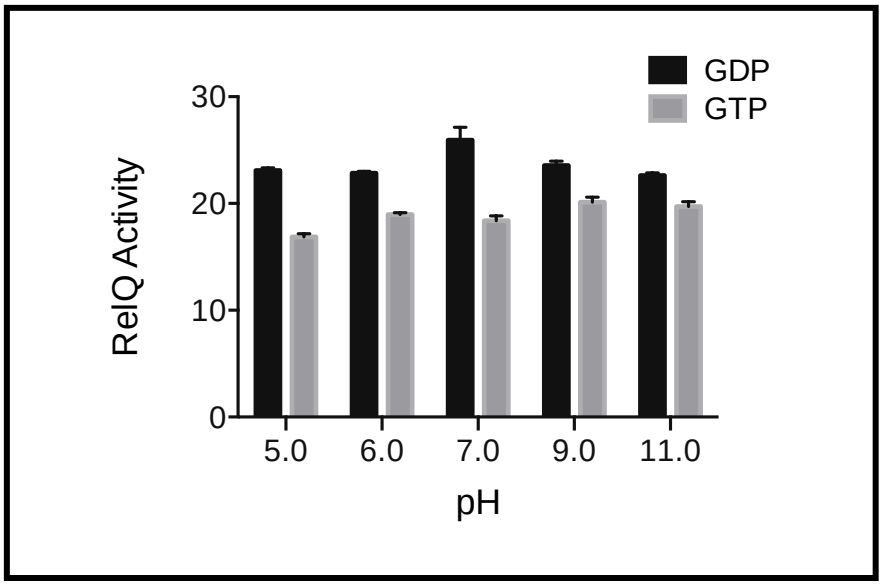

Figure 13. CdRelQ is insensitive to the reaction pH. Conversion of radioactive ATP to magic spot utilizing GDP and GTP substrate is not affected by medium pH**.**

Similarly, CdRelQ utilized all the tested divalent metal cofactors irrespective of their size (Appendix K) for its activity (Figure 14 A). However, BsRelQ activity does appear to be affected on the basis of ionic size (Figure 14 B). We have previously reported that CdRSH is capable of utilizing multiple structurally diverse divalent cations as cofactors with little to no loss of efficacy

compared to magnesium.(106) This capability of both the clostridial synthetases to remain functional at varying pH and their utilization of different divalent cations for (pp)pGpp synthesis may offer survival advantage to *C. difficile* against host immune system during infection. Metal starvation can trigger the SR in some bacteria(123,124) and the mammalian immune system inhibits pathogen growth by limiting metal availability by a so-called host driven 'nutritional immunity'.(125,126) Clostridial synthetases utilization of diverse divalent metal cations could be an adaptation against the host immune response.(105)

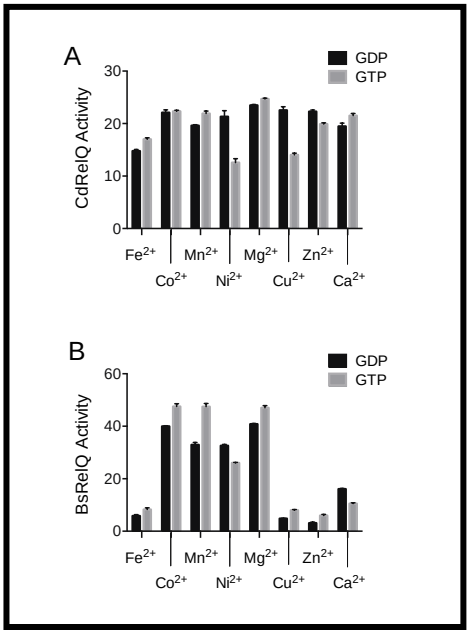

Figure 14. CdRelQ utilizes diverse divalent metal ion cofactors. Pyrophosphotransfer after 60 minutes from γ-^{32}P-ATP to 500 μM of the indicated GXP phosphoacceptor by (A) 2.0 μM CdRelQ or (B) 3.0 μM BsRelQ in the presence of 5.0 mM of the indicated metal ion cofactor. Adapted from Poudel *et al.* 2021.(105)

DISCUSSION

Though the stringent response is a highly conserved regulatory stress reaction exhibited by bacteria the mechanisms by which it induces cellular responses vary among bacterial species. The Gram- positive Firmicutes deviate in many ways from the template established by studies in Gamma -proteobacteria such as *E. coli*. Notably, *E. coli* does not encode SAS enzymes and does not appear to use (p)ppGpp for non-SR regulation of guanosine homeostasis. In this project we explored the biochemistry of the clostridial SAs RelQ. Despite the high sequence conservation between RelQ and SAS from other organisms, our results were not entirely as expected.(105)

We observed that the two clostridial magic spot synthetases enzymes exhibit characteristics that appear to be unique to *C. difficile*. Both the synthetases produced pGpp exclusively utilizing GDP or GTP via hydrolysis of 5' β phosphate bonds. While some SAS enzymes can directly synthesize pGpp using GMP as a substrate, there is little precedent for a synthetase to produce the triphosphate signal using GDP or GTP as substrates.(85,103,104,127-129) There are no known examples of an organism that produces pGpp exclusively. Direct synthesis of pGpp via hydrolysis of GDP or GTP 5' beta phosphate bonds has only been reported as a minor *in vitro* activity of *E. coli* RSH, dependent on the presence of an EKDD motif in the synthetase active site.(98) To date, every organism that synthesizes pGpp directly or indirectly also synthesizes ppGpp and pppGpp.(85,127-130) Utilization of GDP and GTP to exclusively synthesize pGpp by both a RSH and a SAS enzyme has not previously been reported. While it is still possible that RelC synthesizes the longer forms of magic spot despite its non-conserved guanosine binding motif, the dependence of CdRSH and CdRelQ on guanosine β-phosphate bond hydrolysis indicates that pGpp is a very important, and possibly the only, clostridial alarmone. It is also unusual that CdRelQ exhibits a higher affinity for GTP than GDP. The only obvious divergence between CdRelQ and

characterized SAS with substrate preferences for GDP is the presence of a glycine in the first position of the GXP binding motif, which is a polar charged residue in all other SAS homologs except *C. glutamicum* RelS, which has a valine at that position and preferentially utilizes GTP (Figure 3). Previous work in RSH enzymes has posited that an acidic EXDD sequence at the beginning of the guanosine binding motif results in a preference for GDP while a basic RXKD sequence correlates to a preference for GTP.(98) This association does not appear to hold in SAS enzymes, several of which have a basic motif and prefer GDP (Figure 3). However, it is likely that this position does contribute to the enzyme's ability to utilize GDP or GTP. Future mutational analysis will likely be necessary to determine what residues play a role in guanosine β-phosphate bond hydrolysis.(105)

Besides the unexpected triphosphate alarmone product, the characterized clostridial synthetases share another trait that does not appear to be widespread among RSH or SAS family enzymes: a remarkable ability to utilize structurally diverse divalent cation cofactors. While few other synthetases have been tested against a panel of divalent cations, cobalt, zinc, copper, nickel, iron, and calcium do not allow synthetase activity by *M. tuberculosis* Rel and manganese, nickel, and calcium reduce or abolish synthetase activity by *M. exotorquens* Rel.(131,132) Zinc, but not iron or nickel, stimulates enzymatic activity of crystalized RelP from *S. aureus*.(117) There does not appear to be any precedent for the extremely broad range of metals successfully utilized as cofactors by both clostridial synthetases.(106) This could be a *C. difficile* adaptation to so-called 'nutritional immunity,' which is the ability of mammalian immune systems to chelate and sequester metal ions that are limiting factors for the growth of foreign pathogens.(126,133) As metal starvation can trigger the stringent response in some bacteria,(123,134) it is possible that

promiscuous utilization of divalent cations in the enzymes that initiate the clostridial stringent response could provide a survival advantage during infection.(105)

It has been clear for some time that Gram negative *E. coli* is not a suitable model for the Gram-positive stringent response. It appears that even other Firmicutes are not complete models of this pathway in *C. difficile.* Given the role of the stringent response in antibiotic tolerance and virulence, there is interest in inhibiting it as an antimicrobial strategy.(135-138) However, the ubiquity of this signaling pathway among bacteria means that synthetase inhibitors are likely to exhibit a broad spectrum of action which could diminish the protective effect of the gut microbiota. However, the discovery that the stringent response in this organism is mediated by synthetases whose enzymatic product and metal utilization is conserved with each other but different from that of their homologs in other bacterial species raises the possibility that the clostridial enzymes share structural features that distinguish them from synthetases in other organisms. Further characterization of the clostridial synthetase enzymes may provide a foundation for targeted inhibition of the stringent response in this organism, which could be applied as an adjuvant to antibiotic therapy to diminish *C. difficile* antibiotic survival.(105)

SUMMARY

We characterized *C. difficile's* small alarmone synthetase, RelQ and confirmed that CdRelQ is a pyrophospho transfer synthetase and exhibits *in vitro* activity. It utilizes both GDP and GTP as phosphoacceptors and has higher affinity for GTP and its activity did not get compromised at varying pH conditions. In addition, it utilized diverse divalent cations for it synthetic activity. We also discovered that both the clostridial synthetases hydrolyze GDP/GTP independently for their activity and uniquely synthesize pGpp exclusively. To the best of our

knowledge, it is the first reported organism synthesizing only pGpp as its magic spot in the fifty years history of magic spot synthesis. Our study demonstrated that *C. difficile* synthetases activity significantly differs from that of their homologous counterparts which would provide a basis in designing targeted inhibitors against these enzymes. Further, mutational analysis is needed for a clear understanding on why and how the clostridial synthetases hydrolyze GDP/GTP for their synthetic activity.

CHAPTER III

ENVIRONMENTAL CUES TRIGGERING STRINGENT RESPONSE IN *C. DIFFICILE*

PREFACE

The contents of this chapter were published in Journal of Bacteriology in September 2020 and in bioRxiv in August 2021. Reprinted with permission from Pokhrel, A., Poudel, A., Castro, K. B., Celestine, M. J., Oludiran, A., Rinehold, A. J., Resek, A. M., Mhanna, M. A., and Purcell, E. B. (2020) The (p)ppGpp Synthetase RSH Mediates Stationary-Phase Onset and Antibiotic Stress Survival in Clostridioides difficile. *Journal of bacteriology* **202**, e00377-00320 and Poudel, A., Pokhrel, A., Oludiran, A., Coronado, E. J., Alleyne, K., Gilfus, M. M., Gurung, R. K., Adhikari, S. B., and Purcell, E. B. (2021) Unique features of magic spot metabolism in *Clostridioides difficile*. *bioRxiv*, 2021.2008.2002.454818

INTRODUCTION

Since the discovery of the SR, researchers have been interested in elucidating the potential environmental signals that triggers the stress response pathway. Bacteria encounter diverse range of environmental stresses during their life cycle that should trigger the stringent response. (77) Several studies have demonstrated that diverse extracellular stresses including amino acid starvation, alkaline shock, cell wall stress from cell wall active antibiotics, heat stress, oxidative stress and acid stress can trigger the SR.(77,139-141) During the process the intracellular pool of (p)ppGpp is affected simply by modulating the transcription of either RSH or SAS genes.(77) As described in chapter I, the SR has significant contribution in regulating several bacterial

physiology including bacterial growth, virulence, antimicrobial peptide survival, oxidative stress resistance, antibiotic tolerance and persistence.(75,78,88,108,123,127,133,140,142-149) However, there are variations in its regulation among different bacterial species under various environmental conditions.(77) Increased expression of RSH is the predominant response to nutrient limitation in many species.(150) In addition, RSH is also reported to be involved in response to heat stress in *Bacillus subtilis*.(139) Two common SAS found in both *Bacillus subtilis* and *Staphylococcus aureus*, RelQ and RelP, are differentially transcribed; RelP is transcribed during early stationary phase in response to stresses from cell wall active antibiotics, high salt, acidic or alkaline shock and ethanol treatment, while RelQ is primarily transcribed during logarithmic growth phase in response to abrupt nutrients limitation.(79,151) Moreover, there are reports demonstrating the role of these small alarmone synthetases in regulating guanosine homeostasis in order to mediate persistence.(127) In addition to their role in stringent response, small alarmone synthetases are involved in maintaining (p)ppGpp basal level in *Bacillus subtilis* and *E. faecalis*.(97,152)

C. difficile must cope with stresses from dynamic and hostile gastrointestinal tract environment to establish symptomatic infection. Very little is known about the survival of *C. difficile* in diverse extracellular stresses. We hypothesized that (pp)pGpp signaling and the SR could enable *C. difficle* survival under the stress of different categories of antibiotics as well as immune and oxidative stresses. We constructed fluorescent transcriptional reporter strains utilizing an oxygen independent flavoprotein phiLOV2.1 to study the transcriptional regulation of *C. difficle* stringent response genes, *rsh* and *relQ*. Previously we have identified that antibiotics, clindamycin and metronidazole, trigger the expression of both the *relQ* and *rsh* in strain specific manner in *C. difficile*.(106) Clindamycin is a broad spectrum antibiotic whose use is highly

correlated with CDI(153) and metronidazole is one of the drugs being used against CDI whose efficacy is decreasing these days.(154) We further wanted to extend the study and identify other potential stresses triggering the expression of these genes. Furthermore, identifying the stress inducing environmental cues would help in designing alternative therapies for CDI treatment which would target the enzymes responsible for SR and interfere with *C. difficile* antibiotic survival mechanisms. The work presented in this study will provide valuable insights into regulation of the SR in *C. difficile*.

MATERIALS AND METHODS

Construction of transcriptional reporters

The plasmid pRF185::phiLOV2.1 (provided by Gillian Douce, University of Glasgow), containing the *phiLOV2.1* gene under the control of the tetracycline-inducible promoter P_{tet},(155) was digested with BamHI and KpnI to remove the original promoter. The predicted promoters upstream of *rsh* (*CD630_27440* and *CDR20291_2633*) and *relQ* (*CD630_03450* and *CDR20291_0350)* were amplified from 630Δ*erm* and R20291 genomic DNA using the promoter specific forward and reverse primers (Appendix B). P_{rsh} (*rsh* promoter) was amplified separately from 630Δ*erm* and R20291 genomic DNA, while P_{relQ} (*relQ* promoter), which is identical between the two strains, was amplified from 630Δ*erm*. The primers introduced cut sites for BamHI and KpnI, which were used to digest the amplified promoters. The promoters were ligated into the digested pRF185_*phiLOV2.1* plasmid to yield $P_{rsh630\Delta erm}$::*phiLOV2.1*, $P_{rshR20291}$::*phiLOV2.1*, and $P_{relQ630\Delta erm}$::*phiLOV2.1* (Appendix A). The plasmids were subsequently PCR verified for promoter insertion using vector-specific as well as promoter-specific primers. The reporter plasmids were then individually transformed into competent *E. coli* HB101 cells (NEB) carrying the helper plasmid pRK24.(156) HB101 carrying pRK24 and the reporter plasmids were mated with *C.*

difficile 630Δ*erm* and R20291 strains as previously described.(156) $P_{rsh630\Delta erm}$::*phiLOV2.1* and $P_{rshR20291}$::*phiLOV2.1* were mated into their isogenic background strains and $P_{relQ630\Delta erm}$::*phiLOV2.1* was mated into both *C. difficile* strains. Transconjugants were selected on BHIS agar supplemented with 10 μg/mL thaimphenicol and 100 μg/mL kanamycin. Finally, transconjugants were verified by PCR using both promoter-specific and *phiLOV2.12.1*-specific primers.(106)

***In vivo* promoter activity analysis using fluorescent phiLOV reporter strains**

The *in vivo* promoter activity to identify potential signals for triggering SR was studied by exposing the reporter strains to sublethal concentration of diverse stresses as previously described.(106) Briefly, saturated starter cultures of *C. difficile* strains containing the phiLOV2.1 reporter plasmid were grown anaerobically at 37°C in BHIS-Tm10 for 12 to 16 hours and inoculated 1:50 into fresh BHIS-Tm10 containing indicated treatments (8.0μg/mL ampicillin, 0.3μg/mL metronidazole (VWR), 16μg/mL clindamycin1.70 μg/mL vancomycin (VWR), 0.67 μg/mL fidaxomicin (Cayman Chemical), 1.0 mM diamide (MP Biomedicals), 4.0 μM copper sulfate (Fisher Scientific), and grown for 2 hours at 37°C. To monitor temperature-induced promoter activity, log phase (OD_{600}: 0.50-0.70) cells of each of the strains were divided into two halves and incubated in parallel at 37°C and 41°C for 30 mins. pH induced promoter activity was measured by inoculating exponentially growing cells at 1:50 into BHIS-Tm10 containing 0.1M potassium phosphate buffer at pH 6.0, 7.0, 8.0 or 9.0. Similarly, osmotic pressure induced promoter activity was monitored by inoculating exponentially growing cells at 1:50 into BHIS-Tm10 containing 0.5M NaCl and incubating them for two hours. We also monitored the effect of metal starvation on promoter activity by inoculating exponentially growing cells into BHIS-Tm10 containing 2.0mM EDTA (Fischer Scientific). OD_{600} was recorded for each sample upon

collection. To minimize discrepancies in fluorescent signal from cellular autofluorescence, cell numbers in each sample were equalized on collection. Each sample was collected at a volume that would give a cell count equivalent to 3 mL of the culture with the lowest OD_{600}. After collection, cells were pelleted anaerobically in a microcentrifuge and suspended in 400 µL of anaerobic 1X phosphate buffered saline (PBS). Duplicate 200 µL samples were aliquoted into a clear-bottomed black 96-welled microplate (Thermo Fisher Scientific) and were removed from the anaerobic chamber to measure sample fluorescence intensity. Sample fluorescence using 440/30 excitation and 508/20 nm emission filters and sample OD_{630} were measured on a BrandTek plate reader. The instrumental parameters for all fluorescence measurements included a sensitivity limit of 65. Measurements were blanked against 1X PBS and were reported as E508/A630. Statistical analysis was performed using Prism (GraphPad).(105)

C. difficile growth during metal starvation

To assess the effect of metal starvation in *C. difficile* growth behavior, exponentially growing *C. difficile* R20291 cells were inoculated at 1:10 ratio in BHIS medium containing either 2mM EDTA, 2mM of EDTA plus $FeCl_2$ and $ZnCl_2$ or 1mM $FeCl_2$ and $ZnCl_2$. The cells were grown anaerobically for 24 hours while monitoring cell growth every one-hour. Cell growth was monitored by measuring the optical density at 600 nm using an Ultraspec 10 Biochrom cell density meter (Biochrom, Cambridge, United Kingdom). In another experiment, log phase cells at 1:10 ratio were inoculated into BHIS containing respective treatments as mentioned above and incubated for an hour. The cells were briefly centrifuged, and the pellet was resuspended in 1.0mL of fresh BHIS and serially diluted. 100uL of each of the cells were plated into BHIS from 10^{-3} and 10^{-5} dilution and the plates were incubated for 48hours, and visible colonies were enumerated. All

anaerobic bacterial culture took place at 37 °C in a Coy anaerobic chamber (Coy Laboratory Products, Grass Lake, MI) with an atmosphere of 85% N_2, 10% CO_2, 5% H_2.

RESULTS

C. difficile induces *rsh* and *relQ* transcription in response to antibiotic stress

We observed the increased expression of both *rsh* and *relQ* upon exposure to sublethal concentrations of clindamycin and metronidazole (Appendix G) in a strain specific manner (Figure 15 A & B).(106) The *rsh* promoter was unaffected by clindamycin in a laboratory strain, 630Δ*erm*(157) but showed a 50% increase in activity in R20291.(106) Conversely, the *relQ* promoter was upregulated 2.8-fold in 630Δ*erm* but was unaffected in R20291.(106) Upon the exposure to metronidazole, neither of the promoters got stimulated in 630Δ*erm* strain, however, activity from the *rsh* promoter increased 80% in R20291, while the *relQ* promoter showed no response.(106)

We further tested the promoter activity of both the genes when exposed to subinhibitory concentration of ampicillin, vancomycin and fidaxomicin (Appendix G). Ampicillin is one of the most commonly associated antibiotics for CDI.(13) Both vancomycin and fidaxomicin are currently recommended antibiotic treatments against severe CDI.(158-160) In the epidemic strain *C. difficile* R20291 promoter activity in the tetracycline-inducible control strain was unaffected by either antibiotic. Vancomycin had no effect on transcription from the *rsh* or *relQ* promoters. Fidaxomycin stimulated a 96% increase in P_{rsh} activity and a 3.1-fold increase in P*relQ* activity (Figure 16 A). In the laboratory strain *C. difficile* 630Δ*erm* , the P_{rsh} reporter had no response to either drug, while activity from the P_{relQ} reporter increased 3.6-fold upon exposure to vancomycin (Figure 16 B).(105) Ampicillin stimulated a twofold increase in activity of both the promoters in

C. difficile R20291 while their activity remains unaffected in the laboratory strain *C. difficile* 630Δ*erm* (Figure 17).

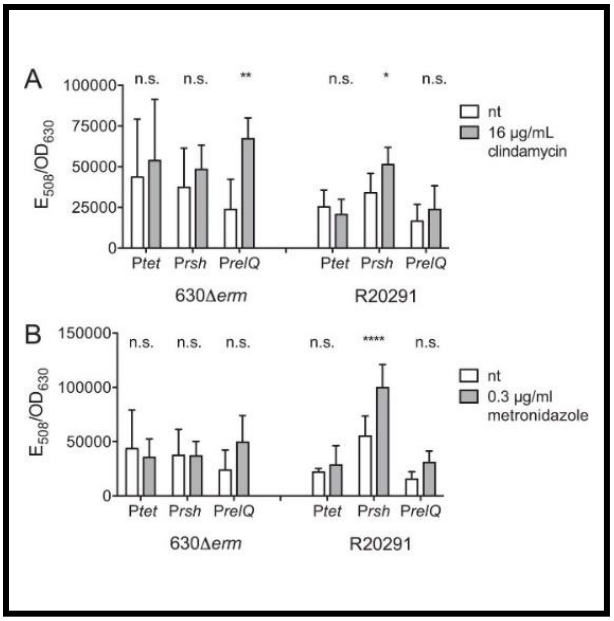

Figure 15. Antibiotic induced transcription of *rsh* and *relQ*. PhiLOV2.1 transcriptional reporter activity after two hours exposure to 16µg/mL of clindamycin (A) and 0.3µg/mL of metronidazole (B) in *C. difficile* 630Δerm and R20291 strains. Adapted from Pokhrel *et al.* 2020.(106)

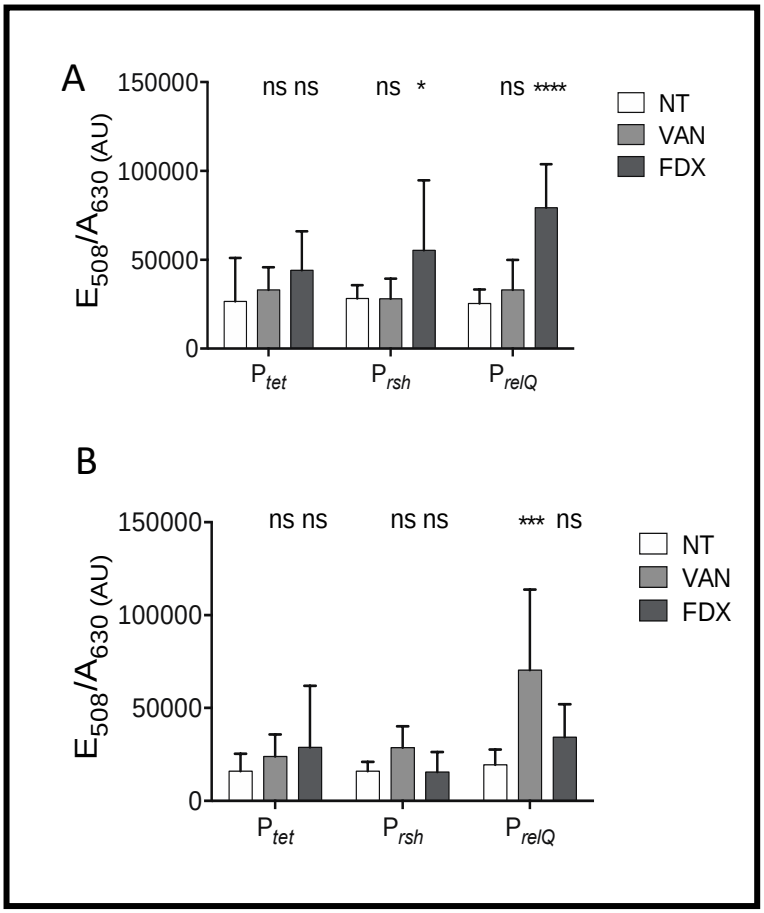

Figure 16. PhiLOV fluorescence normalized to cell density after two hours exposure to 1.7µg/mL vancomycin (VAN) or 0.67µg/mL fidaxomicin (FDX) in *C. difficile* R20291 (A) and 630Δerm (B) strains. Shown are the means and standard deviations of nine biologically independent samples. Conditions treated with antibiotics are compared to untreated by two-way ANOVA. **** $p < 0.0001$, * $p < 0.05$, ns not significant. Adapted from Poudel *et al.* 2021.(105)

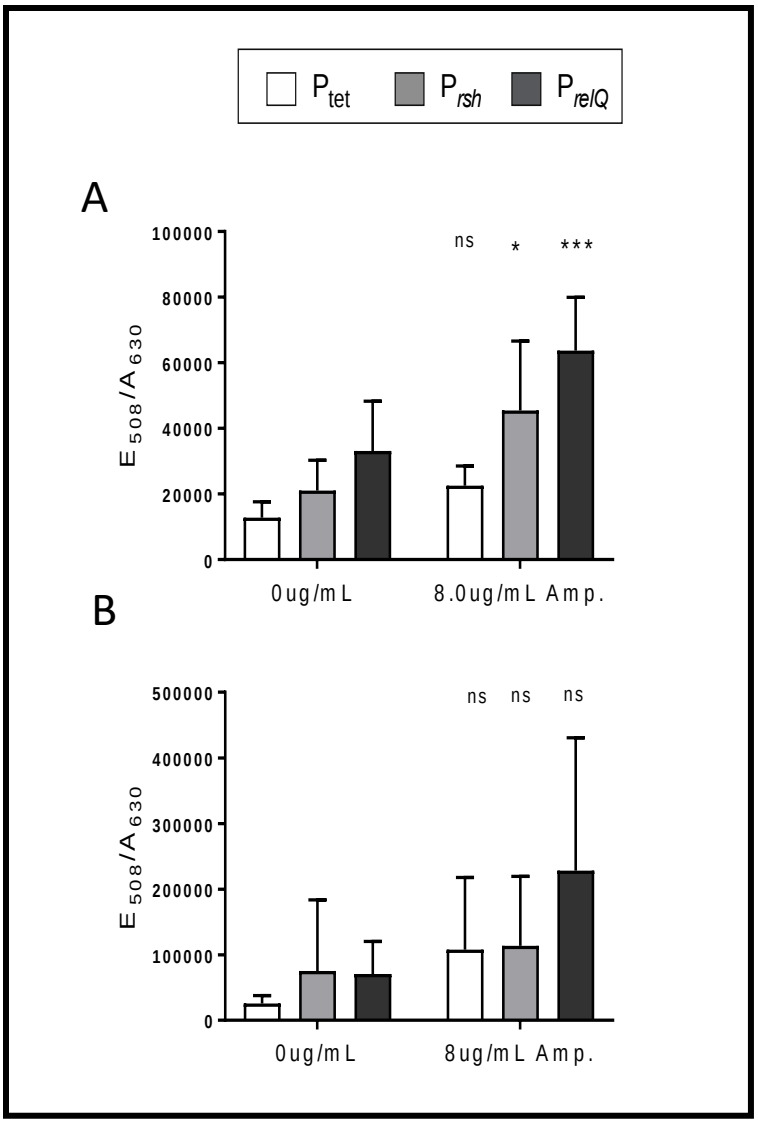

Figure 17. Ampicillin induced transcription of *rsh* and *relQ* genes. PhiLOV2.1 transcriptional reporter activity after two hours exposure to 8.0µg/mL of ampicillin in *C. difficile* R20291 (A) and 630Δerm (B) strains. Shown are the means and standard deviations of nine (A) and six (B) biologically independent samples. Conditions treated with antibiotics are compared to untreated by two-way ANOVA. **** $p < 0.0001$, * $p < 0.05$, ns not significant.

rsh and *relQ* transcription during oxidative, heat, pH and osmotic stress

C. difficile must survive multiple environmental stresses and host defenses in order to colonize the gastrointestinal tract. To assess the potential role of (pp)pGpp signaling and the stringent response in *C. difficile* survival of environmental stress, we monitored *rsh* and *relQ* promoter activity in *C. difficile* R20291 under conditions mimicking potential stressors *in vivo*. *C. difficile* cells were exposed to 41°C to mimic the febrile temperature, however we did not observe any distinguishable activity from the promoters of both the genes suggesting that even high fever within a mammalian host does not activate transcription of (pp)pGpp synthetase genes (Figure 18 A). We employed inhibitory concentrations of copper and diamide (Appendix H) to mimic acute oxidative stress in *C. difficile* cells. We have previously reported that exposure to 4 μM copper, a transition metal that causes oxidative stress in bacteria by generating reactive oxygen species, is sufficient to prevent overnight growth of *C. difficile*.(161) Similarly, diamide mimics oxidative stress in anaerobes by instigating disulfide bonds.(162) Three hours of exposure to copper did not stimulate increased activity from the *rsh* or *relQ* promoters; *rsh* promoter activity was actually somewhat decreased after copper treatment (Figure 19 A). Treatment with diamide stimulated a 3.8-fold increase in *rsh* promoter activity but had no effect on the *relQ* promoter (Figure 19 B). In addition, when *C. difficile* cells were transferred to media buffered at varying pH conditions, we observe the increased activity of P_{rsh} at pH 6 only. Its activity got stimulated by 3.6-fold (Figure 20). Notably, when we measured the pH of spent BHIS after 24 hours of *C. difficile* growth, we found that R20291 acidifies its growth medium to pH 6. Medium acidification by 630Δ*erm* is less pronounced (Table 4).(105) We did not observe any significant stimulation of either of the promoters upon osmotic stress exerted when *C. difficile* cells were treated with subinhibitory concentration (Appendix I) of NaCl (Figure 18 B).

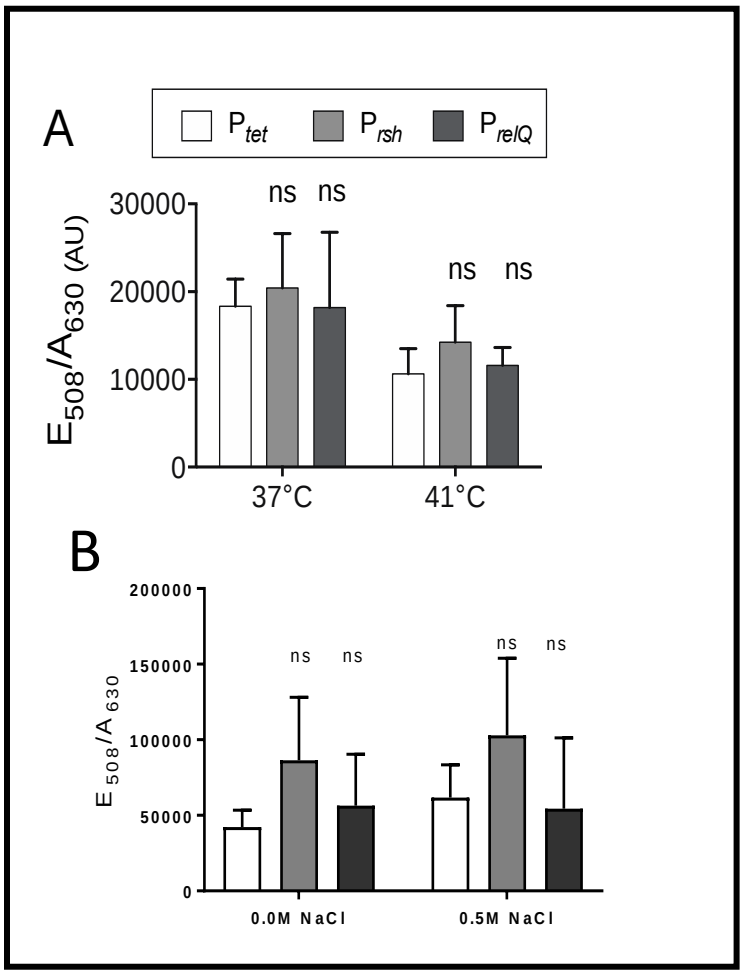

Figure 18. Transcriptional response of *rsh* and *relQ* genes to temperature and osmotic stresses in *C. difficile* R20291. (A) PhiLOV fluorescence normalized to cell density after 30 minutes of incubation at the indicated temperature. Shown are the means and standard deviations of six biologically independent samples. (B) PhiLOV fluorescence normalized to cell density after two hours of exposure to the indicated concentration of NaCl. Shown are the means and standard deviations of six biologically independent samples. Activity from the P*rsh* and P*relQ* promoters was compared to that from the P*tet* promoter in the same condition by two-way ANOVA. * $p < 0.05$, ** $p < 0.01$, ns not significant. Adapted from Poudel *et al.* 2021.(105)

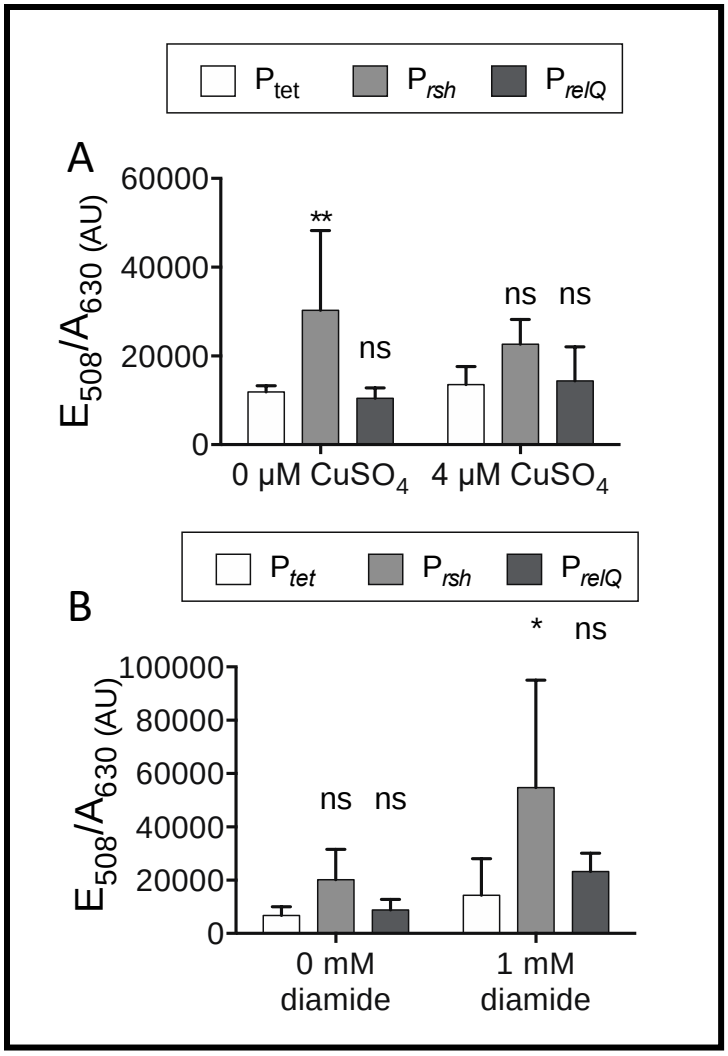

Figure 19. Transcriptional response of (pp)pGpp synthetase genes to oxidative stress in *C. difficile* R20291. (A) PhiLOV fluorescence normalized to cell density after two hours of exposure to the indicated concentration of copper sulfate. Shown are the means and standard deviations of six biologically independent samples. (B) PhiLOV fluorescence normalized to cell density after three hours of exposure to the indicated concentration of diamide. Shown are the means and standard deviations of three biologically independent samples. Activity from the P*rsh* and P*relQ* promoters was compared to that from the P*tet* promoter in the same condition by two-way ANOVA. * $p < 0.05$, ** $p < 0.01$, ns not significant. Adapted from Poudel *et al.* 2021.(105)

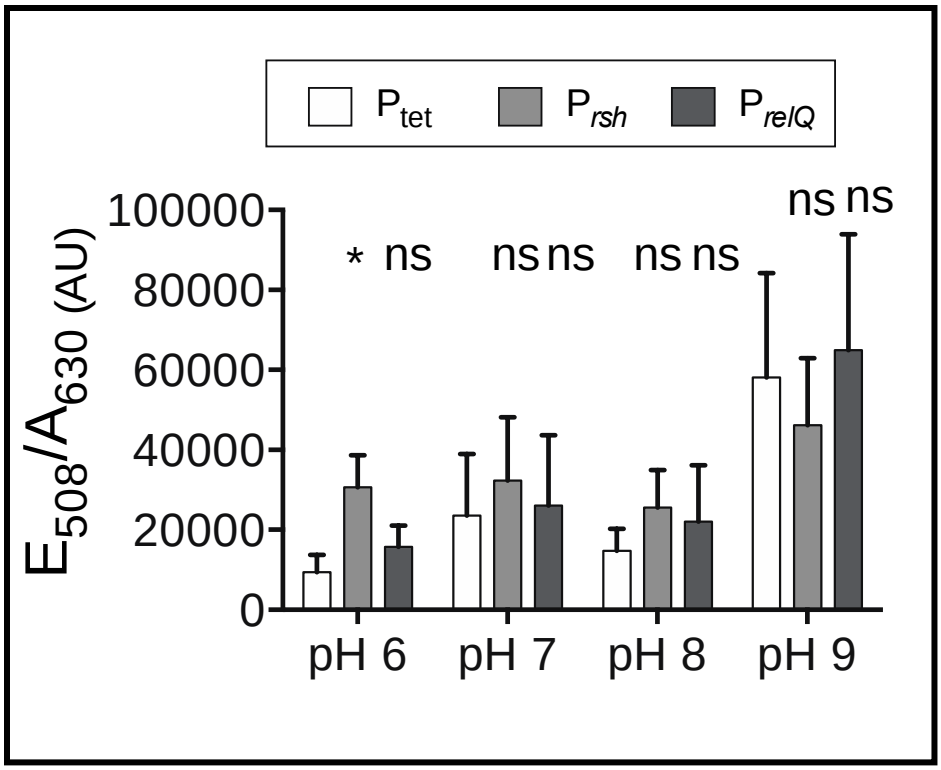

Figure 20. Transcriptional response of (pp)pGpp synthetase genes to varying pH in *C. difficile* R20291 PhiLOV fluorescence normalized to cell density three hours after transfer from unbuffered BHIS to BHIS buffered at the indicated pH with potassium phosphate buffer. Activity from the P*rsh* and P*relQ* promoters was compared to that from the P*tet* promoter in the same condition by two-way ANOVA. * $p < 0.05$, ** $p < 0.01$, ns not significant. Adapted from Poudel *et al.* 2021.(105)

Table 5: Medium acidification by *C. difficile* strains after 24 hours of growth. pH of growth medium was measured before and 24 hours after inoculation with single colonies. Adapted from Poudel *et al.* 2021.(105)

C. difficile strain	pH	
	Fresh BHIS	24 h spent BHIS
R20291	7.44	6.06
630Δerm	7.44	6.94

Metal starvation inhibits *C. difficile* growth and induces transcription of *rsh*

Transition metals are critical components of all forms of life. They are required as cofactors and structural components for many proteins, and their concentration within cells is precisely regulated to avoid both deficiency and toxicity.(163) Approximately 60% of known enzymes contain at least one metal cofactor, among which zinc is the most common enzyme associated transition metal ion followed by iron and manganese.(163) Mammalian immune system chelates and sequester metal ions in a process known as 'nutritional immunity'.(164,165) EDTA metal chelation mimics 'nutritional immunity'. We monitored *rsh* and *relQ* promoter activity in *C. difficile* R20291 under conditions mimicking host 'nutritional immunity'. One hour exposure of the cells to subinhibitory concentration of EDTA (Appendix J) stimulated a 2-fold increase in Prsh promoter activity (Figure 21) suggesting metal starvation induces the SR in *C. difficile*. Promoter activity was not distinguishable when ETDA was neutralized with the addition of a total of equimolar concentration of zinc and ferric chloride (Figure 21). To investigate the growth performance of *C. difficile,* R20291 during metal starvation, we did growth curve assays in BHIS medium supplemented with EDTA. *C. difficile*

growth was significantly inhibited in metal starved growth medium however when 2mM of zinc and ferrous chloride were added along with 2mM of EDTA, the growth remains unaffected as expected (Figure 22 A). We also measured the colony forming units from each of the EDTA treated and non-treated samples along with the samples where EDTA was neutralized with supplementation of metal ions. The CFU in EDTA treated samples was significantly lower in comparison to non-treated and the others indicating the subinhibitory concentration of EDTA was enough to exert stress to the cells (Figure 22 B).

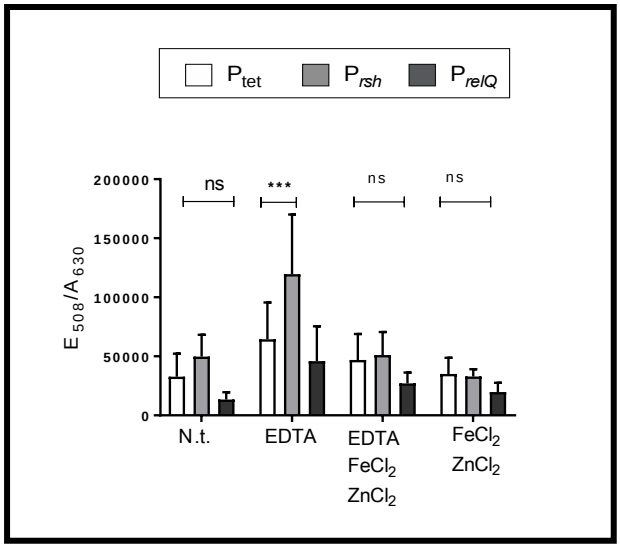

Figure 21. Transcriptional response of (pp)pGpp synthetase genes to metal starvation in *C. difficile* R20291. PhiLOV fluorescence normalized to cell density after one hour of exposure to the 2mM EDTA, 2mM EDTA + 1mM ($FeCl_2$ + $ZnCl_2$) and 1mM ($FeCl_2$ + $ZnCl_2$). Shown are the means and standard deviations of six biologically independent samples. Activity from the P*rsh* and P*relQ* promoters was compared to that from the P*tet* promoter in the same condition by two-way ANOVA. * $p < 0.05$, ** $p < 0.01$, ns not significant.

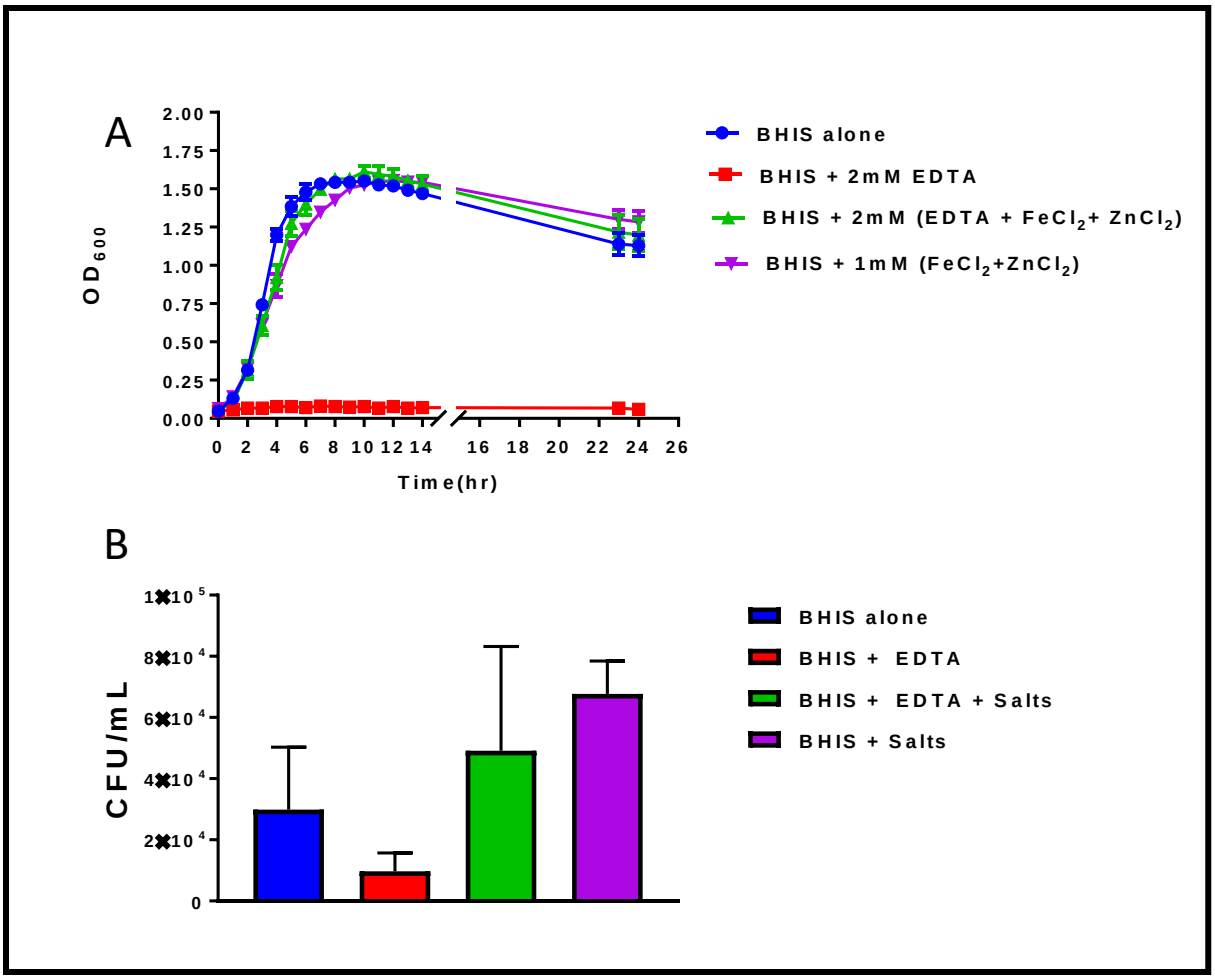

Figure 22. Metal starvation inhibits *C. difficile* R20291 growth. (A) Growth curves at the indicated conditions. (B) CFU after one hour of exposure of cells at the indicated conditions. Shown are the data from three biologically independent samples.

DISCUSSION

In many bacterial species, the stringent response genes are transcriptionally regulated upon the exposure to stressful environmental conditions such as amino acid starvation, alkaline shock, cell wall stress from cell wall active antibiotics, heat stress, oxidative stress, and acid stress.(77,88,139-142) However, the role of the SR in the survival of *C. difficile* against extracellular stresses has not been explored much. In this project we attempted to determine potential environmental signals that induce the SR in *C. difficile*. For this we monitored the activity of promoters of two clostridial stringent response genes, *rsh* and *relQ* using transcriptional reporter strains. Using these tools, we have previously demonstrated that exposure to certain antibiotics stimulates transcription of clostridial stringent response genes in strain specific manner.(106) The historical laboratory 630Δ*erm* strain and the epidemic R20291 strain exhibit different transcriptional responses to antibiotics. In R20291, *rsh* transcription is increased in response to clindamycin and metronidazole while the historical strain does not have a transcriptional response to metronidazole and induces transcription of *relQ* rather than *rsh* upon exposure to clindamycin (Figure 13). Here we confirm that antibiotic stress stimulates transcription of clostridial stringent response genes although the details of the response are strain specific; *relQ* responds to fidaxomicin but not vancomycin in R20291 and to vancomycin but not fidaxomicin in 630Δ*erm*. Similarly, ampicillin, one of the most common drugs associated with CDI, induce the increased transcription of both the genes only in the epidemic R20291 strain. It is tempting to speculate that strain-specific induction of magic spot synthetase genes may contribute to observed differences in antibiotic tolerance among *C. difficile* strains, although this will need to be verified by testing in more clinical strains before a conclusion can be drawn. We have previously found that transcription of *rsh* but not *relQ* is induced by stationary phase onset. Here we report that *rsh* but

not *relQ* are upregulated by oxidative and acid stress in *C. difficile* R20291. It is possible that RSH is the primary mediator of a stress-induced stringent response in this organism and that the primary role of RelQ is regulation of nucleotide metabolism as has been reported in *B. subtilis* and *E. faecalis*.(97,152) Interestingly, our finding that medium acidification caused by stationary phase onset in R20291 is sufficient to induce *rsh* transcription in nutrient-rich fresh growth medium suggests that medium acidification due to metabolic activity may be one of the signals that regulate the expression of stationary phase genes in this organism.

Metal starvation can have detrimental effects on bacterial cell viability. It can trigger the SR in some bacteria and the mammalian immune system inhibits pathogen growth by limiting metal availability.(123,134) In this report, we demonstrated that metal depletion has detrimental effect on *C. difficile* growth however addition of iron and zinc in the medium restored the normal growth pattern. Iron and zinc are vital nutrients for virtually all forms of life.(164) Like in other organisms, we observed that metal starvation induced the increased transcription of *rsh* in *C. difficile* R20291. Taken together, we speculate that immune-mediated metal deprivation could trigger the SR in *C. difficile* and that the promiscuous utilization of diverse divalent metal cations by clostridial synthetases as described in chapter II could provide a survival advantage against such host driven ‘nutritional immunity’.

SUMMARY

Our results indicated that the SR in *C. difficile* is induced via several environmental factors in strain specific manner. We observed multiple classes of antibiotics trigger the expression of both the genes, *relQ* and *rsh*, responsible for SR. Acute oxidative stress and metal starvation like that from the immune system induces *rsh* expression in the R20291 strain. Similarly, acidic

environments stimulated the expression of *rsh* which indicates the high cell density and exhausted environment. However, we did not observe expression of either stringent response gene upon exposure to febrile-like temperature or from osmotic pressure. Previously, we have observed that the translational inhibition of *rsh* gene resulted into a pronounced effect on bacterial antibiotic susceptibility demonstrating the role of SR in *C. difficile* antibiotic survival.(106) Further gene knock out study will be needed to establish the direct role of SR in *C. difficile* survival under diverse stress conditions.

CHAPTER IV

EFFECT OF NANOSECOND PULSES ON VIABILITY OF *CUTIBACTERIUM ACNES*

PREFACE

The content of this chapter was published in Bioelectrochemistry in August 2021. Reprinted with permission from Poudel, Asia; Oludiran, Adenrele; Sözer, Esin B.; Casciola, Maura; Purcell, Erin B; Muratori, Claudia (2021) Growth in a biofilm sensitizes *Cutibacterium acnes* to nanosecond pulsed electric fields. Bioelectrochemistry **140**: 107797.

INTRODUCTION

Cutibacterium acnes (*C. acnes*) is an opportunistic pathogen whose overgrowth and dominance within the dermal microbiome contributes to the pathophysiology of the skin disease acne vulgaris.(166,167) Acne vulgaris is an inflammatory disease that involves the interplay of four main factors: pathological overproduction of sebum, abnormal follicular keratinization, colonization of the pilosebaceous duct by *C. acnes* colonies and biofilms, and inflammation.(168) Current therapeutics for acne treatment involves both topical and systemic applications of vitamin A derived retinoids and antibiotics.(53,65,66) However, the use of retinoids is associated with a range of cutaneous side-effects such as scaling, erythema, dryness, and irritation.(65) Similarly, the use of antibiotics has been associated with alternation of the skin microbiota composition resulting into treatment failure and emergence of antibiotic resistance.(53)

In the present study we aimed to measure the efficacy of nanosecond pulsed electric fields (nsPEF), a new promising cell and tissue ablation technology, to compromise *C. acnes* growth.

The ability of pulsed electric fields (PEF) to inactivate microorganisms in liquid foods and wastewater has been well documented.(169-171) Conventional PEF treatments employ a process referred as electroporation where pulses of millisecond or microsecond duration are applied to compromise the integrity of the cell plasma membrane. Electroporation can be reversible or irreversible based on the pulse parameters. Reversible electroporation results into the formation of pores in the cell membrane which can reseal after a specific time, while irreversible electroporation does permanent damage leading to cell death. nsPEF utilizes much shorter pulses (down to 10 ns) and higher electric field than conventional PEF, to target not only the plasma membrane but also intracellular structures.(172-174). Exposure of cell membranes to nsPEF leads to membrane charging and disrupt the membrane by electromechanical compression resulting into pore formation and membrane rupture.(175,176) When exposed to a strong electric field, a cell becomes polarized due to relocation of ions, and this realignment of charges across the cell creates electrostatic attraction which compresses the cell and its membrane.(176,177) As the electric fields intensifies, both the electromechanical compression and polarization reach a breaking point leading to membrane disruption.(177) nsPEF has been extensively utilized in *in vitro* killing of eukaryotic cells with successful tumor ablation trials in animals and in humans without recurrence and with minimal side effects.(178-182)

Recently there are reports on the effect of nsPEF on bacterial cell viability. However, these studies used different pulse parameters, exposure solutions and methods, suggesting the importance of these factors for bacterial inactivation.(70,71,183,184) In this project we aimed to study the effect of physical stress imparted by nanosecond pulsed electric fields (nsPEF) in the growth of *C. acnes*. The work presented in this study evaluates the potential application of nsPEF as an alternative strategy for the inactivation of *C. acnes*.

MATERIALS AND METHODS

Bacterial strains and growth conditions

The bacterial strain used in this study is *C. acnes* ATCC 29,399 (American Type Culture Collection, Manassass VA). All anaerobic bacterial culture took place at 37 °C in a Coy anaerobic chamber (Coy Laboratory Products, Grass Lake, MI) with an atmosphere of 85% N_2, 10% CO_2, 5% H_2. Cell growth was monitored by measuring the optical density at 600 nm using an Ultraspec 10 Biochrom cell density meter (Biochrom, Cambridge, United Kingdom) for up to 3 days. All plastic consumables were allowed to equilibrate in the anaerobic chamber for a minimum of 72 hours prior to use. Unless otherwise noted, all reagents and supplies were purchased from Fisher Scientific (Fisher Scientific, Waltham MA).(107)

C. acnes is a slowly growing bacterium and difficult to cultivate in laboratory conditions.(185) Since there is no established standard *in vitro* growth protocol, we tested different growth media to establish optimal laboratory growth conditions. Bacterial cultures were grown in TY medium containing 3% peptone, 2% yeast extract and 0.1% sodium thioglycolate and colonies were maintained on TY plates with 3% agar. To avoid contamination, liquid TY media was supplemented with 20 μg/ml of metronidazole (TY-Met) (Beantown Chemical, Hudson NH). Other culture media utilized in this study are 2.5% Brain-Heart Infusion supplemented with 0.5% Bacto-BD yeast extract (BHIS) and 3% agar, chocolate agar plates (Thomas Scientific, Swedesboro NJ), and anaerobic blood agar plates (Thomas Scientific, Swedesboro NJ).(107)

C. acnes biofilm were grown for 72 hours in plastic 24 well plates, either directly on the plate wells bottoms or on glass coverslips. Growth surfaces were coated with 100 μl of 0.1% fibronectin (Thomas Scientific, Swedesboro NJ), poly-D-lysine (Millipore Sigma, Burlington

MA), or poly-L-lysine (Thomas Scientific, Swedesboro NJ) and dried for 4 hours before equilibrating for another 72 hours in anaerobic chamber prior to usage. Exponentially growing *C. acnes* cultures at OD_{600} between 0.5 and 0.8 were diluted at 1:3 into fresh TY-Met media and 2 ml of the diluted culture were directly applied on to the plates which were further incubated for 72 hours for the biofilm formation. To visualize biofilm formation, liquid cultures were removed by pipetting and surfaces were washed with phosphate buffered saline (PBS) at pH 7.0. 0.1% crystal violet was applied for 30 min and washed twice with PBS.(107)

Nanosecond pulsed electric field (nsPEF) treatment

C. acnes samples were prepared by inoculating single colonies into 3 mL of TY-Met medium and growing for 48 h at 37 °C. Starter cultures were diluted 1:10 into TY-Met medium to reach OD_{600} = 0.5–0.8. One hundred microliter samples of this suspension were loaded into 1 mm gap electroporation cuvettes (BioSmith, San Diego, CA), which were closed, sealed with parafilm and brought outside of the anaerobic chamber for nsPEF treatments. In each experiment, samples were kept outside of the chamber for a maximum of 1 hour. Samples were exposed to either nsPEF or sham exposure in TY medium with a conductivity of 0.73 S/m at room temperature (22 ± 2 °C). Trapezoidal pulses of 280 ns duration (100 to 2000, 5 Hz, 28 kV/cm; 0.2–4 kJ/ml) were produced by a custom pulse generation system (Figure 23 A) with an adjustable pulse amplitude (up to 15 kV), duration (200 to 1000 ns) and frequency (1–100 Hz; Pulse Biosciences, Inc., Hayward, CA). The waveform of a 280 ns pulse, 28 kV/cm is reported in Figure 23 B.(107)

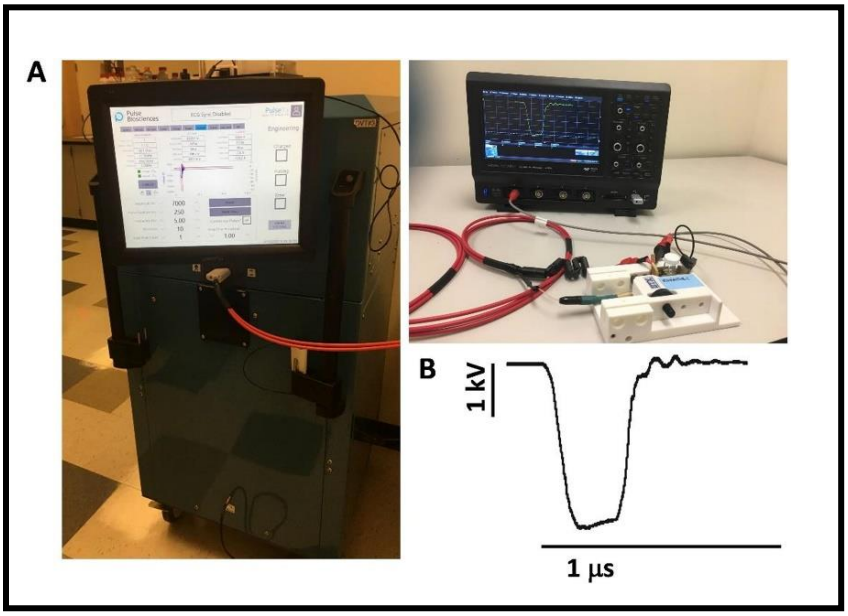

Figure 23. Pulsed electric field exposure system. (A) Trapezoidal pulses of 280 ns duration were produced by a custom pulse generation system and delivered to 1 mm electroporation cuvettes. A digital oscilloscope was used to monitor the pulse amplitude and shape at the cuvette. (B) The shape of a 280 ns, 28 kV/cm electric pulse. Adapted from Poudel *et al.* 2021.(107)

For nsPEF exposure of biofilms-derived cells, samples were harvested by scraping the biofilm from the growth surface. Cells were suspended in 1 ml TY medium and vortexed to disrupt clumps (186) before being aliquoted into electroporation cuvettes for the treatment described above. Samples from each experiment were diluted to the same optical density (OD600 = 0.5–0.8).

Exposure of intact biofilms was accomplished by growing C. acnes biofilms on glass coverslips with an indium tin oxide (ITO) conductive layer and placing these coverslips into 1 mm gap electroporation cuvettes filled with 100 µl of TY medium. The ITO layer was deposited on

one side of the glass coverslips by Diamond Coatings (Halesowen, UK). During nsPEF exposure, the glass surface of the coverslip was resting on the anode and the ITO surface with cells was facing the cathode. The electric field (E) distribution was calculated with Sim4Life light (ZMT ZurichMedTech AG, Zurich, Switzerland) in ohmic quasi-static conditions similarly to what was previously described.(187,188) Two parallel electrodes (20.55 × 12.00 × 1.58 mm3, perfect electric conductors) mimicking the electroporation cuvette were filled with medium (0.73 S/m). The coverslip was modeled as a dielectric cylinder of 8.2 mm diameter, 125 µm thickness with conductivity 0.0043 S/m and coated with a 25 µm think layer of ITO (1.3 MS/m). The coverslip was placed in contact with the anodic electrode with the ITO layer facing the cathode. A 50 × 50 × 50 mm3 cube of air surrounded the electroporation cuvette.(107)

In selected experiments, both planktonic cells and biofilm-derived cells were incubated anaerobically with lysozyme (1 to 10 mg/ml; MP Biomedicals, Santa Ana, CA) for 1 h at 37 °C prior to nsPEF treatment. Sample heating was measured using a thermocouple thermometer (Physitemp, Clifton, NJ).(107)

Determining effect of nsPEF on *C. acnes* viability

Immediately after treatment, both planktonic and biofilm bacteria samples were returned to the anaerobic chamber. Nine hundred microliter of TY medium was added to each cuvette mixed by pipetting. The resulting 1 ml samples were serially diluted to 10-5, 100 µl of each sample was plated on triplicate TY-Met plates and colonies were enumerated after 72 hours. Only counts between 0 and 300 CFU per plate were considered. Bacterial inactivation is expressed as log reduction of viable cells count calculated as log10 CFU/ml differences between sham and nsPEF

exposure samples. All experiments were performed in triplicates and repeated at least three times unless otherwise stated.(107)

Microscopical examination nsPEF effect on cell vaibility

The effect of nsPEF treatment on the cell's viability was visually assessed via fluorescence microscopy using propidium iodide (PI) as a fluorophore. PI poorly penetrates the intact cellular membrane, however upon the membrane breakage, it can easily enter the cytosol and binds the nucleic acids giving strong red fluorescence.(183) For propidium iodide (PI) microscopy experiment, *C. acnes* cells pellet from 1.0mL of two days old starter culture was resuspended in equal volume of TY media containing 10ug/mL of PI (Biotium). 100uL of the resuspended cells were aliquoted into each of the separate electroporation cuvettes for 1000nps and 2000nps treatment. The cells in the cuvettes were prepared and taken outside the anerobic chamber for the nsPEF treatment as mentioned above. The cells in the respective cuvettes were electric pulsed with respective nano second pulse and allowed to sit at room temperature for 15min and resuspended in 45.0mL of degassed TY media to achieve maximum dilution of PI. The cells were centrifuged at 500rpm for 10mins, and the pellet was resuspended in 1.5mL of TY media. The cells were then taken inside the anaerobic chamber where the cells were transferred into the respective rose chambers with the help of a syringe. A rose chamber is a special device designed in our lab to image anaerobic organism that consists of two glass cover slips fixed in two rubber gaskets in opposite sides which is further supported and screwed by metal covering for proper shielding.(189) The cells in the rose chamber are taken outside the anaerobic chamber and imaged using Nikon Ti-E inverted microscope equipped with apochromatic TIRF 60X oil immersion objective lens (N.A. 1.49), pco.edge 4.2 LT sCMOS camera, and SOLA SE II 365 Light Engine as well as complementary DIC components (Nikon Instruments Inc, Melville, NY, USA). The microscope

was maintained at 37°C using a home-built enclosure and a Nevtek Air Stream microscope stage warmer. Nikon Perfect Focus system was employed to eliminate focal drift during recordings.(190)The PI fluorescence was measured using 553nm and 650nm of excitation and emission filters respectively.

RESULTS

In vitro growth optimization of *C. acnes*

C. acnes is a slowly growing bacterium that exists in nature largely as biofilms due to which it has been difficult to cultivate clinical samples *in vitro*. The challenge of growing the bacterium in laboratory set up has led to underdiagnosis in different clinical specimens including implant devices or bone or joint infections. (191,192) There is no consistent reporting on its cultivation time and condition, however studies suggest prolonged cultivation time ranging from 7 to 14 days for its isolation and identification.(193,194) Reported doubling times *in vitro* are 5–6 hours, with liquid cultures reaching stationary phase in 3–4 days (50) Such prolonged cultivation increases the risk of laboratory contamination (195,196) In our initial experiments we attempted to establish optimal laboratory growth conditions for the planed experiments. We tested different growth media commonly used to culture anaerobes and incubation times. Cells were cultured on supplemented brain heart infusion (BHIS) agar, tryptone yeast (TY) agar, chocolate agar or anaerobic blood agar. (197,198) All media yielded round, opaque, and mucoid colonies after 72 hours of growth (Figure 24 A). The chocolate agar plates showed both small and large colonies which could have been due to *C. acnes* heterogeneity or contamination (Figure 24 A). Because TY medium showed high consistent colony counts and is cheaper than the other options tested, growth in liquid culture was assessed in TY. In addition, TY medium contains sodium thioglycolate,

previously shown to facilitate *C. acnes* growth by regulating medium redox potential.(194,195). To avoid contamination, liquid medium was supplemented with 20 μg/mL metronidazole, to which *C. acnes* is resistant.(199,200) We observed that *C. acnes* grows at a moderate speed in this medium and reaches a stationary optical density of 1.2–1.4 within 72 hours (Figure 24 B). Similarly, we got robust *C. acnes* biofilms on glass surfaces at 72 hours of growth. Adhesion of the cells to glass surface was greatly enhanced by coating with poly-L-lysine while coating with fibronectin or poly-D-lysine had more modest effects (Figure 24 C). Since *C. acnes* cultures in electroporation cuvettes were needed to be taken out from the anaerobic chamber for a maximum of 1 hour for the pulse treatment, we assessed the effect of oxygen exposure from seal leakage on cell viability. Both the planktonically growing cells and biofilms derived cells scraped out of biofilms were diluted and plated for viability after 1 hour of incubation at 22 °C in aerobic or anaerobic conditions. After 1 hour of incubation at aerobic condition, all samples were returned to the anaerobic chamber, diluted, and plated to assess viability. One hour of passive exposure to environmental oxygen did not cause meaningful effect on *C. acnes* viability (Figure 24 D), consistent with previous reports of its aerotolerance.(194,201)

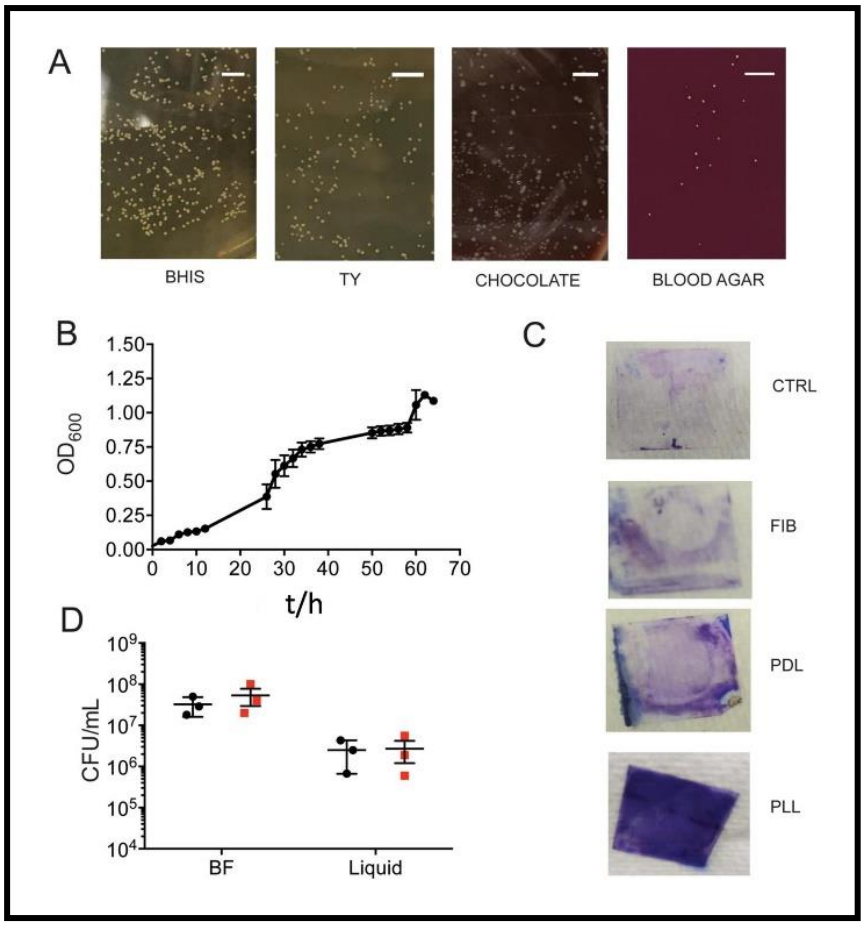

Figure 24. *C. acnes* growth condition optimization: planktonic vs. biofilms. (A) *C. acnes* cells from a frozen glycerol stock were aliquoted into TY medium, let it grow overnight, and plated on the indicated agar plates. Cells on BHIS, TY, and chocolate agar plates were plated at a 10^5 dilution while cells on blood agar plates were seeded at a 10^6 dilution. Scale bar:5 mm. (B) Growth of planktonic *C. acnes* over 72 hours. (C) Crystal violet staining of *C. acnes* biofilms grown for 72 hours on glass coverslips with no coating (CTRL) and coated with 0.1% fibronectin (FIB), 0.1% poly-D-lysine (PDL), or 0.1% poly-L-lysine (PLL). (D) Biofilm (BF) and liquid culture viability after 60 min incubation in an electroporation cuvette in anaerobic (black) or aerobic (red) conditions. Adapted from Poudel *et al.* 2021.(107)

Planktonic *C. acnes* in log phase are resistant to nsPEF

PEF treatments for microbial inactivation are intended to be a non-thermal process. However, an increase in temperature due to Joule heating can be associated with high pulse doses. Therefore, in our preliminary experiments we measured the temperature increase associated with the pulse treatment to exclude any potential heat inactivation effect. We observed an increase in temperature from 20.4 ± 0.2 to 30.9 ± 0.8 °C when the sample was treated with the highest pulse (2000 pulses, 280 ns, 28 kV/cm at 5 Hz) dose that we could test with our exposure system. As *C. acnes* exhibits maximum growth at human body temperatures (30 °C and 37 °C) (202), we discounted the nsPEF-induced heating as an inactivating variable in our experiments.

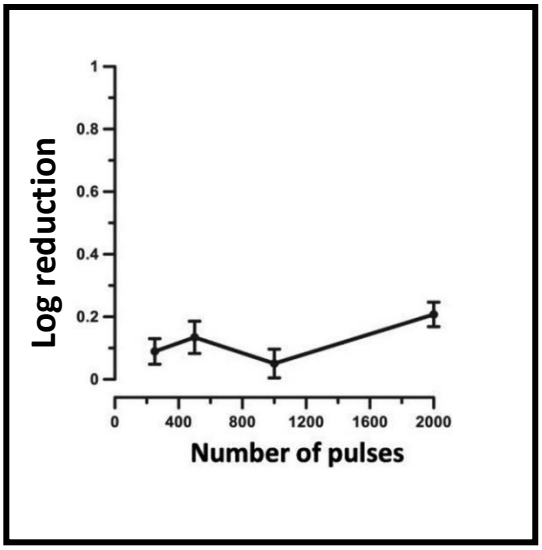

Figure 25. Effect of nsPEF on planktonic *C. acnes* viability. Cells in exponential phase were treated with increasing numbers of 280 ns pulses (250 to 2000 pulses, 28 kV/cm, 5 Hz; 0.5 to 4 kJ/ml) and viability was measured at 72 hours post treatment. Inactivation is expressed as log $(CFU/mL)_{sham}$ – log $(CFU/mL)_{nsPEF}$**.** Adapted and modified from Poudel *et al.* 2021.(107)

We then tested the effect of increasing numbers of 280 ns pulses on the viability of planktonic *C. acnes* in exponential growth phase. The viability of the planktonic cells was not significantly affected by any of the pulse doses tested (Figure 25). Specifically, 2000 pulses, 280 ns pulses, 28 kV/cm at 5 Hz (4 kJ/ml), led to only 0.2 ± 0.02 $\log_{10}$ reduction in *C. acnes* viability.(107)

Lysozyme increases planktonic *C. acnes* sensitivity to nsPEF

Bacteria exhibit variable sensitivity to PEF. It is well known that Gram-positive bacteria are less susceptible to electro-transformation than Gram-negative bacteria due to the differences in their cell wall structure and density.(203) However, there are examples of significant increase in transformation efficiency with an application of cell wall weaking agents.(204) Among these, lysozyme (LY) is a naturally occurring enzyme found in biological fluids including tears, saliva, and milk, and is considered a part of the innate immune system in most mammals.(205) LY degrades bacterial cell wall by disrupting the peptidoglycan layer. It has been used in skin care and as a safe adjunct to antifungals. Liao and their team observed a significant reduction in *C. acnes* viability when *C. acnes* supernatant is incubated with varying concentration of LY.(206) Likewise, LY-triclosan complexes were found to significantly enhance bactericidal activity against several strains of Gram-positive and Gram-negative bacteria.(207) We therefore asked whether destabilizing the cells wall of *C. acnes* with LY increases cells sensitivity to nsPEF. For this planktonic *C. acnes* cells were treated with 0, 1 or 10 mg/ml LY at 37 ^{0}C for an hour. Then the samples were either exposed to 280 ns pulses (1000 and 2000 pulses, 28 kV/cm, 5 Hz; 2 and 4 kJ/ml) or left untreated as parallel sham controls, and colonies were counted at 72 hours post treatment. Our results show that treatment with either nsPEF alone or lysozyme alone did not affect *C. acnes* viability (Figure 26). Instead, we observed increased *C. acnes* growth upon lysozyme treatment suggesting that perturbation of the cell wall may accelerate cell division. However, when

the cells were pretreated with 10 mg/ml LY following nsPEF exposure, the cells were significantly inactivated. Our results reveal for the first time the synergistic effect between LY and nsPEF at killing Gram-positive bacteria.(107)

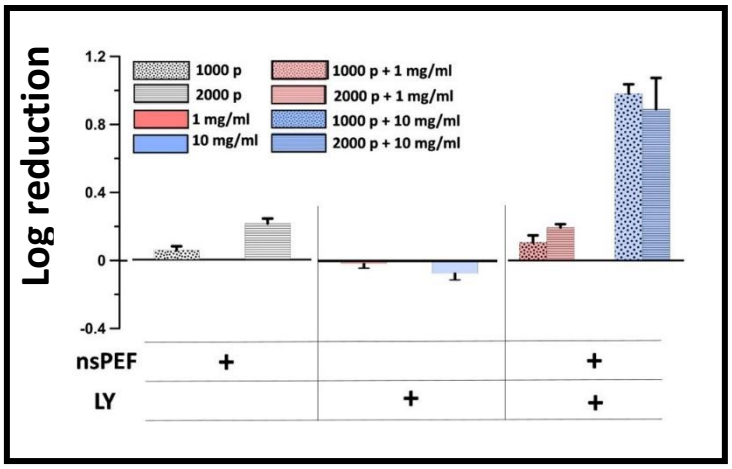

Figure 26. Synergistic cytotoxicity from combination of LY treatment and nsPEF. Planktonic *C. acnes* cells in exponential phase were treated with either nsPEF (1000 and 2000 pulses, 280 ns, 28 kV/cm, 5 Hz; 2 and 4 kJ/ml) or LY (1 or 10 mg/ml) for 1 h or both and viability was measured at 72 h post treatment. Inactivation is expressed as log $(CFU/mL)_{sham}$ – log $(CFU/mL)_{nsPEF}$. Mean +/- s.e., n = 3–5. Adapted and modified from Poudel *et al.* 2021.(107)

C. acnes in biofilms are sensitive to nsPEF

C. acnes biofilm formation plays a significant role in the pathophysiology of acne vulgaris. (49) To investigate the effect of nsPEF on *C. acnes* biofilms viability, cells were grown on poly-L-lysine coated plastic well for 72 hours for biofilms development. Contrary to our results with

planktonic cells biofilms derived cells were significantly inactivated by nsPEF (100 to 2000 pulses, 280 ns pulses, 28 kV/cm, 5 Hz; 0.2 to 4 kJ/ml) as shown in Figure 27 A. Planktonic cells were collected in exponential growth phase while biofilm derived cells were harvested in stationary phase for nsPEF treatment. To determine whether nsPEF sensitivity corelates with *C. acnes* growth phase, we treated both the free-floating cells in the biofilm supernatant and surface attached biofilm-derived cells with nspEF. We observed that nsPEF killed surface attached biofilm cells more efficiently than the free-floating cells even when planktonic cells and biofilms were kept under the exact same culture conditions (Figure 27 B).(107)

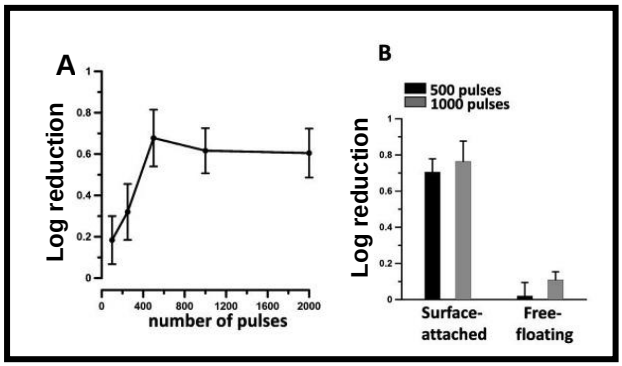

Figure 27. Effect of nsPEF on *C. acnes* biofilms. (A) *C. acnes* cells were grown as biofilms for 72 hours and, before nsPEF, rinsed with growth medium to remove planktonic bacteria, scraped from the plastic surface, and aliquoted in electroporation cuvettes. Samples were treated with increasing numbers of 280 ns pulses (100 to 2000 pulses, 5 Hz, 28 kV/cm; 0.2 to 4 kJ/ml) and viability was measured at 72 hours post treatment. (B) *C. acnes* biofilms were grown for 3 days and both surfaces attached biofilms and free-floating cells in the biofilm suspension were treated with nsPEF (500 and 1000 pulses, 300 ns duration, 28 kV/cm, 5 Hz; 1 and 2 kJ/ml). Viability was measured at 72 hours post treatment. Adapted and modified from Poudel *et al.* 2021.(107)

Since all the tested nsPEF doses failed to inactivate planktonic *C. acnes* while significantly affecting bacteria in biofilms, we investigated whether a lysosomal pretreatment could further increase biofilm sensitivity to nsPEF. For this, biofilms derived cells were pretreated with 10 mg/mL LY for 1 hour before exposure to nsPEF (500 and 1000 pulses, 280 ns pulses, 28 kV/cm, 5 Hz; 1 and 2 kJ/mL) and viability was measured at 72-hour post treatment. In contrast to that of planktonic cells, LY failed to enhance *C. acnes* biofilm sensitivity to nsPEF (Figure 28). Biofilms produce a thick extracellular matrix which is highly resistant to drug penetration. The observations made in this experiment indicates that LY in our experiments did not reach a sufficiently high concentration to affect the bacteria cell wall or the complex structure of biofilm did not allow lysozyme to reach the bacterial cell wall for its optimum activity.(107)

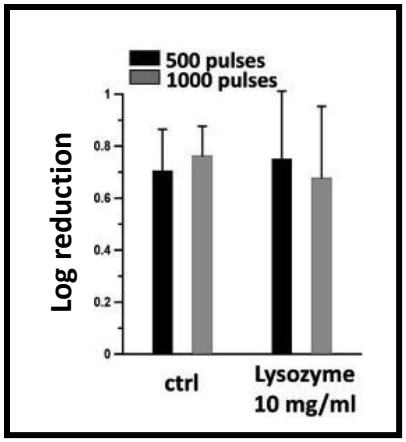

Figure 28. Combined effect of nsPEF and lysosomal pretreatment on *C. acnes* biofilms. Biofilms derived cells were treated with 10 mg/mL LY or left untreated (ctrl). After one hour, cells were treated with nsPEF (500 and 1000 pulses, 280 ns duration, 28 kV/cm, 5 Hz; 1 and 2 kJ/mL) and viability was measured at 72-hour post treatment. Adapted and modified from Poudel *et al.* 2021.(107)

Effect of nsPEF on intact *C. acnes* biofilm

In our study we observed the nsPEF killing effect on biofilm cells that were scrapped from the plastic surface to transfer into the electroporation cuvettes. Therefore, to eliminate the stressful cell handling and possible confounding impact of cell detachment, we investigated the effect of nsPEF on intact biofilm cells. To test intact biofilms on their original substrate, biofilms were grown on glass coverslip with an indium oxide (ITO) conductive layer. The coverslips with adherent biofilms were aseptically placed into 1mm gap electroporation for nsPEF treatment (Figure 29 A). Cells were exposed to 500 or 1000 pulses (280 ns, 5 Hz; 0.1 and 0.2 kJ/ml) at 900 V, which generated a practically uniform electric field of 3.6 kV/cm at the coverslips surface. Even under these conditions we did not observe any difference in nsPEF killing efficiency between the scrapped and intact biofilms derived cells (Figure 29 B).(107) A recent study has also shown highly efficient killing of cells by nsPEF on ITO coverslips that requires about 10-fold lower electric fields than the one used for cells in suspension.(208)

nsPEF disrupt *C. acnes* cell membrane

As *C. acnes* viability was compromised upon the treatment with nansosecond pulses, we wanted to visualize the effect of nsPEF on bacteria. The cells were mixed with a fluorescent dye, propidium iodide, and processed as described above and visualized under microscope. The cells treated with nanoseconds pulses displayed strong fluorescence signal as compared with the cells treated without the electric pulses (Appendix L). Propidium iodide poorly penetrates the intact cellular membrane, however upon the membrane breakage, it can easily enter the cytosol and binds the nucleic acids giving strong red fluorescence.(183)

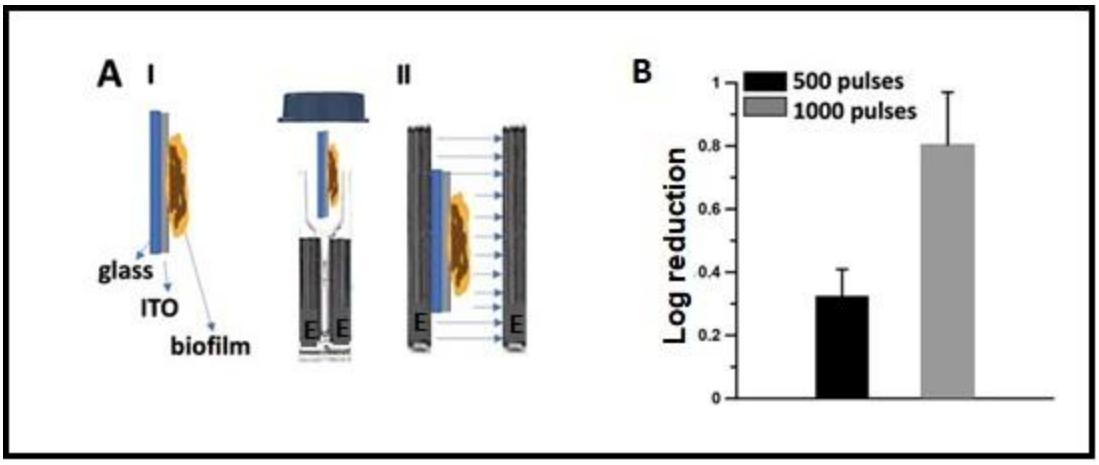

Figure 29. Effect of nsPEF on undisrupted biofilms. (A) Schematic explaining nsPEF delivery to biofilms on ITO glass coverslips in an electroporation cuvette (I). Panel II shows the enlarged view of the gap between the two electrodes marked as (E) with the electric field lines. (B) Biofilms were exposed to either 500 or 1000 pulses (280 ns, 5 Hz, 3.6 kV/cm; 0.1 and 0.2 kJ/mL) and viability was measured at 72 h post treatment. Inactivation is expressed as log (CFU/mL) $_{sham}$ − log (CFU/mL) nsPEF. Mean +/- s.e., n = 9. Adapted from Poudel *et al.* 2021.(107)

DISCUSSION

Current therapeutic choices against acne vulgaris are not effective in managing all grades of inflammatory acne. Vitamin A derived topical retinoids are responsible in causing unwanted side effects whereas antibiotic therapy has been challenged by the emergence of antibiotic resistant *C. acnes* strains. In addition, the increased resilience of bacterial cells growing in biofilms contribute to the spread of antimicrobial resistance and failure of antibiotic therapy. Therefore, there is a growing need of new treatment options that are efficacious against biofilms and do not promote antimicrobial resistance.

There are very limited studies on the use of electrical currents and electrical field against bacterial biofilms viability. For instance, Khan et al 2016, used long 50µs duration electric pulses to kill *Pseudomonas aeruginosa* biofilms and proposed as treatment option in combination with systemic antibacterial therapy.(209) Similarly, low electric fields generated from continuous DC has been utilized to treat biofilms derived from multiple bacterial species including *Staphylococcus aureus*, *Staphylococcus epidermidis*, and *P. aeruginosa*, either alone or in combination with biocides.(210-212) However, none of these studies have directly compared the effect of electric field on killing of both the planktonic and biofilms cells of the same bacterial strain.

In this study we measured of the efficacy nsPEF against the viability of both the planktonic and biofilms derived cells from the same organism. Our results demonstrated that *C. acnes* cells growing planktonically in liquid culture are minimally affected by nsPEF consistent with prior studies with Gram-positive bacteria.(213) These studies have shown slightest reduction in viability of *S. aureus* and *Lacotbacillus acidophilus* respectively upon nsPEF treatment demonstrating that bacteria are far more resistant to PEF treatments than mammalian cells with Gram-positive bacteria being the most resilient.(184,213,214) On contrary to the effect of any other antimicrobial agent, in our study nsPEF appear to affect the viability of *C. acnes* biofilms than the planktonic counterparts. Biofilm is an aggregation of microbial cells embedded in an extracellular matrix (ECM) composed of polysaccharides, proteins, nucleic acids, lipids, and other biomolecules.(215) It protects cells from harmful environmental challenges including UV exposure, meal toxicity, acid exposure, dehydration, phagocytosis and several antibiotics and antimicrobial agents.(216) Besides providing structural support the ECM components also serve as signals, promote migration and genetic exchange, and as ion reservoirs.(217) Therefore, any damage to these structural and biological components of ECM may affect the viability of the cells in biofilms. Since

electric fields are well known in disrupting lipid bilayers(218), damage to dielectric components of the ECM may attribute to the cytotoxic effects of nsPEF. Biofilms cells held together in ECM and are well organized in signal transduction to their adjacent cells than their planktonic counterparts. Therefore, it can be speculated that sensing the damage caused by nsPEF to both the bacterial plasma membrane and ECM components and communicating it via cell-cell signaling leads to enhanced collective cytotoxic response in biofilms than in planktonic cells. Taking into account that 60-80% of human bacterial infections are believed to be caused by bacteria growing in biofilms, our findings demand for further studies on the effects of PEF treatments on microbial communities.

SUMMARY

The effect of increasing numbers of 280ns pulses on the viability of both the planktonic cells and the biofilms derived cells resulted into interesting findings. We observed that biofilms derived cells are sensitive to nsPEF in contrast to the planktonic cells. We also found that lysozyme and nsPEF has synergistic effect in killing planktonic cells. However, when we combined lysozyme with nsPEF treatment against biofilm-derived cells, we did not observe any synergistic effect in killing the cells. We speculate that lysozyme made the planktonic cells more vulnerable by weakening the cell wall and allowing nsPEF to act more efficiently. On the other hand, the complex structure of biofilm did not allow lysozyme to reach the bacterial cell wall for its optimum activity. Additionally, when we treated the free-floating cells in the biofilm supernatant and surface attached biofilm-derived cells with nspEF, we observed that surface attached biofilm cells were more sensitive than the free-floating cells. Overall, our results demonstrate that while all the tested nsPEF doses failed to inactivate planktonic *C. acnes*, they significantly impaired bacteria in

biofilms. It is the first report of its kind showing that the bacteria growing as biofilms are more sensitive to nsPEF treatments.

CHAPTER V

CONCLUSIONS AND FUTURE DIRECTIONS

The work presented in this dissertation investigated the mechanisms of extracellular stresses survival of two clinically important Gram-positive organisms, *C. difficile* and *C. acnes*. In chapter II and III, we explored the (pp)pGpp mediated stress response mechanism in *C. difficile*. Previously we have shown that *C. difficile* encodes a long bifunctional RSH and a monofunctional RelQ and have studied the functional aspects of long RSH.(106) Utilizing standard protein purification techniques and radiolabeled thin layer chromatography and phosphorous NMR, we characterized *C. difficile's* small alarmone synthetase, RelQ in this study. We confirmed that like CdRSH, CdRelQ is a pyrophospho transfer synthetase and exhibits *in vitro* (pp)pGpp synthetic activity. However, unlike CdRSH, CeRelQ activity is concentration dependent as it exhibited little or no pyrophosphotransfer activity at concentration below 0.4µM. This concentration dependence of CdRelQ indicates that it may require to undergo oligomerization for its functional activity as in other Gram-positive organisms(116-118), however further experimentation utilizing size exclusion chromatography is needed for its verification. Unlike many of its Gram-positive homologs, CdRelQ utilizes both GDP and GTP as phosphoacceptors and has higher affinity for GTP. In addition, it utilized diverse divalent cations for its (pp)pGpp synthetic activity which is unique as no reported organisms were able to make use of such diverse cations. This ability of utilizing different divalent ions for (pp)pGpp synthetic activity may provide *C. difficile* survival advantage against host derived 'nutritional immunity' during infection. We also discovered that like CdRSH, CdRelQ activity is not compromised at varying pH conditions. Surprisingly, we discovered that both the clostridial synthetases, CdRSH and CdRelQ, hydrolyze GDP/GTP independently for their (pp)pGpp synthetic activity and uniquely synthesize pGpp exclusively. *C.*

difficile turns out to be the first reported organism synthesizing only pGpp as its magic spot in the fifty years history of magic spot synthesis. This unique trait of *C. difficile* synthetases warrants further mutational analysis to check out why and how the clostridial synthetases hydrolyze GDP/GTP for their synthetic activity. Similarly, structural analysis of these enzymes may provide additional understanding about their unique substrate preferences. Previous study in RSH enzymes has shown that an acidic EXDD and basic RXKD sequence at the beginning of the guanosine binding motif resulted in a preference for GDP and GTP respectively.(98) However, SAS enzymes do not follow this hypothesis as several of them have a basic motif and prefers GDP. Altogether, our results demonstrate that *C. difficile* stringent response enzymes activity markedly differs from that of their homologous counterparts. This differences in magic spot metabolism suggest that other Firmicutes may not serve as complete model of the stringent response pathway in *C. difficile* which would provide a basis in designing targeted inhibitors against these enzymes.

The stringent response pathway is a conserved stress signaling pathway, however, the factors regulating the expression of stringent response genes vary among the bacterial species.(77) In chapter III, we determined some of the environmental cues regulating the SR in *C. difficile* utilizing transcriptional fluorescence reporter strains. We found that the SR in *C. difficile* is induced via several environmental factors in strain specific manner. Multiple classes of antibiotics triggered the expression of clostridial stringent response genes suggesting the role of stringent response in *C. difficile* survival under antibiotic stress. In earlier study, we have demonstrated that the translational inhibition of *rsh* gene resulted into an increase on bacterial antibiotic susceptibility demonstrating the role of SR in *C. difficile* antibiotic survival.(106) Since *C. difficile* must cross diverse gastrointestinal environments to establish infection, we investigated whether these environmental conditions would trigger the SR response. When we exposed R20291 strain in an

acute oxidative stress and metal starvation like that from the immune system, we observed increase activity of *rsh* promoter. We also found that acidic environments stimulated the expression of *rsh* gene. Interestingly, febrile like temperature and osmotic pressure did not induce expression of either of stringent response genes. It is likely that RSH is the primary mediator of a stress triggered stringent response whereas RelQ plays a role in regulation of nucleotide metabolism in this organism as has been reported in other Gram-positive organisms. Future gene knock out study will establish the direct role of SR in *C. difficile* survival under diverse stress conditions.

The fourth chapter of this dissertation is thematically related to the studies presented in earlier chapters. In this chapter, we investigated the effect of physical stress exerted by nanosecond pulsed electric fields on *C. acnes* viability. Nanosecond pulse stimulation has emerged as an alternative for microbial inactivation. Since the technique is totally of physical nature, it is difficult for the microorganism to develop resistance against it.(68,219) We studied the effect of increasing numbers of 280ns pulses on the viability of both the planktonic and the biofilms derived cells that resulted into exciting findings. We found that *C. acnes* cells in biofilms are sensitive to nsPEF in contrast to the planktonic cells. We also observed the synergistic killing of planktonic cells by lysozyme and nsPEF. When it comes in killing of biofilms derived cells, we did not observe the synergy between lysozyme and nsPEF. We speculate that lysozyme weakened the cell wall of the planktonic cells and made them more vulnerable to physical stress imparted by nsPEF. On the other hand, the structural components of biofilm did not allow lysozyme to reach the bacterial cell wall for its optimum activity. Cells in biofilms are more resilient to antibiotics than planktonic cells and spreads antimicrobial resistance to adherent cells via horizontal gene transfer.(55,220) Our results showing bacteria growing as biofilms are more sensitive to nsPEF treatments would contribute to controlling the growing problem of antimicrobial resistance. Moreover, expanding

the study to other bacterial species forming biofilms and evaluating the relevance of nsPEF parameters as well as measuring potential synergistic effect between nsPEF and standard biocides will provide clearer picture on the application of nsPEF for microbial inactivation.

REFERENCES

1. Sizar O., U. C. G. (2020) *Gram Positive Bacteria*, StatPearls, Treasure Island, FL, USA
2. Mai-Prochnow, A., Clauson, M., Hong, J., and Murphy, A. B. (2016) Gram positive and Gram negative bacteria differ in their sensitivity to cold plasma. *Sci. Rep.* **6**, 38610
3. Silhavy, T. J., Kahne, D., and Walker, S. (2010) The bacterial cell envelope. *Cold Spring Harb. Perspect. Biol.* **2**, a000414-a000414
4. Yang, D. C., Blair, K. M., and Salama, N. R. (2016) Staying in Shape: the Impact of Cell Shape on Bacterial Survival in Diverse Environments. *Microbiol. Mol. Biol. Rev.* **80**, 187-203
5. Doernberg, S. B., Lodise, T. P., Thaden, J. T., Munita, J. M., Cosgrove, S. E., Arias, C. A., Boucher, H. W., Corey, G. R., Lowy, F. D., Murray, B., Miller, L. G., Holland, T. L., and Group, f. t. G.-P. C. o. t. A. R. L. (2017) Gram-Positive Bacterial Infections: Research Priorities, Accomplishments, and Future Directions of the Antibacterial Resistance Leadership Group. *Clin. Infect. Dis.* **64**, S24-S29
6. Munita, J. M., Bayer, A. S., and Arias, C. A. (2015) Evolving resistance among Gram-positive pathogens. *Clin. Infect. Dis.* **61 Suppl 2**, S48-S57
7. Trastoy, R., Manso, T., Fernández-García, L., Blasco, L., Ambroa, A., Molino, M. L. P. d., Bou, G., García-Contreras, R., Wood, T. K., and Tomás, M. (2018) Mechanisms of Bacterial Tolerance and Persistence in the Gastrointestinal and Respiratory Environments. *Clin. Microbiol. Rev.* **31**, e00023-00018
8. Sandhu, B. K., and McBride, S. M. (2018) Clostridioides difficile. *Trends Microbiol.* **26**, 1049-1050
9. O'Donoghue, C., and Kyne, L. (2011) Update on Clostridium difficile infection. *Curr. Opin. Gastroenterol.* **27**, 38-47
10. Tenover, F. C., Tickler, I. A., and Persing, D. H. (2012) Antimicrobial-resistant strains of Clostridium difficile from North America. *Antimicrob. Agents Chemother.* **56**, 2929-2932
11. He, M., Miyajima, F., Roberts, P., Ellison, L., Pickard, D. J., Martin, M. J., Connor, T. R., Harris, S. R., Fairley, D., Bamford, K. B., D'Arc, S., Brazier, J., Brown, D., Coia, J. E., Douce, G., Gerding, D., Kim, H. J., Koh, T. H., Kato, H., Senoh, M., Louie, T., Michell, S., Butt, E., Peacock, S. J., Brown, N. M., Riley, T., Songer, G., Wilcox, M., Pirmohamed, M., Kuijper, E., Hawkey, P., Wren, B. W., Dougan, G., Parkhill, J., and Lawley, T. D. (2013) Emergence and global spread of epidemic healthcare-associated Clostridium difficile. *Nat. Genet.* **45**, 109-113
12. Hazleton, K. Z., Martin, C. G., Arnolds, K. L., Nusbacher, N. M., Moreno-Huizar, N., Armstrong, M., Reisdorph, N., and Lozupone, C. A. (2019) Dietary fat and fiber impacts intestinal microbiome resilience to antibiotics and Clostridoides difficile infection in mice. *bioRxiv*, 828939
13. Leffler, D. A., and Lamont, J. T. (2015) Clostridium difficile Infection. *N. Engl. J. Med.* **372**, 1539-1548
14. Mefferd, C. C., Bhute, S. S., Phan, J. R., Villarama, J. V., Do, D. M., Alarcia, S., Abel-Santos, E., and Hedlund, B. P. (2020) A High-Fat/High-Protein, Atkins-Type Diet Exacerbates Clostridioides (Clostridium) difficile Infection in Mice, whereas a High-Carbohydrate Diet Protects. *mSystems* **5**, e00765-00719
15. Lessa, F. C., Mu, Y., Bamberg, W. M., Beldavs, Z. G., Dumyati, G. K., Dunn, J. R., Farley, M. M., Holzbauer, S. M., Meek, J. I., Phipps, E. C., Wilson, L. E., Winston, L. G., Cohen,

J. A., Limbago, B. M., Fridkin, S. K., Gerding, D. N., and McDonald, L. C. (2015) Burden of Clostridium difficile Infection in the United States. *N. Engl. J. Med.* **372**, 825-834
16. Rupnik, M., Wilcox, M. H., and Gerding, D. N. (2009) Clostridium difficile infection: new developments in epidemiology and pathogenesis. *Nat. Rev. Microbiol.* **7**, 526-536
17. Sorg, J. A., and Sonenshein, A. L. (2008) Bile salts and glycine as cogerminants for Clostridium difficile spores. *J. Bacteriol.* **190**, 2505-2512
18. Howerton, A., Ramirez, N., and Abel-Santos, E. (2011) Mapping interactions between germinants and Clostridium difficile spores. *J. Bacteriol.* **193**, 274-282
19. Sun, X., and Hirota, S. A. (2015) The roles of host and pathogen factors and the innate immune response in the pathogenesis of Clostridium difficile infection. *Mol. Immunol.* **63**, 193-202
20. Ng, J., Hirota, S. A., Gross, O., Li, Y., Ulke-Lemee, A., Potentier, M. S., Schenck, L. P., Vilaysane, A., Seamone, M. E., Feng, H., Armstrong, G. D., Tschopp, J., Macdonald, J. A., Muruve, D. A., and Beck, P. L. (2010) Clostridium difficile toxin-induced inflammation and intestinal injury are mediated by the inflammasome. *Gastroenterology* **139**, 542-552, 552 e541-543
21. Britton, R. A., and Young, V. B. (2014) Role of the intestinal microbiota in resistance to colonization by Clostridium difficile. *Gastroenterology* **146**, 1547-1553
22. Peng, Z., Jin, D., Kim, H. B., Stratton, C. W., Wu, B., Tang, Y. W., and Sun, X. (2017) Update on Antimicrobial Resistance in Clostridium difficile: Resistance Mechanisms and Antimicrobial Susceptibility Testing. *J. Clin. Microbiol.* **55**, 1998-2008
23. Spigaglia, P. (2016) Recent advances in the understanding of antibiotic resistance in Clostridium difficile infection. *Ther Adv Infect Dis* **3**, 23-42
24. Trastoy, R., Manso, T., Fernández-García, L., Blasco, L., Ambroa, A., Pérez del Molino, M. L., Bou, G., García-Contreras, R., Wood, T. K., and Tomás, M. (2018) Mechanisms of Bacterial Tolerance and Persistence in the Gastrointestinal and Respiratory Environments. *Clin. Microbiol. Rev.* **31**, e00023-00018
25. Zheng, L., Kelly, C. J., and Colgan, S. P. (2015) Physiologic hypoxia and oxygen homeostasis in the healthy intestine. A Review in the Theme: Cellular Responses to Hypoxia. *Am. J. Physiol. Cell Physiol.* **309**, C350-C360
26. Wetzel, D., and McBride, S. M. (2020) The Impact of pH on Clostridioides difficile Sporulation and Physiology. *Appl. Environ. Microbiol.* **86**, e02706-02719
27. Buffie, C. G., Bucci, V., Stein, R. R., McKenney, P. T., Ling, L., Gobourne, A., No, D., Liu, H., Kinnebrew, M., Viale, A., Littmann, E., van den Brink, M. R. M., Jenq, R. R., Taur, Y., Sander, C., Cross, J. R., Toussaint, N. C., Xavier, J. B., and Pamer, E. G. (2015) Precision microbiome reconstitution restores bile acid mediated resistance to Clostridium difficile. *Nature* **517**, 205-208
28. Fachi, J. L., Felipe, J. d. S., Pral, L. P., da Silva, B. K., Corrêa, R. O., de Andrade, M. C. P., da Fonseca, D. M., Basso, P. J., Câmara, N. O. S., de Sales e Souza, É. L., dos Santos Martins, F., Guima, S. E. S., Thomas, A. M., Setubal, J. C., Magalhães, Y. T., Forti, F. L., Candreva, T., Rodrigues, H. G., de Jesus, M. B., Consonni, S. R., Farias, A. d. S., Varga-Weisz, P., and Vinolo, M. A. R. (2019) Butyrate Protects Mice from Clostridium difficile-Induced Colitis through an HIF-1-Dependent Mechanism. *Cell Rep.* **27**, 750-761.e757
29. Collins, J., Danhof, H., and Britton, R. A. (2019) The role of trehalose in the global spread of epidemic Clostridium difficile. *Gut Microbes* **10**, 204-209

30. Hryckowian, A. J., Van Treuren, W., Smits, S. A., Davis, N. M., Gardner, J. O., Bouley, D. M., and Sonnenburg, J. L. (2018) Microbiota-accessible carbohydrates suppress Clostridium difficile infection in a murine model. *Nat. Microbiol.* **3**, 662-669
31. Martin-Verstraete, I., Peltier, J., and Dupuy, B. (2016) The Regulatory Networks That Control Clostridium difficile Toxin Synthesis. *Toxins (Basel)* **8**, 153
32. Giordano, N., Hastie, J. L., Smith, A. D., Foss, E. D., Gutierrez-Munoz, D. F., and Carlson, P. E., Jr. (2018) Cysteine Desulfurase IscS2 Plays a Role in Oxygen Resistance in Clostridium difficile. *Infect. Immun.* **86**, e00326-00318
33. Joo, H.-S., Fu, C.-I., and Otto, M. (2016) Bacterial strategies of resistance to antimicrobial peptides. *Philos. Trans. R. Soc. B: Biol. Sci.* **371**, 20150292
34. Fang, Ferric C., Frawley, Elaine R., Tapscott, T., and Vázquez-Torres, A. (2016) Bacterial Stress Responses during Host Infection. *Cell Host Microbe* **20**, 133-143
35. LeGrand, E. K., and Day, J. D. (2016) Self-harm to preferentially harm the pathogens within: non-specific stressors in innate immunity. *Proc. Biol. Sci.* **283**, 20160266
36. Frädrich, C., Beer, L.-A., and Gerhard, R. (2016) Reactive Oxygen Species as Additional Determinants for Cytotoxicity of Clostridium difficile Toxins A and B. *Toxins (Basel)* **8**, 25
37. Girinathan, B. P., Braun, S. E., and Govind, R. (2014) Clostridium difficile glutamate dehydrogenase is a secreted enzyme that confers resistance to H2O2. *Microbiology (Reading)* **160**, 47-55
38. Seekatz, A. M., Theriot, C. M., Rao, K., Chang, Y.-M., Freeman, A. E., Kao, J. Y., and Young, V. B. (2018) Restoration of short chain fatty acid and bile acid metabolism following fecal microbiota transplantation in patients with recurrent Clostridium difficile infection. *Anaerobe* **53**, 64-73
39. Rowland, I., Gibson, G., Heinken, A., Scott, K., Swann, J., Thiele, I., and Tuohy, K. (2018) Gut microbiota functions: metabolism of nutrients and other food components. *Eur. J. Nutr.* **57**, 1-24
40. Schäffler, H., and Breitrück, A. (2018) Clostridium difficile - From Colonization to Infection. *Front. Microbiol.* **9**, 646-646
41. Kelly, C. P. (1996) Immune response to Clostridium difficile infection. *Eur. J. Gastroenterol. Hepatol.* **8**, 1048-1053
42. Jump, R. L. (2013) Clostridium difficile infection in older adults. *Aging health* **9**, 403-414
43. Czepiel, J., Dróżdż, M., Pituch, H., Kuijper, E. J., Perucki, W., Mielimonka, A., Goldman, S., Wultańska, D., Garlicki, A., and Biesiada, G. (2019) Clostridium difficile infection: review. *Eur.J. Clin. Microbiol. Infect. Dis.* **38**, 1211-1221
44. Marciniak, C., Chen, D., Stein, A. C., and Semik, P. E. (2006) Prevalence of Clostridium Difficile Colonization at Admission to Rehabilitation. *Arch. Phys. Med. Rehabil.* **87**, 1086-1090
45. Macleod-Glover, N., and Sadowski, C. (2010) Efficacy of cleaning products for C. difficile: environmental strategies to reduce the spread of Clostridium difficile-associated diarrhea in geriatric rehabilitation. *Can. Fam. Physician* **56**, 417-423
46. Mounsey, A., Lacy Smith, K., Reddy, V. C., and Nickolich, S. (2020) Clostridioides difficile Infection: Update on Management. *Am. Fam. Physician* **101**, 168-175
47. Khanna, S., and Gerding, D. N. (2019) Current and future trends in clostridioides (clostridium) difficile infection management. *Anaerobe* **58**, 95-102

48. Khanna, S. (2021) Advances in Clostridioides difficile therapeutics. *Expert Rev. Anti Infect. Ther.* **19**, 1067-1070
49. Platsidaki, E., and Dessinioti, C. (2018) Recent advances in understanding Propionibacterium acnes (Cutibacterium acnes) in acne. *F1000Research* **7**, F1000 Faculty Rev-1953
50. Hall, G. S., Pratt-Rippin, K., Meisler, D. M., Washington, J. A., Roussel, T. J., and Miller, D. (1994) Growth curve for Propionibacterium acnes. *Curr. Eye Res.* **13**, 465-466
51. Portillo, M., Eugenia, a., Corvec, S., phane, Borens, O., and Trampuz, A. (2013) Propionibacterium acnes: An Underestimated Pathogen in Implant-Associated Infections. *BioMed Res. Int.* **2013**, 10
52. Nord, C. E., and Oprica, C. (2006) Antibiotic resistance in Propionibacterium acnes. Microbiological and clinical aspects. *Anaerobe* **12**, 207-210
53. Dessinioti, C., and Katsambas, A. (2017) Propionibacterium acnes and antimicrobial resistance in acne. *Clin. Dermatol.* **35**, 163-167
54. Crane, J. K., Hohman, D. W., Nodzo, S. R., and Duquin, T. R. (2013) Antimicrobial Susceptibility of Propionibacterium acnes isolates from Shoulder Surgery. *Antimicrob. Agents Chemother.* **57**, 3424-3426
55. Coenye, T., Peeters, E., and Nelis, H. J. (2007) Biofilm formation by Propionibacterium acnes is associated with increased resistance to antimicrobial agents and increased production of putative virulence factors. *Res. Microbiol.* **158**, 386-392
56. Burkhart, C. N., and Burkhart, C. G. (2003) Microbiology's principle of biofilms as a major factor in the pathogenesis of acne vulgaris. *Int. J. Dermatol.* **42**, 925-927
57. Decker, A., and Graber, E. M. (2012) Over-the-counter Acne Treatments: A Review. *J. Clin. Aesthet. Dermatol.* **5**, 32-40
58. Joo, Y., Kang, H., Choi, E. H., Nelson, J. S., and Jung, B. (2012) Characterization of a new acne vulgaris treatment device combining light and thermal treatment methods. *Skin Res. Technol.* **18**, 15-21
59. Lim, H. W., Collins, S. A. B., Resneck, J. S., Bolognia, J. L., Hodge, J. A., Rohrer, T. A., Van Beek, M. J., Margolis, D. J., Sober, A. J., Weinstock, M. A., Nerenz, D. R., Smith Begolka, W., and Moyano, J. V. (2017) The burden of skin disease in the United States. *J. Am. Acad. Dermatol.* **76**, 958-972.e952
60. Strauss, J. S., Krowchuk, D. P., Leyden, J. J., Lucky, A. W., Shalita, A. R., Siegfried, E. C., Thiboutot, D. M., Van Voorhees, A. S., Beutner, K. A., Sieck, C. K., and Bhushan, R. (2007) Guidelines of care for acne vulgaris management. *J. Am. Acad. Dermatol.* **56**, 651-663
61. Lee, S. Y., You, C. E., and Park, M. Y. (2007) Blue and red light combination LED phototherapy for acne vulgaris in patients with skin phototype IV. *Lasers Surg. Med.* **39**, 180-188
62. Davies, J., and Davies, D. (2010) Origins and evolution of antibiotic resistance. *Microbiol. Mol. Biol. Rev.* **74**, 417-433
63. MacLean, R. C., and San Millan, A. (2019) The evolution of antibiotic resistance. *Science* **365**, 1082-1083
64. Fair, R. J., and Tor, Y. (2014) Antibiotics and bacterial resistance in the 21st century. *Perspect. Medicin. Chem.* **6**, 25-64
65. Dreno, B. (2004) Topical Antibacterial Therapy for Acne Vulgaris. *Drugs* **64**, 2389-2397

66. Dreno, B., Thiboutot, D., Gollnick, H., Bettoli, V., Kang, S., Leyden, J. J., Shalita, A., and Torres, V. (2014) Antibiotic stewardship in dermatology: limiting antibiotic use in acne. *Eur. J. Dermatol.* **24**, 330-334
67. Adler, B. L., Kornmehl, H., and Armstrong, A. W. (2017) Antibiotic Resistance in Acne Treatment. *JAMA Dermatology* **153**, 810-811
68. Novickij, V., Zinkevičienė, A., Stanevičienė, R., Gruškienė, R., Servienė, E., Vepštaitė-Monstavičė, I., Krivorotova, T., Lastauskienė, E., Sereikaitė, J., Girkontaitė, I., and Novickij, J. (2018) Inactivation of Escherichia coli Using Nanosecond Electric Fields and Nisin Nanoparticles: A Kinetics Study. *Front. Microbiol.* **9**
69. Wang, T., Chen, H., Yu, C., and Xie, X. (2019) Rapid determination of the electroporation threshold for bacteria inactivation using a lab-on-a-chip platform. *Environ. Int.* **132**, 105040
70. Frey, W., Gusbeth, C., and Schwartz, T. (2013) Inactivation of Pseudomonas putida by Pulsed Electric Field Treatment: A Study on the Correlation of Treatment Parameters and Inactivation Efficiency in the Short-Pulse Range. *J. Membr. Biol.* **246**, 769-781
71. Perni, S., Chalise, P. R., Shama, G., and Kong, M. G. (2007) Bacterial cells exposed to nanosecond pulsed electric fields show lethal and sublethal effects. *Int. J. Food Microbiol.* **120**, 311-314
72. Magnusson, L. U., Farewell, A., and Nyström, T. (2005) ppGpp: a global regulator in Escherichia coli. *Trends Microbiol.* **13**, 236-242
73. Boutte, C. C., and Crosson, S. (2013) Bacterial lifestyle shapes stringent response activation. *Trends Microbiol.* **21**, 174-180
74. Cashel, M., and Gallant, J. (1969) Two Compounds implicated in the Function of the RC Gene of Escherichia coli. *Nature* **221**, 838-841
75. Potrykus, K., and Cashel, M. (2008) (p)ppGpp: Still Magical? *Annu. Rev. Microbiol.* **62**, 35-51
76. Harms, A., Maisonneuve, E., and Gerdes, K. (2016) Mechanisms of bacterial persistence during stress and antibiotic exposure. *Science* **354**, aaf4268
77. Irving, S. E., and Corrigan, R. M. (2018) Triggering the stringent response: signals responsible for activating (p)ppGpp synthesis in bacteria. *Microbiology* **164**, 268-276
78. Dalebroux, Z. D., Svensson, S. L., Gaynor, E. C., and Swanson, M. S. (2010) ppGpp conjures bacterial virulence. *Microbiol. Mol. Biol. Rev.* **74**, 171-199
79. Nanamiya, H., Kasai, K., Nozawa, A., Yun, C.-S., Narisawa, T., Murakami, K., Natori, Y., Kawamura, F., and Tozawa, Y. (2008) Identification and functional analysis of novel (p)ppGpp synthetase genes in Bacillus subtilis. *Mol. Microbiol.* **67**, 291-304
80. Ruwe, M., Rückert, C., Kalinowski, J., and Persicke, M. (2018) Functional Characterization of a Small Alarmone Hydrolase in Corynebacterium glutamicum. *Front. Microbiol.* **9**, 916-916
81. Atkinson, G. C., Tenson, T., and Hauryliuk, V. (2011) The RelA/SpoT Homolog (RSH) Superfamily: Distribution and Functional Evolution of ppGpp Synthetases and Hydrolases across the Tree of Life. *PLoS One* **6**, e23479
82. Das, B., and Bhadra, R. K. (2020) (p)ppGpp Metabolism and Antimicrobial Resistance in Bacterial Pathogens. *Front. Microbiol.* 10.3389/fmicb.2020.563944
83. Hauryliuk, V., Atkinson, G. C., Murakami, K. S., Tenson, T., and Gerdes, K. (2015) Recent functional insights into the role of (p)ppGpp in bacterial physiology. *Nat Rev Microbiol* **13**, 298-309

84. Gaca, A. O., Kudrin, P., Colomer-Winter, C., Beljantseva, J., Liu, K., Anderson, B., Wang, J. D., Rejman, D., Potrykus, K., Cashel, M., Hauryliuk, V., and Lemos, J. A. (2015) From (p)ppGpp to (pp)pGpp: Characterization of Regulatory Effects of pGpp Synthesized by the Small Alarmone Synthetase of Enterococcus faecalis. *J. Bacteriol.* **197**, 2908-2919
85. Yang, J., Anderson, B. W., Turdiev, A., Turdiev, H., Stevenson, D. M., Amador-Noguez, D., Lee, V. T., and Wang, J. D. (2020) The nucleotide pGpp acts as a third alarmone in Bacillus, with functions distinct from those of (p) ppGpp. *Nat.Commun.* **11**, 5388
86. Irving, S. E., Choudhury, N. R., and Corrigan, R. M. (2021) The stringent response and physiological roles of (pp)pGpp in bacteria. *Nat. Rev. Microbiol.* **19**, 256-271
87. Kanjee, U., Gutsche, I., Alexopoulos, E., Zhao, B., El Bakkouri, M., Thibault, G., Liu, K., Ramachandran, S., Snider, J., Pai, E. F., and Houry, W. A. (2011) Linkage between the bacterial acid stress and stringent responses: the structure of the inducible lysine decarboxylase. *EMBO J* **30**, 931-944
88. Abranches, J., Martinez, A. R., Kajfasz, J. K., Chavez, V., Garsin, D. A., and Lemos, J. A. (2009) The molecular alarmone (p)ppGpp mediates stress responses, vancomycin tolerance, and virulence in Enterococcus faecalis. *J. Bacteriol.* **191**, 2248-2256
89. Ma, Z., King, K., Alqahtani, M., Worden, M., Muthuraman, P., Cioffi, C. L., Bakshi, C. S., and Malik, M. (2019) Stringent response governs the oxidative stress resistance and virulence of Francisella tularensis. *PloS one* **14**, e0224094
90. Schäfer, H., Beckert, B., Frese, C. K., Steinchen, W., Nuss, A. M., Beckstette, M., Hantke, I., Driller, K., Sudzinová, P., Krásný, L., Kaever, V., Dersch, P., Bange, G., Wilson, D. N., and Turgay, K. (2020) The alarmones (p)ppGpp are part of the heat shock response of Bacillus subtilis. *PLoS genetics* **16**, e1008275
91. Ronneau, S., and Hallez, R. (2019) Make and break the alarmone: regulation of (p)ppGpp synthetase/hydrolase enzymes in bacteria. *FEMS Microbiol Rev* **43**, 389-400
92. Takada, H., Roghanian, M., Caballero-Montes, J., Van Nerom, K., Jimmy, S., Kudrin, P., Trebini, F., Murayama, R., Akanuma, G., Garcia-Pino, A., and Hauryliuk, V. (2021) Ribosome association primes the stringent factor Rel for tRNA-dependent locking in the A-site and activation of (p)ppGpp synthesis. *Nucleic Acids Res* **49**, 444-457
93. Brown, A., Fernández, I. S., Gordiyenko, Y., and Ramakrishnan, V. (2016) Ribosome-dependent activation of stringent control. *Nature* **534**, 277-280
94. Steinchen, W., Vogt, M. S., Altegoer, F., Giammarinaro, P. I., Horvatek, P., Wolz, C., and Bange, G. (2018) Structural and mechanistic divergence of the small (p)ppGpp synthetases RelP and RelQ. *Sci. Rep.* **8**, 2195
95. Gaca, A. O., Colomer-Winter, C., and Lemos, J. A. (2015) Many means to a common end: the intricacies of (p)ppGpp metabolism and its control of bacterial homeostasis. *J Bacteriol* **197**, 1146-1156
96. Gaca, A. O., Kajfasz, J. K., Miller, J. H., Liu, K., Wang, J. D., Abranches, J., and Lemos, J. A. (2013) Basal Levels of (p)ppGpp in Enterococcus faecalis: the Magic beyond the Stringent Response. *mBio* **4**
97. Kriel, A., Brinsmade, S. R., Tse, J. L., Tehranchi, A. K., Bittner, A. N., Sonenshein, A. L., and Wang, J. D. (2014) GTP dysregulation in Bacillus subtilis cells lacking (p)ppGpp results in phenotypic amino acid auxotrophy and failure to adapt to nutrient downshift and regulate biosynthesis genes. *J. Bacteriol* **196**, 189-201

98. Sajish, M., Kalayil, S., Verma, S. K., Nandicoori, V. K., and Prakash, B. (2009) The significance of EXDD and RXKD motif conservation in Rel proteins. *J. Biol. Chem.* **284**, 9115-9123
99. Petchiappan, A., Naik, S. Y., and Chatterji, D. (2020) RelZ-Mediated Stress Response in Mycobacterium smegmatis: pGpp Synthesis and Its Regulation. *J. Bacteriol.* **202**, e00444-00419
100. Sajish, M., Tiwari, D., Rananaware, D., Nandicoori, V. K., and Prakash, B. (2007) A Charge Reversal Differentiates (p)ppGpp Synthesis by Monofunctional and Bifunctional Rel Proteins. *J. Biol. Chem.* **282**, 34977-34983
101. Geiger, T., Kastle, B., Gratani, F. L., Goerke, C., and Wolz, C. (2014) Two small (p)ppGpp synthases in Staphylococcus aureus mediate tolerance against cell envelope stress conditions. *J. Bacteriol.* **196**, 894-902
102. Ruwe, M., Kalinowski, J., and Persicke, M. (2017) Identification and Functional Characterization of Small Alarmone Synthetases in Corynebacterium glutamicum. *Front. Microbiol.* **8**, 1601-1601
103. Zhang, Y., Zbornikova, E., Rejman, D., and Gerdes, K. (2018) Novel (p)ppGpp Binding and Metabolizing Proteins of Escherichia coli. *mBio* **9**, e02188-02117
104. Ooga, T., Ohashi, Y., Kuramitsu, S., Koyama, Y., Tomita, M., Soga, T., and Masui, R. (2009) Degradation of ppGpp by nudix pyrophosphatase modulates the transition of growth phase in the bacterium Thermus thermophilus. *J. Biol. Chem.* **284**, 15549-15556
105. Poudel, A., Pokhrel, A., Oludiran, A., Coronado, E. J., Alleyne, K., Gilfus, M. M., Gurung, R. K., Adhikari, S. B., and Purcell, E. B. (2021) Unique features of magic spot metabolism in Clostridioides difficile. *bioRxiv*, 2021.2008.2002.454818
106. Pokhrel, A., Poudel, A., Castro, K. B., Celestine, M. J., Oludiran, A., Rinehold, A. J., Resek, A. M., Mhanna, M. A., and Purcell, E. B. (2020) The (p)ppGpp Synthetase RSH Mediates Stationary-Phase Onset and Antibiotic Stress Survival in Clostridioides difficile. *J. Bacteriol.* **202**, JB.00377-00320
107. Poudel, A., Oludiran, A., Sözer, E. B., Casciola, M., Purcell, E. B., and Muratori, C. (2021) Growth in a biofilm sensitizes Cutibacterium acnes to nanosecond pulsed electric fields. *Bioelectrochemistry* **140**, 107797
108. Geiger, T., Goerke, C., Fritz, M., Schafer, T., Ohlsen, K., Liebeke, M., Lalk, M., and Wolz, C. (2010) Role of the (p)ppGpp synthase RSH, a RelA/SpoT homolog, in stringent response and virulence of Staphylococcus aureus. *Infect. Immun.* **78**, 1873-1883
109. Hauryliuk, V., Atkinson, G. C., Murakami, K. S., Tenson, T., and Gerdes, K. (2015) Recent functional insights into the role of (p)ppGpp in bacterial physiology. *Nat. Rev. Microbiol.* **13**, 298-309
110. Jimmy, S., Saha, C. K., Kurata, T., Stavropoulos, C., Oliveira, S. R. A., Koh, A., Cepauskas, A., Takada, H., Rejman, D., Tenson, T., Strahl, H., Garcia-Pino, A., Hauryliuk, V., and Atkinson, G. C. (2020) A widespread toxin−antitoxin system exploiting growth control via alarmone signaling. *Proc. Natl. Acad. Sci. U.S.A.* **117**, 10500-10510
111. Das, B., Pal, R. R., Bag, S., and Bhadra, R. K. (2009) Stringent response in Vibrio cholerae: genetic analysis of spoT gene function and identification of a novel (p)ppGpp synthetase gene. *Mol. Microbiol.* **72**, 380-398
112. Pokhrel, A., Poudel, A., and Purcell, E. B. (2018) A Purification and In Vitro Activity Assay for a (p)ppGpp Synthetase from Clostridium difficile. *J Vis Exp*, e58547

113. Gasteiger, E., Gattiker, A., Hoogland, C., Ivanyi, I., Appel, R. D., and Bairoch, A. (2003) ExPASy: The proteomics server for in-depth protein knowledge and analysis. *Nucleic Acids Res* **31**, 3784-3788
114. Pokhrel, A. (2021) *Evaluating the Role of the Stringent Response Mechanisms in Clostridiodies difficile Survival and Pathogenesis.* PhD Doctoral Dissertation, Chemistry and Biochemistry, Old Dominion University, Norfolk, Virginia, United States, DOI:10.25777/05ee-2b17
115. Schneider, C. A., Rasband, W. S., and Eliceiri, K. W. (2012) NIH Image to ImageJ: 25 years of image analysis. *Nat. Methods* **9**, 671-675
116. Steinchen, W., Schuhmacher, J. S., Altegoer, F., Fage, C. D., Srinivasan, V., Linne, U., Marahiel, M. A., and Bange, G. (2015) Catalytic mechanism and allosteric regulation of an oligomeric (p)ppGpp synthetase by an alarmone. *Proc. Natl. Acad. Sci. U.S.A.* **112**, 13348-13353
117. Manav, M. C., Beljantseva, J., Bojer, M. S., Tenson, T., Ingmer, H., Hauryliuk, V., and Brodersen, D. E. (2018) Structural basis for (p)ppGpp synthesis by the Staphylococcus aureus small alarmone synthetase RelP. *J. Biol. Chem.* **293**, 3254-3264
118. Beljantseva, J., Kudrin, P., Andresen, L., Shingler, V., Atkinson, G. C., Tenson, T., and Hauryliuk, V. (2017) Negative allosteric regulation of Enterococcus faecalis small alarmone synthetase RelQ by single-stranded RNA. *Proc. Natl. Acad. Sci. U. S. A.* **114**, 3726-3731
119. Nardi-Schreiber, A., Sapir, G., Gamliel, A., Kakhlon, O., Sosna, J., Gomori, J. M., Meiner, V., Lossos, A., and Katz-Brull, R. (2017) Defective ATP breakdown activity related to an ENTPD1 gene mutation demonstrated using 31P NMR spectroscopy. *Chem.Commun.* **53**, 9121-9124
120. Spoerner, M., Karl, M., Lopes, P., Hoering, M., Loeffel, K., Nuehs, A., Adelsberger, J., Kremer, W., and Kalbitzer, H. R. (2017) High pressure 31P NMR spectroscopy on guanine nucleotides. *J. Biomol. NMR* **67**, 1-13
121. Liu, Y., Gu, Y., and Yu, X. (2017) Assessing tissue metabolism by phosphorous-31 magnetic resonance spectroscopy and imaging: a methodology review. *Quant Imaging Med Surg* **7**, 707-726
122. Barron, N. L. a. A. R. (2013) P-31 NMR Spectroscopy. creativecommons.org
123. Colomer-Winter, C., Gaca, A. O., and Lemos, J. A. (2017) Association of Metal Homeostasis and (p)ppGpp Regulation in the Pathophysiology of Enterococcus faecalis. *Infect. Immun.* **85**, e00260-00217
124. Miethke, M., Klotz, O., Linne, U., May, J. J., Beckering, C. L., and Marahiel, M. A. (2006) Ferri-bacillibactin uptake and hydrolysis in Bacillus subtilis. *Mol. Microbiol.* **61**, 1413-1427
125. Weiss, G., and Carver, P. L. (2018) Role of divalent metals in infectious disease susceptibility and outcome. *Clin. Microbiol. Infect.* **24**, 16-23
126. Becker, K. W., and Skaar, E. P. (2014) Metal limitation and toxicity at the interface between host and pathogen. *FEMS Microbiol. Rev.* **38**, 1235-1249
127. Gaca, A. O., Colomer-Winter, C., and Lemos, J. A. (2015) Many Means to a Common End: the Intricacies of (p)ppGpp Metabolism and Its Control of Bacterial Homeostasis. *J. Bacteriol.* **197**, 1146-1156

128. Fung, D. K., Yang, J., Stevenson, D. M., Amador-Noguez, D., and Wang, J. D. (2020) Small Alarmone Synthetase SasA Expression Leads to Concomitant Accumulation of pGpp, ppApp, and AppppA in Bacillus subtilis. *Front. Microbiol.* **11**
129. Tagami, K., Nanamiya, H., Kazo, Y., Maehashi, M., Suzuki, S., Namba, E., Hoshiya, M., Hanai, R., Tozawa, Y., Morimoto, T., Ogasawara, N., Kageyama, Y., Ara, K., Ozaki, K., Yoshida, M., Kuroiwa, H., Kuroiwa, T., Ohashi, Y., and Kawamura, F. (2012) Expression of a small (p)ppGpp synthetase, YwaC, in the (p)ppGpp(0) mutant of Bacillus subtilis triggers YvyD-dependent dimerization of ribosome. *MicrobiologyOpen* **1**, 115-134
130. Yang, N., Xie, S., Tang, N.-Y., Choi, M. Y., Wang, Y., and Watt, R. M. (2019) The Ps and Qs of alarmone synthesis in Staphylococcus aureus. *PLoS One* **14**, e0213630
131. Avarbock, D., Avarbock, A., and Rubin, H. (2000) Differential Regulation of Opposing RelMtb Activities by the Aminoacylation State of a tRNA·Ribosome·mRNA·RelMtb Complex. *Biochemistry* **39**, 11640-11648
132. Sobala, M., Bruhn-Olszewska, B., Cashel, M., and Potrykus, K. (2019) Methylobacterium extorquens RSH Enzyme Synthesizes (p)ppGpp and pppApp in vitro and in vivo, and Leads to Discovery of pppApp Synthesis in Escherichia coli. *Front. Microbiol.* **10**, 859-859
133. Weiss, L. A., and Stallings, C. L. (2013) Essential roles for Mycobacterium tuberculosis Rel beyond the production of (p)ppGpp. *J. Bacteriol.* **195**, 5629-5638
134. Miethke, M., Westers, H., Blom, E.-J., Kuipers, O. P., and Marahiel, M. A. (2006) Iron starvation triggers the stringent response and induces amino acid biosynthesis for bacillibactin production in Bacillus subtilis. *J. Bacteriol.* **188**, 8655-8657
135. Krishnan, S., and Chatterji, D. (2020) Pleiotropic Effects of Bacterial Small Alarmone Synthetases: Underscoring the Dual-Domain Small Alarmone Synthetases in Mycobacterium smegmatis. *Front Microbiol* **11**, 594024
136. Syal, K., Flentie, K., Bhardwaj, N., Maiti, K., Jayaraman, N., Stallings, C. L., and Chatterji, D. (2017) Synthetic (p)ppGpp Analogue Is an Inhibitor of Stringent Response in Mycobacteria. *Antimicrob. Agents Chemother.* **61**, e00443-00417
137. Wexselblatt, E., Oppenheimer-Shaanan, Y., Kaspy, I., London, N., Schueler-Furman, O., Yavin, E., Glaser, G., Katzhendler, J., and Ben-Yehuda, S. (2012) Relacin, a novel antibacterial agent targeting the Stringent Response. *PLoS Pathog.* **8**, e1002925-e1002925
138. Dutta, N. K., Klinkenberg, L. G., Vazquez, M.-J., Segura-Carro, D., Colmenarejo, G., Ramon, F., Rodriguez-Miquel, B., Mata-Cantero, L., Porras-De Francisco, E., Chuang, Y.-M., Rubin, H., Lee, J. J., Eoh, H., Bader, J. S., Perez-Herran, E., Mendoza-Losana, A., and Karakousis, P. C. (2019) Inhibiting the stringent response blocks Mycobacterium tuberculosis entry into quiescence and reduces persistence. *Sci Adv* **5**, eaav2104-eaav2104
139. Schäfer, H., Beckert, B., Frese, C. K., Steinchen, W., Nuss, A. M., Beckstette, M., Hantke, I., Driller, K., Sudzinová, P., Krásný, L., Kaever, V., Dersch, P., Bange, G., Wilson, D. N., and Turgay, K. (2020) The alarmones (p)ppGpp are part of the heat shock response of Bacillus subtilis. *PLoS Genet.* **16**, e1008275
140. Ma, Z., King, K., Alqahtani, M., Worden, M., Muthuraman, P., Cioffi, C. L., Bakshi, C. S., and Malik, M. (2019) Stringent response governs the oxidative stress resistance and virulence of Francisella tularensis. *PLoS One* **14**, e0224094-e0224094
141. Kanjee, U., Gutsche, I., Alexopoulos, E., Zhao, B., El Bakkouri, M., Thibault, G., Liu, K., Ramachandran, S., Snider, J., Pai, E. F., and Houry, W. A. (2011) Linkage between the

bacterial acid stress and stringent responses: the structure of the inducible lysine decarboxylase. *EMBO J.* **30**, 931-944

142. Aedo, S., and Tomasz, A. (2016) Role of the Stringent Stress Response in the Antibiotic Resistance Phenotype of Methicillin-Resistant Staphylococcus aureus. *Antimicrob. Agents Chemother.* **60**, 2311-2317
143. Corrigan, R. M., Bellows, L. E., Wood, A., and Gründling, A. (2016) ppGpp negatively impacts ribosome assembly affecting growth and antimicrobial tolerance in Gram-positive bacteria. *Proc. Natl. Acad. Sci. U.S.A.* **113**, E1710-E1719
144. Nguyen, D., Joshi-Datar, A., Lepine, F., Bauerle, E., Olakanmi, O., Beer, K., McKay, G., Siehnel, R., Schafhauser, J., Wang, Y., Britigan, B. E., and Singh, P. K. (2011) Active Starvation Responses Mediate Antibiotic Tolerance in Biofilms and Nutrient-Limited Bacteria. *Science* **334**, 982-986
145. Hammer, B. K., Tateda, E. S., and Swanson, M. S. (2002) A two-component regulator induces the transmission phenotype of stationary-phase Legionella pneumophila. *Mol. Microbiol.* **44**, 107-118
146. Pizarro-Cerdá, J., and Tedin, K. (2004) The bacterial signal molecule, ppGpp, regulates Salmonella virulence gene expression. *Mol. Microbiol.* **52**, 1827-1844
147. Vogt, S. L., Green, C., Stevens, K. M., Day, B., Erickson, D. L., Woods, D. E., and Storey, D. G. (2011) The stringent response is essential for Pseudomonas aeruginosa virulence in the rat lung agar bead and Drosophila melanogaster feeding models of infection. *Infect. Immun.* **79**, 4094-4104
148. Pulschen, A. A., Sastre, D. E., Machinandiarena, F., Crotta Asis, A., Albanesi, D., de Mendoza, D., and Gueiros-Filho, F. J. (2017) The stringent response plays a key role in Bacillus subtilis survival of fatty acid starvation. *Mol. Microbiol.* **103**, 698-712
149. Hobbs, J. K., and Boraston, A. B. (2019) (p)ppGpp and the Stringent Response: An Emerging Threat to Antibiotic Therapy. *ACS Infect. Dis.* **5**, 1505-1517
150. Ronneau, S., and Hallez, R. (2019) Make and break the alarmone: regulation of (p)ppGpp synthetase/hydrolase enzymes in bacteria. *FEMS Microbiol. Rev.* **43**, 389-400
151. Thackray, P. D., and Moir, A. (2003) SigM, an extracytoplasmic function sigma factor of Bacillus subtilis, is activated in response to cell wall antibiotics, ethanol, heat, acid, and superoxide stress. *J. Bacteriol.* **185**, 3491-3498
152. Gaca, A. O., Kajfasz, J. K., Miller, J. H., Liu, K., Wang, J. D., Abranches, J., and Lemos, J. A. (2013) Basal levels of (p)ppGpp in Enterococcus faecalis: the magic beyond the stringent response. *mBio* **4**, e00646-00613
153. Denève, C., Deloménie, C., Barc, M.-C., Collignon, A., and Janoir, C. (2008) Antibiotics involved in Clostridium difficile-associated disease increase colonization factor gene expression. *J. Med. Microbiol.* **57**, 732-738
154. Vardakas, K. Z., Polyzos, K. A., Patouni, K., Rafailidis, P. I., Samonis, G., and Falagas, M. E. (2012) Treatment failure and recurrence of Clostridium difficile infection following treatment with vancomycin or metronidazole: a systematic review of the evidence. *Int. J. Antimicrob. Agents* **40**, 1-8
155. Buckley, A. M., Jukes, C., Candlish, D., Irvine, J. J., Spencer, J., Fagan, R. P., Roe, A. J., Christie, J. M., Fairweather, N. F., and Douce, G. R. (2016) Lighting Up Clostridium Difficile: Reporting Gene Expression Using Fluorescent Lov Domains. *Sci. Rep.* **6**, 23463

156. Purcell, E. B., McKee, R. W., McBride, S. M., Waters, C. M., and Tamayo, R. (2012) Cyclic diguanylate inversely regulates motility and aggregation in Clostridium difficile. *J. Bacteriol.* **194**, 3307-3316
157. Hussain, H. A., Roberts, A. P., and Mullany, P. (2005) Generation of an erythromycin-sensitive derivative of Clostridium difficile strain 630 (630Δerm) and demonstration that the conjugative transposon Tn916ΔE enters the genome of this strain at multiple sites. *J. Med. Microbiol.* **54**, 137-141
158. Singh, T., Bedi, P., Bumrah, K., Singh, J., Rai, M., and Seelam, S. (2019) Updates in Treatment of Recurrent Clostridium difficile Infection. *J. Clin. Med. Res.* **11**, 465-471
159. Stevens, V. W., Khader, K., Echevarria, K., Nelson, R. E., Zhang, Y., Jones, M., Timbrook, T. T., Samore, M. H., and Rubin, M. A. (2020) Use of Oral Vancomycin for Clostridioides difficile Infection and the Risk of Vancomycin-Resistant Enterococci. *Clin. Infect. Dis.* **71**, 645-651
160. Al-Jashaami, L. S., and DuPont, H. L. (2016) Management of Clostridium difficile Infection. *Gastroenterol Hepatol (N Y)* **12**, 609-616
161. Oludiran, A., Courson, D. S., Stuart, M. D., Radwan, A. R., Poutsma, J. C., Cotten, M. L., and Purcell, E. B. (2019) How Oxygen Availability Affects the Antimicrobial Efficacy of Host Defense Peptides: Lessons Learned from Studying the Copper-Binding Peptides Piscidins 1 and 3. *Int. J. Mol. Sci.* **20**, 5289
162. Rocha, E. R., Tzianabos, A. O., and Smith, C. J. (2007) Thioredoxin reductase is essential for thiol/disulfide redox control and oxidative stress survival of the anaerobe Bacteroides fragilis. *J. Bacteriol.* **189**, 8015-8023
163. Andreini, C., Bertini, I., Cavallaro, G., Holliday, G. L., and Thornton, J. M. (2008) Metal ions in biological catalysis: from enzyme databases to general principles. *J. Biol. Inorg. Chem.* **13**, 1205-1218
164. Kehl-Fie, T. E., and Skaar, E. P. (2010) Nutritional immunity beyond iron: a role for manganese and zinc. *Curr. Opin. Chem. Biol.* **14**, 218-224
165. Skaar, E. P. (2010) The battle for iron between bacterial pathogens and their vertebrate hosts. *PLoS Pathog.* **6**, e1000949-e1000949
166. Dréno, B., Pécastaings, S., Corvec, S., Veraldi, S., Khammari, A., and Roques, C. (2018) Cutibacterium acnes (Propionibacterium acnes) and acne vulgaris: a brief look at the latest updates. *J. Eur. Acad. Dermatol. Venereol.* **32**, 5-14
167. Szabó, K., Erdei, L., Bolla, B. S., Tax, G., Bíró, T., and Kemény, L. (2017) Factors shaping the composition of the cutaneous microbiota. *Br. J. Dermatol.* **176**, 344-351
168. Toyoda, M., and Morohashi, M. (2001) Pathogenesis of acne. *Med. Electron Microsc.* **34**, 29-40
169. Sale, A. J., and Hamilton, W. A. (1967) Effects of high electric fields on microorganisms: I. Killing of bacteria and yeasts. *Biochim. Biophys. Acta* **148**, 781-788
170. Mahnič-Kalamiza, S., Vorobiev, E., and Miklavčič, D. (2014) Electroporation in Food Processing and Biorefinery. *J. Membr. Biol.* **247**, 1279-1304
171. Gusbeth, C., Frey, W., Volkmann, H., Schwartz, T., and Bluhm, H. (2009) Pulsed electric field treatment for bacteria reduction and its impact on hospital wastewater. *Chemosphere* **75**, 228-233
172. Batista Napotnik, T., Reberšek, M., Vernier, P. T., Mali, B., and Miklavčič, D. (2016) Effects of high voltage nanosecond electric pulses on eukaryotic cells (in vitro): A systematic review. *Bioelectrochemistry* **110**, 1-12

173. Beebe, S. J., Chen, Y.-J., Sain, N. M., Schoenbach, K. H., and Xiao, S. (2012) Transient features in nanosecond pulsed electric fields differentially modulate mitochondria and viability. *PLoS One* **7**, e51349-e51349
174. Thompson, G. L., Roth, C. C., Kuipers, M. A., Tolstykh, G. P., Beier, H. T., and Ibey, B. L. (2016) Permeabilization of the nuclear envelope following nanosecond pulsed electric field exposure. *Biochem. Biophys. Res. Commun.* **470**, 35-40
175. Beebe, S. J., and Schoenbach, K. H. (2005) Nanosecond pulsed electric fields: a new stimulus to activate intracellular signaling. *J Biomed Biotechnol* **2005**, 297-300
176. Weaver, J. C., and Chizmadzhev, Y. A. (1996) Theory of electroporation: A review. *Bioelectrochem. Bioenerg.* **41**, 135-160
177. Liu, Z., Zhao, L., Zhang, Q., Huo, N., Shi, X., Li, L., Jia, L., Lu, Y., Peng, Y., and Song, Y. (2019) Proteomics-Based Mechanistic Investigation of Escherichia coli Inactivation by Pulsed Electric Field. *Front. Microbiol.* **10**
178. Ibey, B. L., Roth, C. C., Pakhomov, A. G., Bernhard, J. A., Wilmink, G. J., and Pakhomova, O. N. (2011) Dose-Dependent Thresholds of 10-ns Electric Pulse Induced Plasma Membrane Disruption and Cytotoxicity in Multiple Cell Lines. *PLoS One* **6**, e15642
179. Muratori, C., Pakhomov, A. G., Xiao, S., and Pakhomova, O. N. (2016) Electrosensitization assists cell ablation by nanosecond pulsed electric field in 3D cultures. *Sci. Rep.* **6**, 23225
180. Rossi, A., Pakhomova, O. N., Mollica, P. A., Casciola, M., Mangalanathan, U., Pakhomov, A. G., and Muratori, C. (2019) Nanosecond Pulsed Electric Fields Induce Endoplasmic Reticulum Stress Accompanied by Immunogenic Cell Death in Murine Models of Lymphoma and Colorectal Cancer. *Cancers (Basel)* **11**, 2034
181. Rossi, A., Pakhomova, O. N., Pakhomov, A. G., Weygandt, S., Bulysheva, A. A., Murray, L. E., Mollica, P. A., and Muratori, C. (2019) Mechanisms and immunogenicity of nsPEF-induced cell death in B16F10 melanoma tumors. *Sci. Rep.* **9**, 431-431
182. Beebe, S. J., Fox, P. M., Rec, L. J., Willis, E. L. K., and Schoenbach, K. H. (2003) Nanosecond, high-intensity pulsed electric fields induce apoptosis in human cells. *The FASEB Journal* **17**, 1493-1495
183. Guionet, A., Joubert-Durigneux, V., Packan, D., Cheype, C., Garnier, J.-P., David, F., Zaepffel, C., Leroux, R.-M., Teissié, J., and Blanckaert, V. (2014) Effect of nanosecond pulsed electric field on Escherichia coli in water: inactivation and impact on protein changes. *J. Appl. Microbiol.* **117**, 721-728
184. Vadlamani, A., Detwiler, D. A., Dhanabal, A., and Garner, A. L. (2018) Synergistic bacterial inactivation by combining antibiotics with nanosecond electric pulses. *Appl. Microbiol. Biotechnol.* **102**, 7589-7596
185. Bossard, D. A., Ledergerber, B., Zingg, P. O., Gerber, C., Zinkernagel, A. S., Zbinden, R., Achermann, Y., and Patel, R. (2016) Optimal Length of Cultivation Time for Isolation of Propionibacterium acnes in Suspected Bone and Joint Infections Is More than 7 Days. *J. Clin. Microbiol.* **54**, 3043-3049
186. Purcell, E. B., McKee, R. W., Bordeleau, E., Burrus, V., and Tamayo, R. (2015) Regulation of Type IV Pili Contributes to Surface Behaviors of Historical and Epidemic Strains of Clostridium difficile. *J. Bacteriol.* **198**, 565-577
187. Gianulis, E. C., Labib, C., Saulis, G., Novickij, V., Pakhomova, O. N., and Pakhomov, A. G. (2017) Selective susceptibility to nanosecond pulsed electric field (nsPEF) across different human cell types. *Cell. Mol. Life Sci.* **74**, 1741-1754

188. Michel, O., Pakhomov, A. G., Casciola, M., Saczko, J., Kulbacka, J., and Pakhomova, O. N. (2020) Electropermeabilization does not correlate with plasma membrane lipid oxidation. *Bioelectrochemistry* **132**, 107433
189. Courson, D. S., Pokhrel, A., Scott, C., Madrill, M., Rinehold, A. J., Tamayo, R., Cheney, R. E., and Purcell, E. B. (2019) Single cell analysis of nutrient regulation of Clostridioides (Clostridium) difficile motility. *Anaerobe* **59**, 205-211
190. Oludiran, A. C., D.S.; Stuart, M.D.; Radwan, A.R.; Poutsma, J.C.; Cotten, M.L.; Purcell, E.B. (2019) How Oxygen Availability Affects the Antimicrobial Efficacy of Host Defense Peptides: Lessons Learned from Studying the Copper-Binding Peptides Piscidins 1 and 3. *Int. J. Mol. Sci.* **20**, 5289
191. Costerton, J. W., Cheng, K. J., Geesey, G. G., Ladd, T. I., Nickel, J. C., Dasgupta, M., and Marrie, T. J. (1987) Bacterial Biofilms in Nature and Disease. *Annu. Rev. Microbiol.* **41**, 435-464
192. Bossard, D. A., Ledergerber, B., Zingg, P. O., Gerber, C., Zinkernagel, A. S., Zbinden, R., and Achermann, Y. (2016) Optimal Length of Cultivation Time for Isolation of Propionibacterium acnes in Suspected Bone and Joint Infections Is More than 7 Days. *J. Clin. Microbiol.* **54**, 3043-3049
193. Schäfer, P., Fink, B., Sandow, D., Margull, A., Berger, I., and Frommelt, L. (2008) Prolonged Bacterial Culture to Identify Late Periprosthetic Joint Infection: A Promising Strategy. *Clin. Infect. Dis.* **47**, 1403-1409
194. María Eugenia Portillo, S. C., Olivier Borens and Andrej Trampuz. (2013) Propionibacterium acnes: An Underestimated Pathogen inImplant-Associated Infections. *BioMed Res. Int.*
195. Shannon, S. K., Mandrekar, J., Gustafson, D. R., Rucinski, S. L., Dailey, A. L., Segner, R. E., Burman, M. K., Boelman, K. J., Lynch, D. T., Rosenblatt, J. E., and Patel, R. (2013) Anaerobic Thioglycolate Broth Culture for Recovery of Propionibacterium acnes from Shoulder Tissue and Fluid Specimens. *J. Clin. Microbiol.* **51**, 731-732
196. Dora, C., Altwegg, M., Gerber, C., Böttger, E. C., and Zbinden, R. (2008) Evaluation of Conventional Microbiological Procedures and Molecular Genetic Techniques for Diagnosis of Infections in Patients with Implanted Orthopedic Devices. *J. Clin. Microbiol.* **46**, 824-825
197. Smith, C. J., Markowitz, S. M., and Macrina, F. L. (1981) Transferable tetracycline resistance in Clostridium difficile. *Antimicrob. Agents Chemother.* **19**, 997-1003
198. Deschler, E. K., Thompson, P. P., and Kowalski, R. P. (2012) Evaluation of the new OxyPlate™ Anaerobic System for the isolation of ocular anaerobic bacteria. *Int J Ophthalmol* **5**, 582-585
199. Achermann, Y., Goldstein, E. J. C., Coenye, T., and Shirtliff, M. E. (2014) Propionibacterium acnes: from Commensal to Opportunistic Biofilm-Associated Implant Pathogen. *Clin. Microbiol. Rev.* **27**, 419
200. Boisrenoult, P. (2018) Cutibacterium acnes prosthetic joint infection: Diagnosis and treatment. *Orthop. Traumatol. Surg. Res.* **104**, S19-S24
201. Cove, J. H., Holland, K. T., and Cunliffe, W. J. (1983) Effects of Oxygen Concentration on Biomass Production, Maximum Specific Growth Rate and Extracellular Enzyme Production by Three Species of Cutaneous Propionibacteria Grown in Continuous Culture. *Microbiology* **129**, 3327-3334

202. Schlecht, S., Freudenberg, M. A., and Galanos, C. (1997) Culture and biological activity ofPropionibacterium acnes. *Infection* **25**, 247-249
203. Pyne, M. E., Moo-Young, M., Chung, D. A., and Chou, C. P. (2013) Development of an electrotransformation protocol for genetic manipulation of Clostridium pasteurianum. *Biotechnol Biofuels* **6**, 50-50
204. Aune, T. E. V., and Aachmann, F. L. (2010) Methodologies to increase the transformation efficiencies and the range of bacteria that can be transformed. *Appl. Microbiol. Biotechnol.* **85**, 1301-1313
205. Varahan, S., Iyer, V. S., Moore, W. T., and Hancock, L. E. (2013) Eep Confers Lysozyme Resistance to Enterococcus faecalis via the Activation of the Extracytoplasmic Function Sigma Factor SigV. *J. Bacteriol.* **195**, 3125-3134
206. Liao, A.-H., Hung, C.-R., Lin, C.-F., Lin, Y.-C., and Chen, H.-K. (2017) Treatment effects of lysozyme-shelled microbubbles and ultrasound in inflammatory skin disease. *Sci. Rep.* **7**, 41325-41325
207. Hoq, M. I., Mitsuno, K., Tsujino, Y., Aoki, T., and Ibrahim, H. R. (2008) Triclosan–lysozyme complex as novel antimicrobial macromolecule: A new potential of lysozyme as phenolic drug-targeting molecule. *Int. J. Biol. Macromol.* **42**, 468-477
208. Pakhomova, O. N., Gregory, B., Semenov, I., and Pakhomov, A. G. (2014) Calcium-mediated pore expansion and cell death following nanoelectroporation. *Biochim. Biophys. Acta Biomembr.* **1838**, 2547-2554
209. Khan, S. I., Blumrosen, G., Vecchio, D., Golberg, A., McCormack, M. C., Yarmush, M. L., Hamblin, M. R., and Austen, W. G., Jr. (2016) Eradication of multidrug-resistant pseudomonas biofilm with pulsed electric fields. *Biotechnol. Bioeng.* **113**, 643-650
210. Schmidt-Malan, S. M., Karau, M. J., Cede, J., Greenwood-Quaintance, K. E., Brinkman, C. L., Mandrekar, J. N., and Patel, R. (2015) Antibiofilm Activity of Low-Amperage Continuous and Intermittent Direct Electrical Current. *Antimicrob. Agents Chemother.* **59**, 4610-4615
211. Brinkman, C. L., Schmidt-Malan, S. M., Karau, M. J., Greenwood-Quaintance, K., Hassett, D. J., Mandrekar, J. N., and Patel, R. (2016) Exposure of Bacterial Biofilms to Electrical Current Leads to Cell Death Mediated in Part by Reactive Oxygen Species. *PLoS One* **11**, e0168595
212. Blenkinsopp, S. A., Khoury, A. E., and Costerton, J. W. (1992) Electrical enhancement of biocide efficacy against Pseudomonas aeruginosa biofilms. *Appl. Environ. Microbiol.* **58**, 3770-3773
213. Vadlamani, R. A., Dhanabal, A., Detwiler, D. A., Pal, R., McCarthy, J., Seleem, M. N., and Garner, A. L. (2020) Nanosecond electric pulses rapidly enhance the inactivation of Gram-negative bacteria using Gram-positive antibiotics. *Appl. Microbiol. Biotechnol.* **104**, 2217-2227
214. Martens, S. L., Klein, S., Barnes, R. A., TrejoSanchez, P., Roth, C. C., and Ibey, B. L. (2020) 600-ns pulsed electric fields affect inactivation and antibiotic susceptibilities of Escherichia coli and Lactobacillus acidophilus. *AMB Express* **10**, 55-55
215. Gannesen, A. V., Zdorovenko, E. L., Botchkova, E. A., Hardouin, J., Massier, S., Kopitsyn, D. S., Gorbachevskii, M. V., Kadykova, A. A., Shashkov, A. S., Zhurina, M. V., Netrusov, A. I., Knirel, Y. A., Plakunov, V. K., and Feuilloley, M. G. J. (2019) Composition of the Biofilm Matrix of Cutibacterium acnes Acneic Strain RT5. *Front. Microbiol.* **10**

216. Hall-Stoodley, L., Costerton, J. W., and Stoodley, P. (2004) Bacterial biofilms: from the Natural environment to infectious diseases. *Nature Reviews Microbiology* **2**, 95-108
217. Karygianni, L., Ren, Z., Koo, H., and Thurnheer, T. (2020) Biofilm Matrixome: Extracellular Components in Structured Microbial Communities. *Trends Microbiol.*
218. Tieleman, D. P. (2004) The molecular basis of electroporation. *BMC Biochem.* **5**, 10
219. Del Pozo, J. L., Rouse, M. S., and Patel, R. (2008) Bioelectric effect and bacterial biofilms. A systematic review. *Int. J. Artif. Organs* **31**, 786-795
220. Kuehnast, T., Cakar, F., Weinhäupl, T., Pilz, A., Selak, S., Schmidt, M. A., Rüter, C., and Schild, S. (2018) Comparative analyses of biofilm formation among different Cutibacterium acnes isolates. *Int. J. Med. Microbiol.* **308**, 1027-1035

APPENDIX A

STRAINS AND PLASMIDS

Name	Description	Reference
Escherichia coli		
BL21	fhuA2 [lon] ompT gal [dcm] ΔhsdS	New England Biolabs (NEB)
DH5α	F-φ80lacZΔM15 Δ(lacZYA-argF)U169 recA1 endA1 hsdR17(r-, m+) phoA supE44 thi-1 gyrA96 relA1 λ-tonA	NEB
HB101		NEB
HB101 pRK24	HB101 transformed with pRK24	(160)
EP036	pMMBneo::R20291_relQ-His6 in BL21	This study
EP056	pET24a::R20291_relQ-His6 in BL21	This study
Clostridioides difficile		
630Δerm	Wild type 630 lacking erythromycin resistance gene *ermB*	(161)
R20291	Wild type	
CEP 18	pRF185::phiLOV2.1 in R20291	(107)
CEP 19	pRF185::phiLOV2.1 in 630Δerm	(107)
CEP 21	PrelQ630Δerm::phiLOV2.1 in R20291	(107)
CEP 22	Prsh630Δerm::phiLOV2.1 in 630Δerm	(107)
CEP 23	PrelQ630Δerm::phiLOV2.1 in 630Δerm	(107)
CEP25	PrshR20291::phiLOV2.1 in R20291	(107)
Cutibacterium acnes		
C. acnes ATCC 29399	Isolated from human forehead	American Type Culture Collection, Manassass VA
Plasmids		
pMMBneo	Low copy expression vector, Ptac, neo casettee, kanR	(113)

pET24a	Expression vector via T7 promoter, kanR	Novagen
pRF185	tetR	(159)
pMMBneo::relQ	R20291 relQ ligated into KpnI/PstI sites of pMMBneo	This study
pRF185::phiLOV2.1	phiLOV2.1 downstream of tetracycline-inducible promoter ligated into BamHI/KpnI sites of pRF185	(107)
PrelQ630Δerm::phiLOV2.1	Predicted promoter upstream of 630Δerm relQamplified and ligated into BamHI/KpnI sites of pRF185::phiLOV2. 1	(107)
Prsh630Δerm::phiLOV2.1	Predicted promoter upstream of 630Δermrshamplified and ligated into BamHI/KpnI sites of pRF185::phiLOV2.1	(107)
PrshR20291::phiLOV2.1	Predicted promoter upstream of R20291 rshamplified and ligated into BamHI/KpnIsites of pRF185::phiLOV2.1	(107)
pET28::SAS1	pET28 plasmid carrying *Bacillus subtilis* SAS1 gene	Generously obtained from Mingxu Fang, University of California, San Diego and Carl E. Bauer, Indiana University, Bloomington

APPENDIX B

OLIGONUCLEOTIDE PRIMER SEQUENCES

Name	Sequence (5’ to 3’)	Reference
5relQ_NdeI	TACATATGGAATACGAAAAATGG	This study
3relQ_XhoI	GTGCTCGAGCTGAACTACTTTATC	This study
relQ_a_F	CAGGTACCAGCAATATGGAATACGAAAAATGGA	This study
relQ_a_R	CCCTGCAGCTAATGGTGATGGTGATGGTGCTGAACTACTTTATCATC	This study
relQ_F	CAAGAATTCCACTATGGAGCTTGTAATCA	(107)
relQ_R	CAAGGATCCCATATTGCTCACCCTTTATTTG	(107)
pRF185_F	CTGGACTTCATGAAAAACTAAAAAAAATATTG	(107)
pRF185_R	CACCGACGAGCAAGGCAAGACCG	(107)
phiLOV2.1_F	GCTAGCCCAGGTATGATTGAAAAAAGTTTTGTTATTACTG	(107)
phiLOV2.1_R	CATGGATCCTTATTAAACATGATCTG	(107)
Prsh_F BamHI	TATAGGATCCGGAAAGTTACCAGGTGAAGTTGA	(107)
Prsh_R KpnI	ATATGGTACCCCACCTATTTTGTATAAAATTTTAATATATATG	(107)
PrelQ_F BamHI	TATAGGATCCATGGCAAGCAAGTTATATCG	(107)
PrelQ_R KpnI	ATATGGTACCCCTTTATTTGTTTTTTATGACCTTC	(107)
pMMB_F	CGACATCATAACGGTTCTGG	This study
pMMB_R	TTCACTTCTGAGTTCGGCAT	This study

APPENDIX C

CdRelQ OVEREXPRESSION DOES NOT ARREST *E. COLI* GROWTH

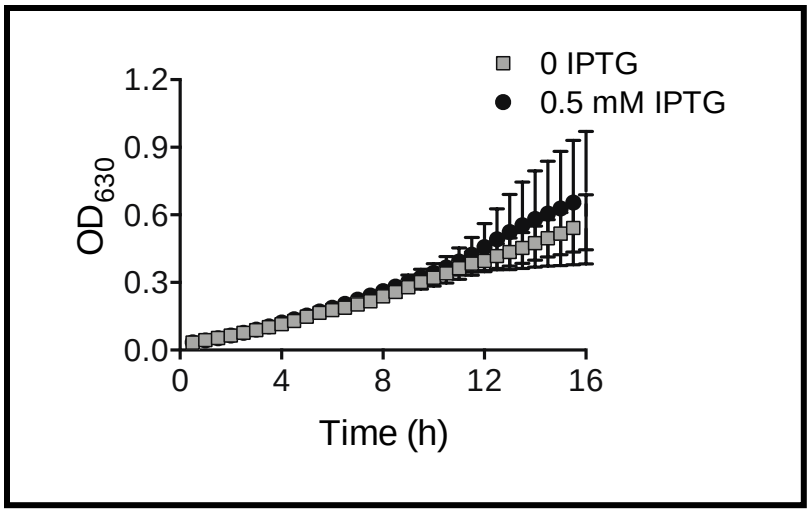

Growth of *E. coli* BL21 carrying pMMBneo::CdRelQ-His6 in the absence of presence of 0.5 mM IPTG inducer. Shown are the means and standard deviations of two biologically independent samples measured in triplicate, with one contaminated sample excluded from analysis. Adapted from Poudel *et al.* 2021.(105)

APPENDIX D

ITC THERMOGRAM AND WISEMAN PLOTS OF CDRELQ INTERACTIONS WITH GXP AT 37°C

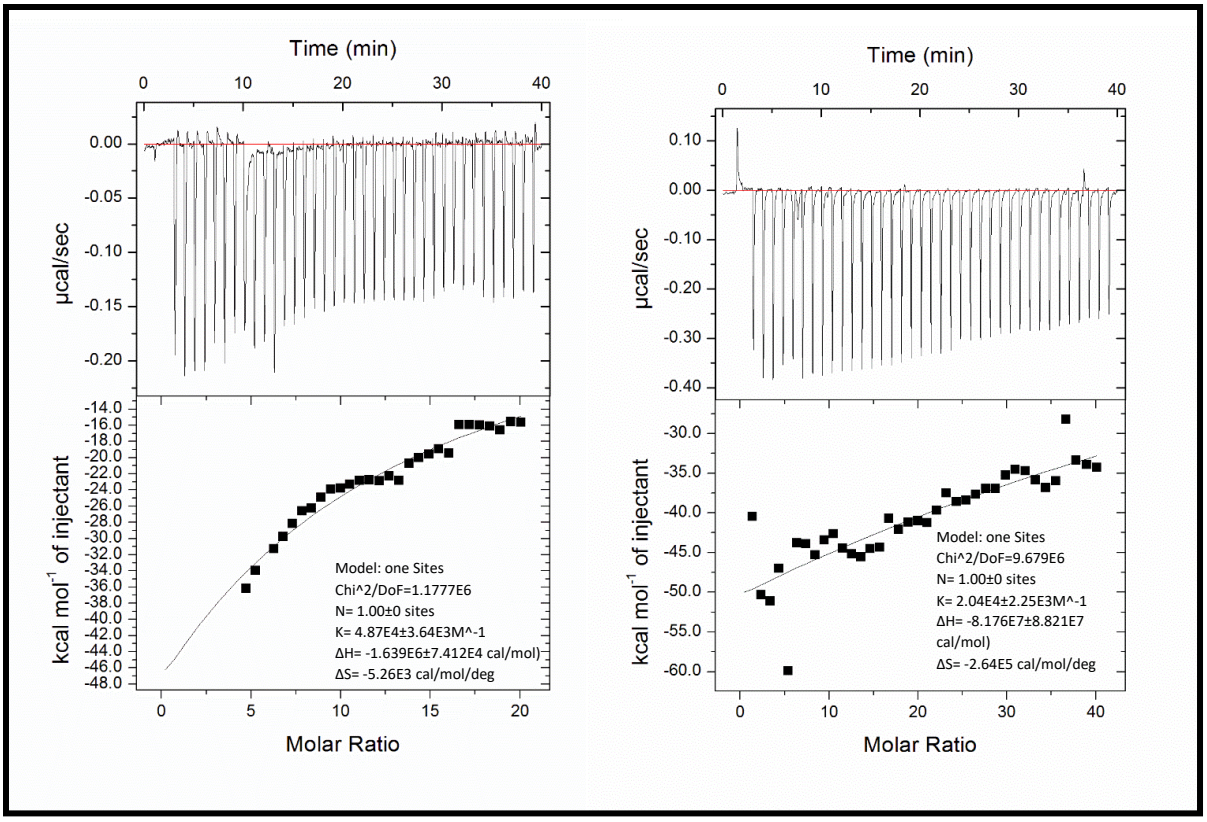

Binding of CdRelQ to GTP (left) and GDP (right). The upper panels show raw data for titration of GXP with CdRelQ, and the lower panels show the integrated heats of binding obtained from the raw data. The data were fitted to a single-binding site model. Each value is the average of three repeat experiments and the standard deviation ± are shown.

APPENDIX E

CdRelQ SYNTHETASE PRODUCTS ARE ALKALI LABILE

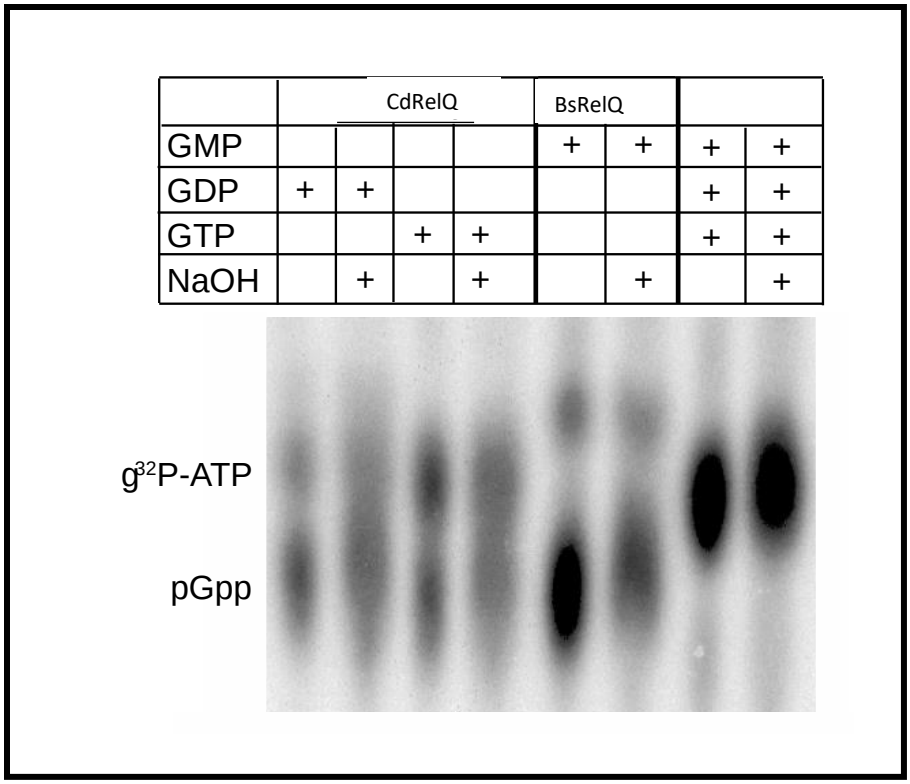

Pyrophosphotransfer reactions were treated with 0.4M NaOH, leading to dissolution of distinct pGpp spots.

APPENDIX F

NMR SPECTRA OF NUCLEOTIDE STANDARDS

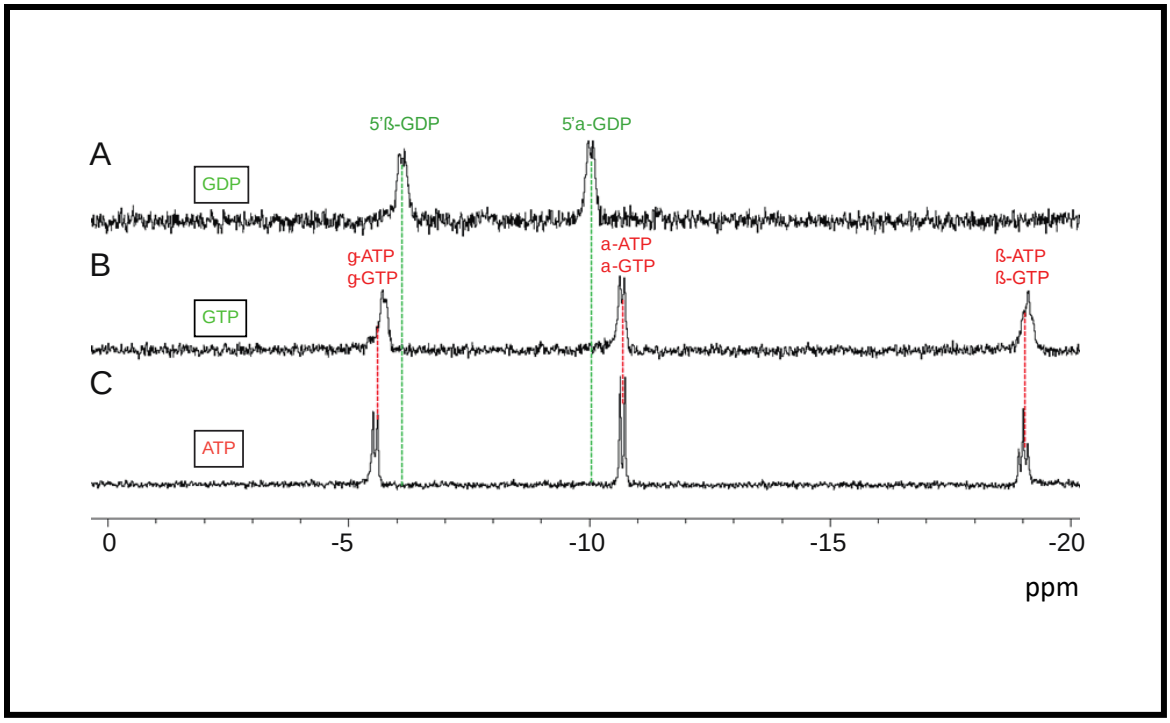

^{31}P NMR spectra of (A) GDP, (B) GTP, and (C) ATP.

APPENDIX G

SUBLETHAL CONCENTRATION OF ANTIBIOTICS

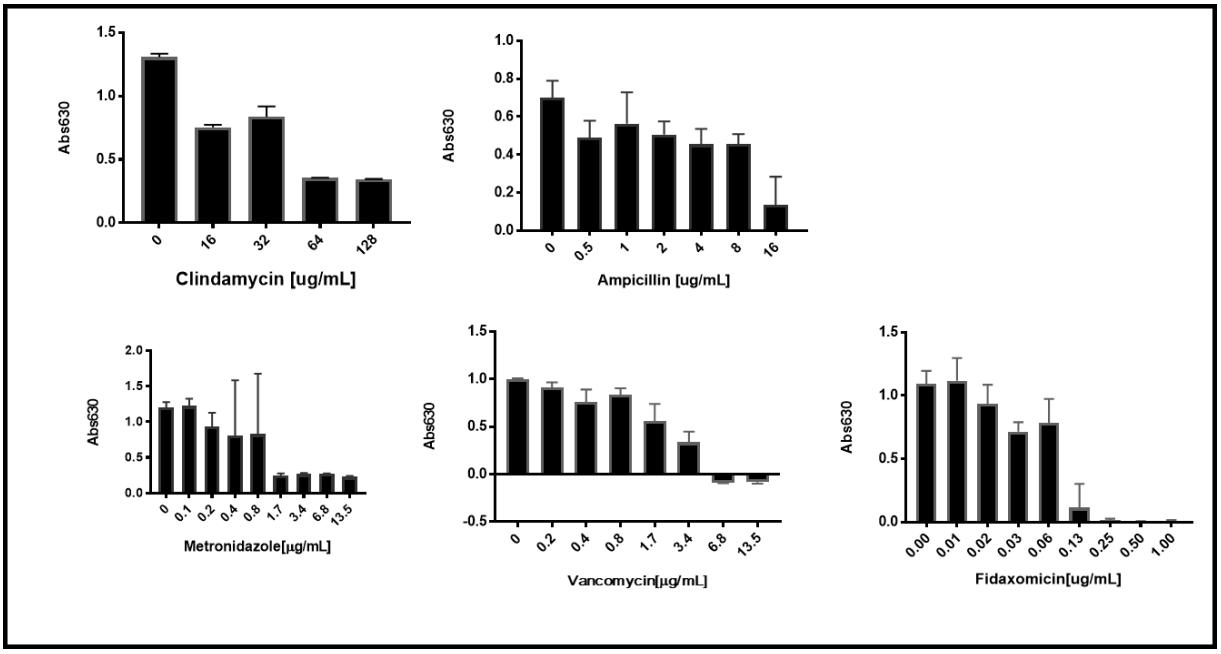

Sublethal concentration	Clindamycin (µg/mL)	Ampicillin (µg/mL)	Metronidazole (µg/mL)	Vancomycin (µg/mL)	Fidaxomicin (µg/mL)
0.25X	4.00	2.00	0.075	0.43	0.17
0.5X	8.00	4.00	0.15	0.85	0.33
1.0X	16.00	8.00	0.30	1.70	0.67

C. difficile R20291 cell density after overnight growth in BHIS medium containing the indicated concentrations of either antibiotic. Log phase cells of R20291 were inoculated at 1:10 into fresh BHIS media treated with increasing concentrations of either antibiotic. Cells were incubated anaerobically at 37°C to monitor cell accumulation and growth inhibition. Shown are the means and standard deviations of at least three biologically independent samples.

APPENDIX H

INHIBITORY CONCENTRATION OF DIAMIDE

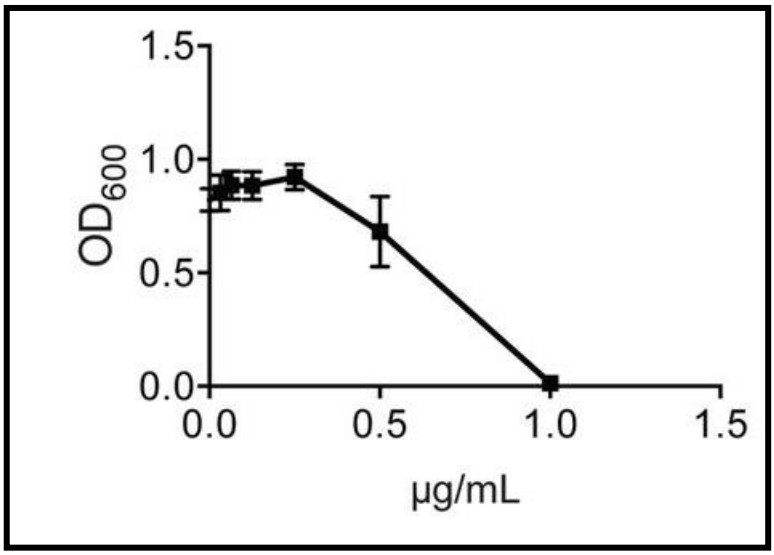

C. difficile R20291 cell density after overnight growth in TY medium at 37°C containing the indicated concentration of diamide. Shown are the means and standard deviations of at least three biologically independent samples.

APPENDIX I

SUBINHIBITORY CONCENTRATION OF NaCl

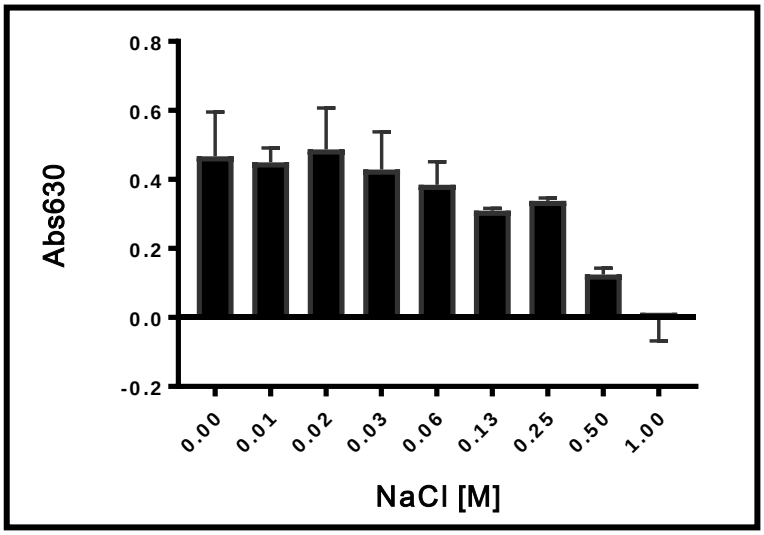

Sublethal concentration	NaCl [M]
0.25X	0.125
0.5X	0.25
1.0X	0.50

C. difficile R20291 cell density after overnight growth in BHIS medium containing the indicated concentrations of NaCl. Log phase cells of R20291 were inoculated at 1:10 into fresh BHIS media treated with increasing concentrations of NaCl. Cells were incubated anaerobically at 37°C to monitor cell accumulation and growth inhibition. Shown are the means and standard deviations of at least six biologically independent samples.

APPENDIX J

SUBINHIBITORY CONCENTRATION OF EDTA

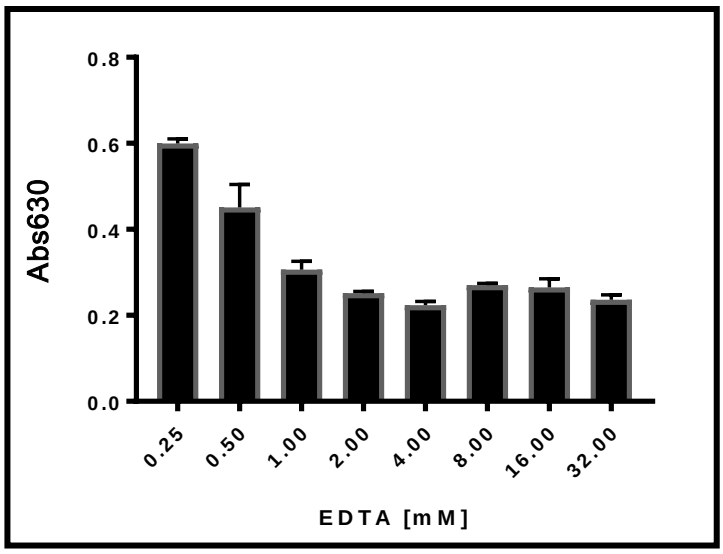

Sublethal concentration	EDTA [mM]
0.25X	0.50
0.5X	1.00
1.0X	2.00

C. difficile R20291 cell density after overnight growth in BHIS medium containing the indicated concentrations of EDTA. Log phase cells of R20291 were inoculated at 1:10 into fresh BHIS media treated with increasing concentrations of EDTA. Cells were incubated anaerobically at 37°C to monitor cell accumulation and growth inhibition. Shown are the means and standard deviations of at least six biologically independent samples.

APPENDIX K

EFFECTIVE IONIC RADIUS OF DIFFERENT METAL CATIONS

Cation	Effective ionic radius (Å)
Fe^{2+}	0.75
Co^{2+}	0.79
Mn^{2+}	0.81
Ni^{2+}	0.83
Mg^{2+}	0.86
Cu^{2+}	0.87
Zn^{2+}	0.88
Ca^{2+}	1.1

Metal ions are arranged in increasing ionic size . Adapted from Poudel *et al.* 2021.(105)

APPENDIX L

nsPEF CAN DISRUPT C. ACNES CELL MEMBRANE

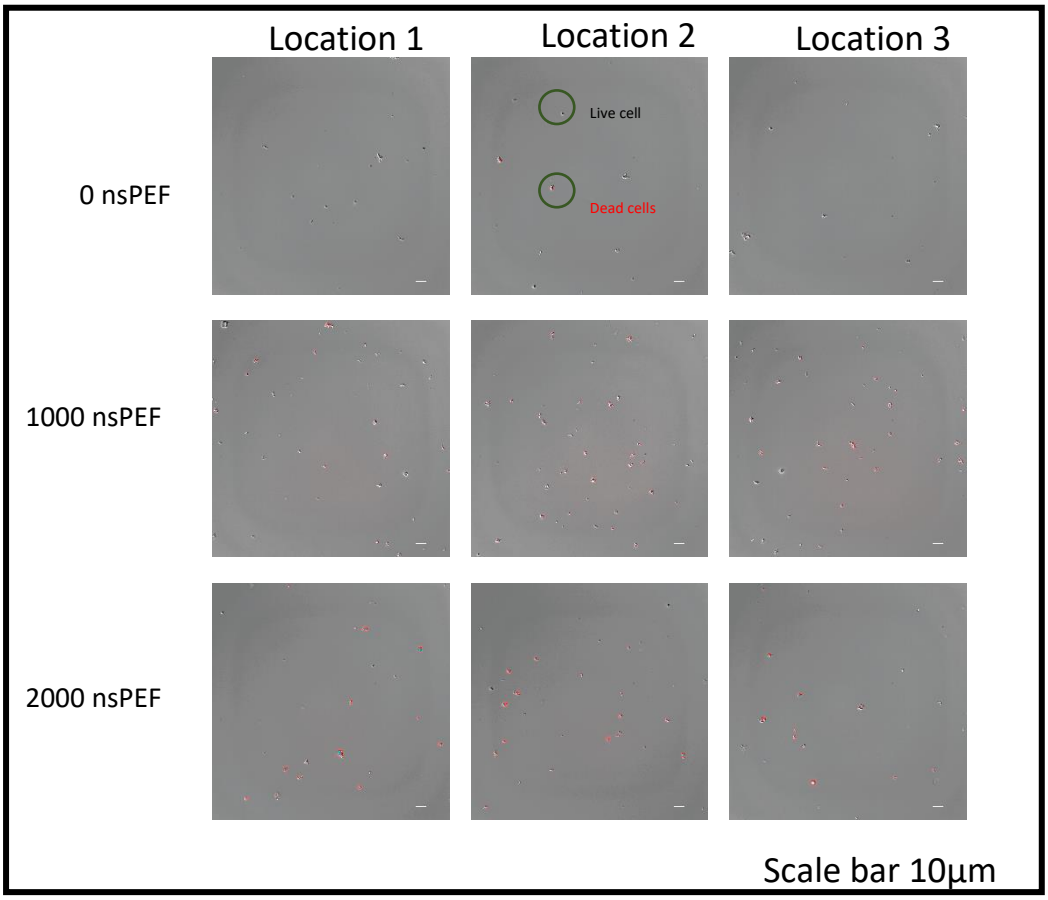

Representative fluorescence images of *C.acnes* after treatment with respective nsPEF. Propidium iodide poorly penetrates the intact cellular membrane, however upon the membrane breakage, it can easily enter the cytosol and binds the nucleic acids giving strong red fluorescence. More red fluorescence cells observed in the sample treated with 2000 nsPEF in comparison to the samples treated with 1000 nsPEF.

APPENDIX M

APPROVAL TO USE ^{32}P

Old Dominion University
Radiation Safety Committee

Application for the Possession and Use of Radioactive Materials

Directions: This application is to be completed only by Authorized Users or persons applying concurrently for Authorized User status (RSO-1). *Complete in duplicate, sign both copies, and return* to the Environmental Health and Safety Office/Radiation Safety Office. When approved by the Radiation Safety Committee, one copy will be returned to the applicant to serve as his/her authorization. *This authorization expires two years from the approval date.* An amendment must be submitted for approval before any change in protocol.

1. **Applicant:** Erin Purcell

   Department: Chemistry and Biochemistry

2. **Application Type:** ☑ New ☐ Renewal ☐ Amendment

3. **Office:**

   Building Alfriend Room 201 Phone (757) 683-4240

4. **Location(s) of Proposed Use:**

   Building Alfriend Room(s) 206, 107 Phone none

5. **Radionuclides for Possession:**

   (a) **Radionuclide:** 32-P Possession Limit (mCi): 1.0

   Chemical/Physical Form: aqueous gamma-32-P ATP (adenosine triphosphate)

   (b) **Radionuclide:** _____ Possession Limit (mCi): _____

   Chemical/Physical Form: _____

   (c) **Radionuclide:** _____ Possession Limit (mCi): _____

   Chemical/Physical Form: _____

   (d) **Radionuclide:** _____ Possession Limit (mCi): _____

   Chemical/Physical Form: _____

   (e) **Radionuclide:** _____ Possession Limit (mCi): _____

   Chemical/Physical Form: _____

RSO-2 (rev. 7/02)

1

6. Sealed Sources Only:

Complete this part for each sealed source proposed for use. Low activity check sources and exempt check sources need not be listed.

(a) Source:

Radionuclide: _____ Half-life: _____

Activity: _____(mCi)

Principal radiation emitted (check one or more) and energy(s) of the emission(s):

☐ Alpha Energy _____(MeV)

☐ Beta Energy _____max. ___ (MeV)

☐ Gamma or x-ray Energy _____(MeV)

☐ Positron Energy _____(MeV)

Date calibrated: _____

Manufacturer: _____

Model No.: _____

Serial No.: _____

(b) Source description:

(c) Describe the proposed use(s) of the source giving particular attention to health and safety aspects:

7. **Unsealed Sources Only:**

Complete this part for *each* radionuclide proposed for use. Use a separate page for each radionuclide.

(a) Radionuclide:

Radionuclide 32-P Half-life 14.3 days

Principal radiation emitted (check one or more) and energy(s) of the emission(s):

- ☐ Alpha Energy _____(MeV)
- ☑ Beta Energy 1.71 max. (MeV)
- ☐ Gamma or x-ray Energy _____(MeV)
- ☐ Positron Energy _____(MeV)

(b) Experimental Protocol:
Outline experimental protocol, with particular attention to health and safety aspects of the proposed use. Use additional sheet(s) if necessary.

See attached page.

(c) Waste:

Estimate activity and volume (or number) of waste that will be generated by proposed use.

- ☑ Aqueous: Activity/Volume per month 0.005 mCi
- ☐ Other liquid (specify): Activity/Volume per month _____
- ☐ Liquid scintillation vials Activity/Number per month _____
- ☐ Animal carcasses Activity/Number per month _____
- ☑ Solid (dry)/Incinerable Activity/Volume per month 0.020 mCi
- ☐ Solid (dry)/Non-Incinerable Activity/Volume per month _____
- ☐ Other (specify): Activity/Volume/Number per month _____

(d) Associated Wastes:

If applicable, describe any mixed waste (e.g. carcinogenic, hazardous etc.) that will be generated as a result of proposed use

Experimental Protocol

Gamma-32-P ATP (adenosine triphosphate) will be used as a reagent for phosphotransfer experiments. Briefly, gamma-32-P ATP will be added to reaction mixes with crude cell extract or purified enzyme and either GDP (guanosine diphosphate) or GTP (guanosine triphosphate). At selected timepoints, aliquots of this reaction mixture will be spotted onto PEI cellulose plates and air dried. When experiments are complete, cellulose plates will be used for thin layer chromatography (TLC) in aqueous buffer buffer, dried, and exposed to a phosphorimager plate for visualization.

On occasion, radioactive guanosine tetraphosphate (ppGpp) formed when the beta and gamma phosphate from gamma-32-P ATP is transferred to a GDP substrate will be isolated from the TLC plates by cutting the radionuclide-containing portion of the TLC plate in water or buffer, precipitating the phosphate species in salt solution, and rehydrating the precipitated 32-P ppGpp. This purified 32-P ppGpp will be used as a substrate in subsequent TLC reactions performed as above.

Radionuclides will be stored in a locked acrylic container within a -20 degree freezer. This container will be transported to a radioactivity workstation and opened behind an acrylic shield to retrieve materials. Reaction mixes will be assembled with all components except for the radioactive substrate before experiments are initiated by adding the 32-P ATP. All steps involving radioactive materials—reaction assembly and spotting, running, and exposing the TLC plates--will occur behind plexiglass shielding. All work will occur over a disposable absorbant bench pad with a water resistant backing (bench diaper), which will be disposed in the radioactive solid waste after use. Personnel will wear appropriate PPE (gloves and labcoats) and will use a GM pancake detector to monitor for environmental contamination during and after the experiment.

We anticipate using roughly 0.25 mCi/month. These protocols will generate incinerable dry waste in the form of plastic tubes and pipet tips, bench pads and paper towels used for cleaning, and the TLC plates. Dry waste will be stored in a shielded container for EHS pickup. Reactions will be designed to occur in minimal volume, to limit the production of aqueous waste. When the TLC is performed properly, the radioactive phosphate species will remain on the cellulose plate and not enter the running buffer, but used buffer will be considered radioactive and stored and disposed of as aqueous radioactive waste, as will buffer or water used to soak and precipitate 32-P ppGpp. Aqueous radioactive waste will be stored in a shielded container for EHS pickup.

8. **Equipment and Facilities:**

(a) Instruments and Equipment:

Check available instruments and equipment

- ☐ Fume hood Room # _____
- ☑ Appropriate signs, tape and labeling
- ☑ Personal protective equipment (PPE)
  - ☑ Disposable gloves
  - ☑ Lab coats
  - ☐ Safety glasses
- ☑ Waterproof backed absorbent material for benches
- ☐ Remote pipette(s)
- ☐ Trays to contain spills
- ☐ Film badges
- ☑ Portable radiation detection instrument(s) Specify type GM pancake detector
- ☐ Liquid scintillation counter
- ☐ Gamma scintillation counter

(b) Facilities:

Attach a floor plan of areas where radioactive materials are used or stored showing fixtures such as sinks, hoods, benches, cold rooms etc., and major pieces of equipment such as refrigerators, freezers, centrifuges desks, radwaste containers etc. Indicate work areas, radioactive material storage areas, radioactive waste storage areas, entrances and exits. *Indicate room numbers.*

See attached page.

9. **Security and Emergency Procedures:**

(a) Security

Describe what provisions have been made to insure that radioactive materials are secure from unauthorized persons. Also describe a key control plan designed to restrict access to areas where radioactive materials are used and stored.

See attached page.

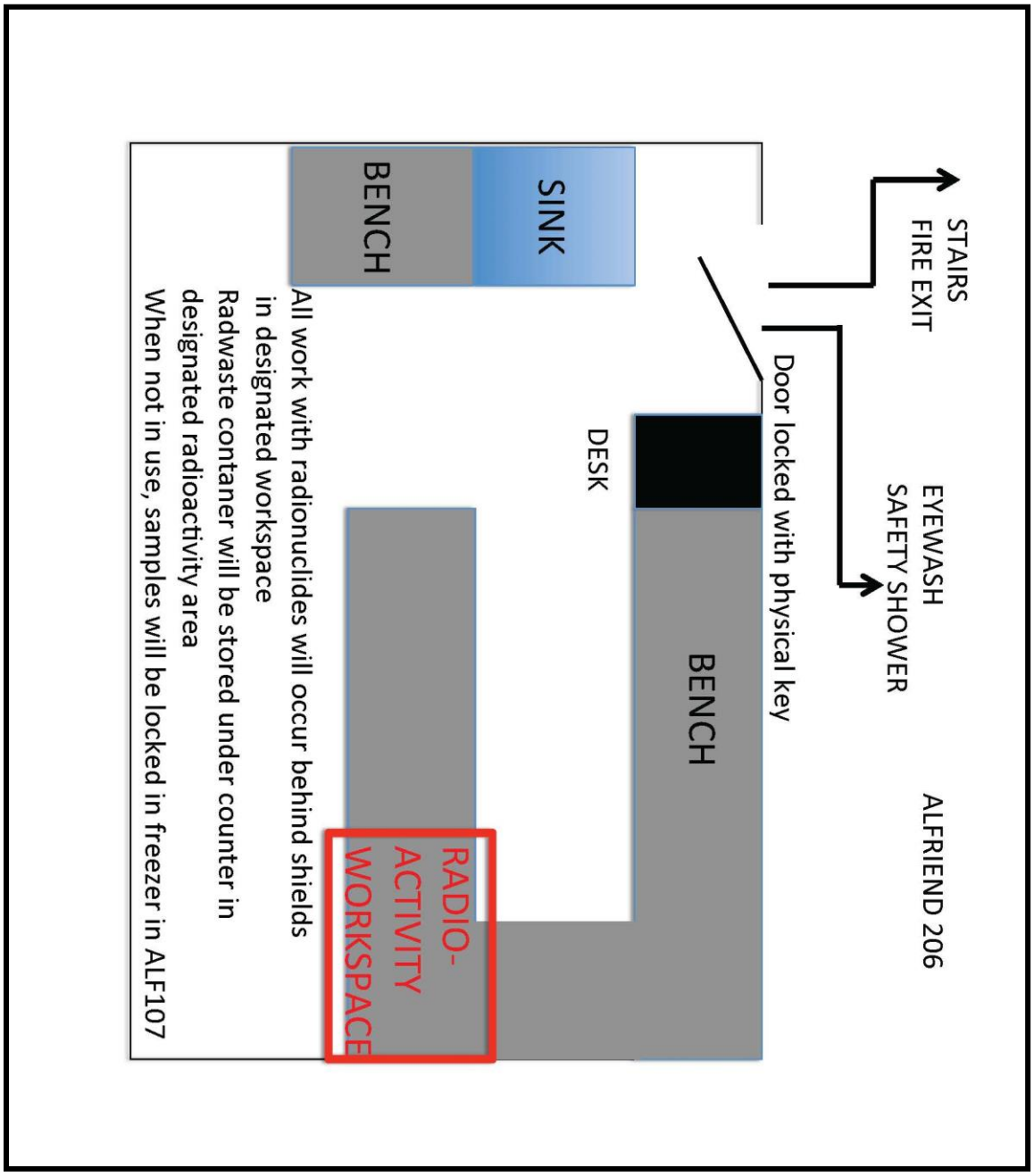
STAIRS
FIRE EXIT
EYEWASH
SAFETY SHOWER
ALFRIEND 206
Door locked with physical key
BENCH
DESK
SINK
BENCH
RADIO-
ACTIVITY
WORKSPACE
All work with radionuclides will occur behind shields
in designated workspace
Radwaste contaner will be stored under counter in
designated radioactivity area
When not in use, samples will be locked in freezer in ALF107

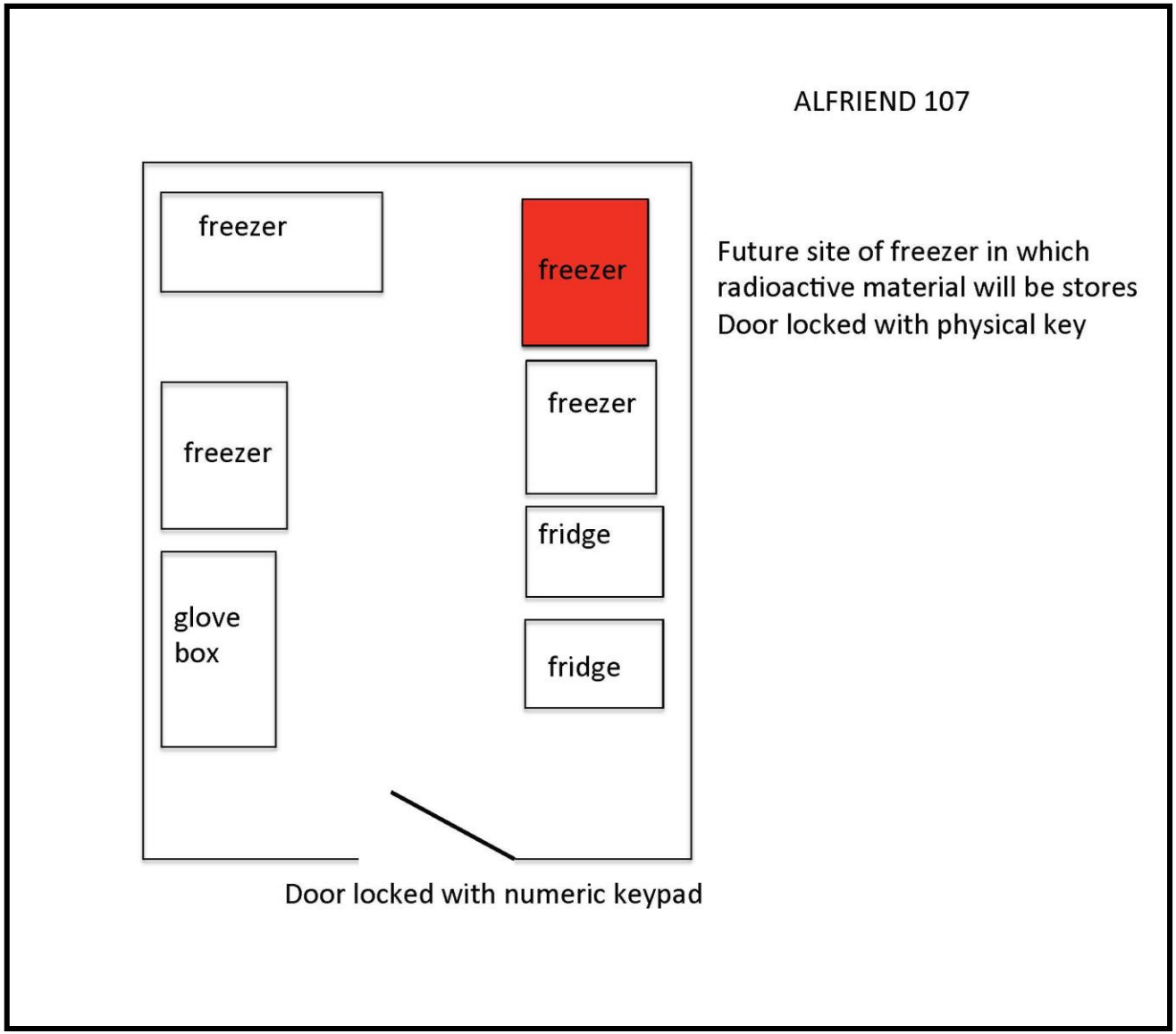
ALFRIEND 107
freezer
freezer
freezer
freezer
fridge
glove box
fridge
Future site of freezer in which radioactive material will be stores
Door locked with physical key
Door locked with numeric keypad

Security Procedures

Stock vials of gamma-32-ATP and any radionuclide products purified from TLC plates will be stored in an acylic lockbox secured to the inside of a -20 degree freezer (in Alfriend 107). Only qualified laboratory personnel will have either the key or the combination to the lock securing the box to the freezer and the separate lock to open the box. All work involving radionuclides will occur in Alfriend 206, which is kept locked when unoccupied. Only qualified laboratory personnel have the key to the room. A record of who has keys will be kept with other radiation safety documentation in a designated binder. Shielded waste will be stored in Alfriend 206.

Emergency Procedures

All radionuclides will be present as aqueous liquids, so spill procedures will be universal. Upon a spill, all work in the lab will be stopped and a sign placed on the door to prevent anyone from entering until the spill is cleaned up. Lab personnel, wearing appropriate PPE (lab coat, disposable gloves), keeping portable acrylic shields between their torsos/faces and the spill, will first use a Geiger coutner to define the area affected by the spill, then absorb all liquid with paper towels and dispose of them in the radioactive solid waste container. Personnel will then spray the affected area with radioactive spill cleaner (Count-Off or similar), absorb the liquid with paper towels, dispose of the paper towels in the radioactive waste, and survey the area with the Geiger counter. This procedure will be repeated until no radiation is detected. At this point, personnel will swipe the area with Kimwipes or filter paper to conduct a liquid scintillation test and ensure that there is no remaining contamination. After the area is confirmed to be clean of radioactivity, the sign will be removed from the door and normal laboratory operations will resume. The spill will be recorded in the use log and inventory to account for the radioactive material.

Laboratory monitoring

The lab will be monitored for radioactive contamination by liquid scintillation wipe tests (using the liquid scintillation counter owned by EHS) once monthly. The following surfaces within ALF206 will be tested:

- benchtop within radioactivity workspace
- floor within radioactivity workspace
- outside of radioactive waste containers
- pipets used within radioactivity workspace
- drawer handles within radioactivity workspace
- sink
- lab door handle

The radioactive workspace will be surveyed by GM pancake detector before and after each use of radionuclides.

Record keeping

Printed copies of materials pertaining to the use of radionuclides will be kept together in a designated binder, which will be kept on the reference shelf in ALF206. These will include:

- records of receipt of radionuclides
- use records—every time material is removed from the source vial, user will record the volume and activity removed. Every time materials are added to the dry or liquid waste container, the approximate activity added to that waste container will be recorded. After every use of radioactivity, the use logs will be updated so that the withdrawals of activity from the source vial equal the deposit of activity into the waste containers.
- Disposal records- whenever a source vial is discarded, it will be recorded and removed from the current inventory
- Records of monthly wipe tests
- All approvals from and communications with the radiation safety committee

(b) Emergency Procedures:

Describe the emergency procedure(s) that will be followed in case of a spill or accident. Describe decontamination procedures.

See attached page

(c) Emergency Contacts:

List two names and phone numbers to be called after hours in case of emergency.

Name Erin Purcell Phone (773) 354-2571

Name David Courson (spouse) Phone (773) 354-2570

10. Monitoring and Recordkeeping:

(a) Laboratory monitoring:

Describe your laboratory monitoring program. Include a description of your swipe survey schedule (specifically the frequency of surveys), areas to be surveyed, and documentation of surveys. *Note:* Survey frequency must be commensurate with the type(s), form(s), and activities of radionuclides proposed for use. For most applications swipe surveys must be conducted on a monthly basis. See the Radiation Safety Policy and Procedures Manual for guidance.

See attached page.S

(b) Recordkeeping:

Describe your method of inventory control and accounting, including records of receipt, use and disposal.

See attached page.

11. Personnel:

List all persons who will use or will be potentially exposed to radiation as the result of proposed use.

Erin B. Purcell (AU)

11. Certification:

The signature below affirms that the applicant has read and will comply with the rules, regulations, and procedures of the Old Dominion University Radiation Safety Committee and Radiation Safety Officer. The applicant accepts responsibility for maintaining current knowledge of those rules, regulations, and procedures and responsibility for the actions of those persons working under his/her authorization. Any changes in the use protocol, personnel and the location of use will be reported to the Radiation Safety Officer in a timely manner.

Signature Erin B Purcell **Date** Nov. 22, 2016

Radiation Safety Committee:

Approved / RSC Chair _____ **Approved / RSO** _____

Approved / RSC Member _____ **Approved / RSC Member** _____

Approved / RSC Member _____

(a) Dosimetry Indicated

- ☐ Whole Body
- ☐ Whole Body + Extremity
- ☐ Bioassay

(b) Special conditions attached to approval:

(c) Date of approval: _____

(d) Expiration date: _____

RSO-2 (rev. 7/02)

APPENDIX N

RIGHTS AND PERMISSION

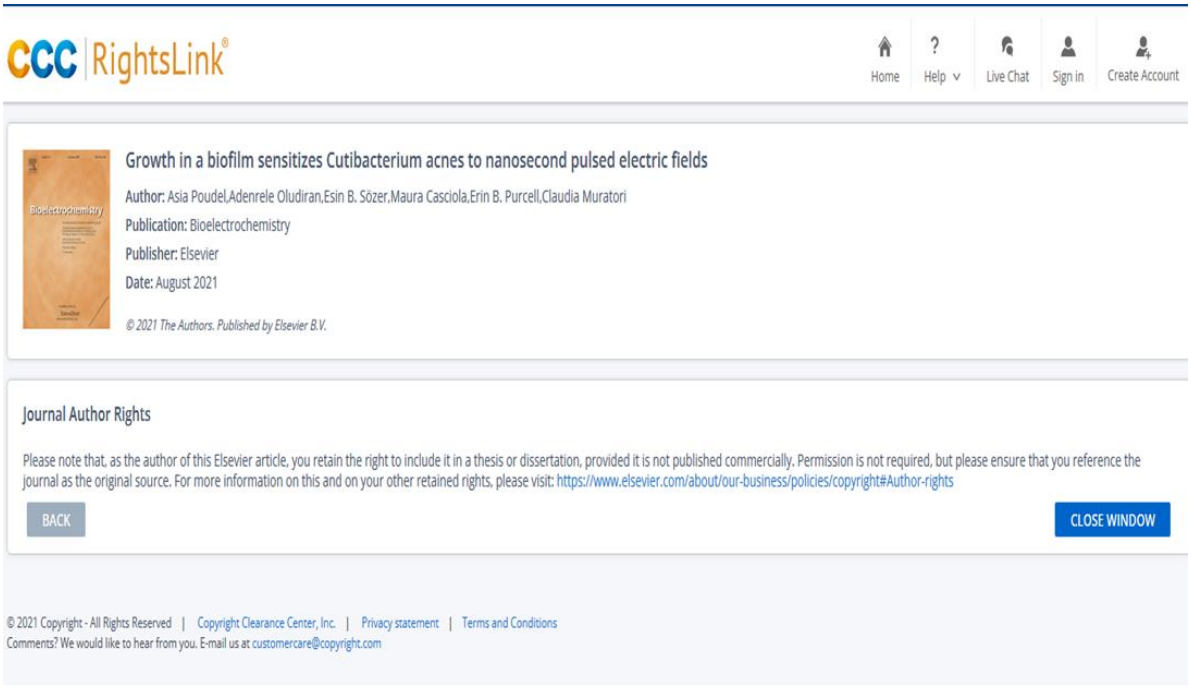

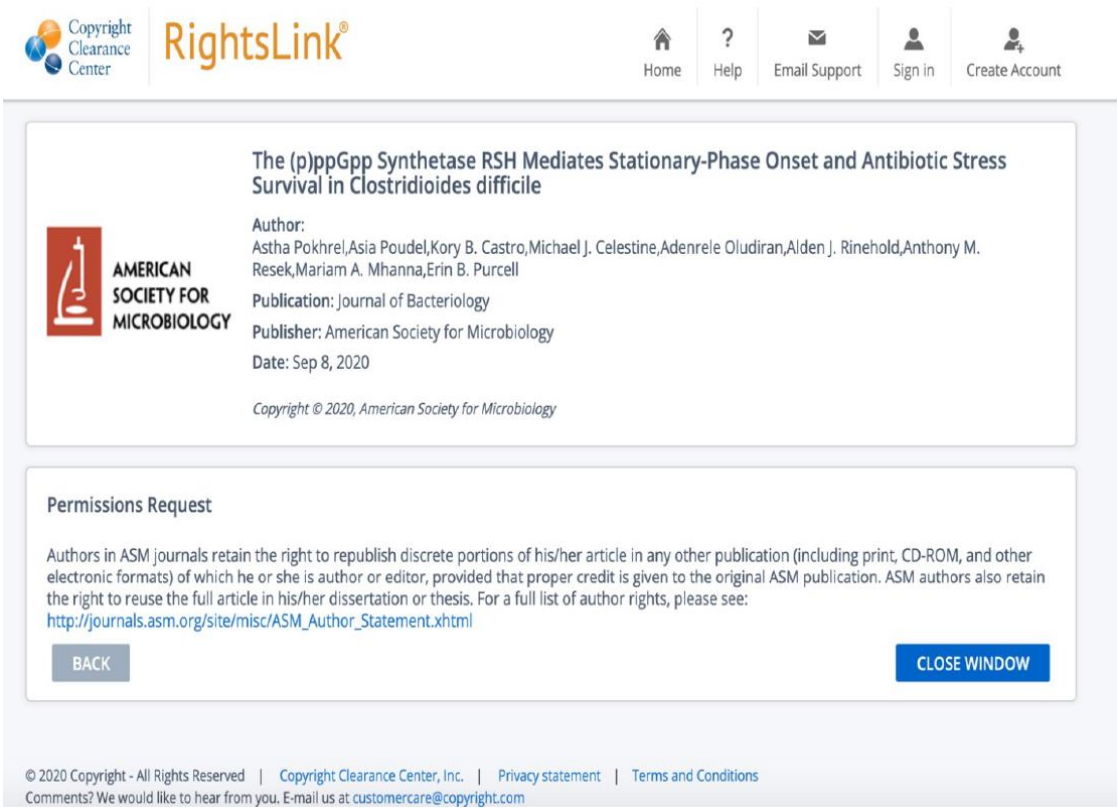
Copyright Clearance Center
RightsLink®
Home
Help
Email Support
Sign in
Create Account
The (p)ppGpp Synthetase RSH Mediates Stationary-Phase Onset and Antibiotic Stress Survival in Clostridioides difficile
Author:
Astha Pokhrel,Asia Poudel,Kory B. Castro,Michael J. Celestine,Adenrele Oludiran,Alden J. Rinehold,Anthony M. Resek,Mariam A. Mhanna,Erin B. Purcell
Publication: Journal of Bacteriology
Publisher: American Society for Microbiology
Date: Sep 8, 2020
Copyright © 2020, American Society for Microbiology
AMERICAN SOCIETY FOR MICROBIOLOGY
Permissions Request
Authors in ASM journals retain the right to republish discrete portions of his/her article in any other publication (including print, CD-ROM, and other electronic formats) of which he or she is author or editor, provided that proper credit is given to the original ASM publication. ASM authors also retain the right to reuse the full article in his/her dissertation or thesis. For a full list of author rights, please see:
http://journals.asm.org/site/misc/ASM_Author_Statement.xhtml
BACK
CLOSE WINDOW
© 2020 Copyright - All Rights Reserved | Copyright Clearance Center, Inc. | Privacy statement | Terms and Conditions
Comments? We would like to hear from you. E-mail us at customercare@copyright.com

New Results

Unique features of magic spot metabolism in *Clostridioides difficile*

Asia Poudel, Astha Pokhrel, Adenrele Oludiran, Estevan J. Coronado, Kwincy Alleyne, Marrett M. Gilfus, Raj K. Gurung, Surya B. Adhikari, Erin B. Purcell

doi: https://doi.org/10.1101/2021.08.02.454818

ARTICLE INFORMATION

doi https://doi.org/10.1101/2021.08.02.454818

History August 2, 2021.

VITA

Asia Poudel

Department of Chemistry and Biochemistry

Old Dominion University

Norfolk, VA, 23529

Education

Ph.D. (Anticipated December 2021) in Chemistry and Biochemistry, Old Dominion University, Norfolk, VA

M.S. (May 2021) in Chemistry and Biochemistry, Old Dominion University, Norfolk, VA

M.Sc. (September 2010) in Microbiology, Tribhuvan University, Nepal

Selected Presentations

Developing molecular tools to determine stringent response in *Clostridium difficile*. **Asia Poudel** & Erin B. Purcell. EVMS Graduate Research Conference, EVMS 2018

The molecular basis of antibiotic resistance in *Clostridium difficile*. **Asia Poudel** & Erin B. Purcell. Mid Atlantic Microbial Pathogenesis Meeting, Wintergreen, VA, 2019

Clostridial stringent response enzymes utilize diverse divalent cations. **Asia Poudel**, Astha Pokhrel & Erin B. Purcell. Microbial Pathogenesis & Host Response (virtual meeting), CSHL 2021

Publications

Astha Pokhrel, **Asia Poudel**, and Erin B. Purcell. A Purification and InVitro Activity Assay for a (p)ppGpp Synthetase from Clostridium difficile. JoVE. 2018.

Astha Pokhrel, **Asia Poudel**, Kory B. Castro, Michael J. Celestine, Adenrele Oludiran, Alden J. Rinehold, Anthony M. Resek, Mariam A. Mhanna, Erin B. Purcell. The (p)ppGpp synthetase RSH mediates stationary phase onset and antibiotic stress survival in *Clostridioides difficile.* Journal of Bacteriology Jul 2020

Asia Poudel, Adenrele oludiran, Esin B. Sözer, Maura Casciola, Erin B. Purcell, Claudia Muratori. Growth in a biofilm sensitizes *Cutibacterium acnes* to nanosecond pulsed electric fields. Bioelectrochemistry Volume 140, August 2021, 107797

Asia Poudel, Astha Pokhrel, Adenrele Oludiran, Estevan J. Coronado, Kwincy Alleyne, Marrett M. Gilfus, Erin B. Purcell. Unique features of magic spot metabolism in *Clostridioides difficile.* bioRxiv, 2021.2008.2002.454818